USGS
science for a changing world

U.S. DEPARTMENT OF THE INTERIOR

U.S. GEOLOGICAL SURVEY

Characterization of Coal and Coal Combustion Products from a Coal-burning Power Plant -- Preliminary Report and Results of Analyses

Edited by

George N. Breit[1]
and
Robert B. Finkelman[2]

Open-File Report 98-342

[1] Denver, Colorado
[2] Reston, Virginia

Table of Contents

List of Tables

List of Figures

A. INTRODUCTION

by Robert B. Finkelman U. S. Geological Survey, Reston, Virginia and **George N. Breit**, U. S. Geological Survey, Denver, Colorado

The U.S. Geological Survey, the Kentucky Geological Survey, and the Kentucky Center for Applied Energy Research are conducting a multi-disciplinary study of the physical and chemical properties of solid coal-combustion waste products. The purpose of the project is to provide comprehensive and accurate physical and chemical characterization of these waste materials. Included in the investigation are studies of how the waste materials may interact with the environment. Results of the environmental studies are intended to enhance objective assessments of the environmental impact of these materials.

Figure A1 is a schematic of the project organization, some of the analytical techniques applied to the samples, and references to relevant sections of this report. Materials collected as part of the study include samples of feed coal, bottom ash, fly ash, limestone, flue-gas-desulfurization sludge, and waste-pond slurry. With the full cooperation of the power plant operator these materials were collected monthly for two years from two subunits (unit 1 and unit 3) of the power plant. Unit 1 burns relatively high-sulfur coal from the Illinois and Appalachian basins. This unit was equipped with a limestone slurry flue-gas desulfurization (FGD) circuit during our sampling. Unit 3 burns low-sulfur coal from the central Appalachian basin.

Background

In March 1994 the U.S. Geological Survey (USGS) contacted the Kentucky Geological Survey (KGS) for the purpose of setting up a cooperative research program on trace elements in coal and coal waste products. On April 4, 1994 Cortland Eble of the KGS contacted the cooperating utility. A sampling plan was developed and approved by the operator. Sample collection at the power plant commenced in July 1994 and continued on a monthly basis through June 1996.

Project Objectives

The power plant samples presented us with opportunities to achieve the following goals.

* Determine the concentration, distribution, and modes of occurrence of trace elements in the high-volume combustion waste products.
* Observe temporal variation in the properties of high-volume combustion waste products with respect to temporal variations in the properties of the feed coal.
* Document differences in the behavior of elements between units burning high-sulfur and low-sulfur coals.
* Observe the effects on trace element distribution caused by the installation of an FGD system on unit 1.
* Determine the mineralogy, magnetic properties, isotopic composition, organic chemistry, and radionuclide content of selected samples.

Purpose of this Report

This report is a summary of what was accomplished during the first year of the project. The information is conveyed in the following series of short contributions prepared by project researchers. Results presented in this report are for the samples collected during the first 4 to 12 months of sampling. The report contains preliminary data and interpretations and does not reflect the final analysis of any of the participating researchers or their organizations.

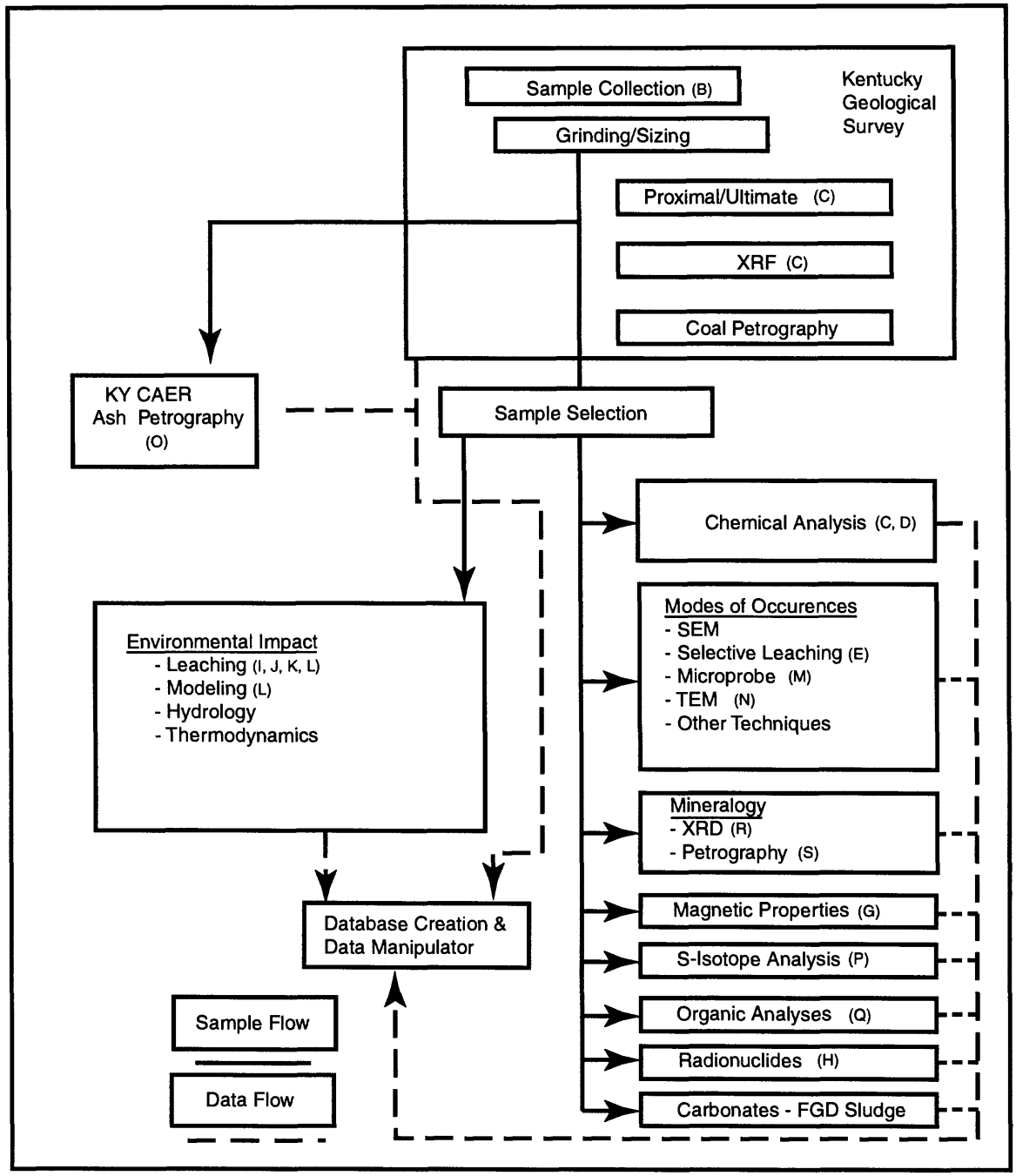

Figure A1. Diagram of sample and data flow for characterization of sampled coal, fly ash, bottom ash and flue gas desulfurization sludge. Letters in parentheses identify relevant sections of this volume. [KY CAER, Center for Applied Energy Research, Lexington, Kentucky; XRF, x-ray fluorescence; SEM, scanning electron microscope; TEM, transmission electron microscope; XRD, x-ray diffraction; FGD, flue gas desulfurization).

B. SAMPLE COLLECTION PROCEDURE

by Cortland F. Eble, Kentucky Geological Survey, Lexington, Kentucky

This section describes the sampling procedures used at the power plant to collect feed coal, fly ash, bottom ash, flue-gas-desulfurization (FGD) sludge, limestone for the FGD unit and solids from the disposal pond. Along with the sampling procedures, a brief description of the operation of the power plant is included to put sample collection in the context of plant operations. In most cases, ideal methods of sampling could not be used because of limitations within the power plant, and resources to handle large amounts of material were not available. Splits of samples provided to members of the project are the basis of the subsequent sections of this volume.

Coal

Coal is transferred from a storage yard to the power plant by a conveyor belt at a rate depending on the needs of the furnace. The coal is then stored in a holding silo that overlies a gravimetric feeder. Each furnace has six holding silos. Coal brought to the silos has a maximum dimension between 5 and 8 centimeters, although most of it is less than 10 mesh (< 2 mm). The coal is then demand fed from the silos through the gravimetric feeders into pulverizers. The pulverizers are ball mills that grind the coal to less than 200 mesh (<250 μm). The pulverized coal is then injected with preheated air into the furnaces. Heat from the resulting fireball (internal furnace temperature >2600 degrees F) converts water contained in a network of pipes in the furnace walls into steam. The steam moves through a turbine that drives the electric generator.

With the help of power plant staff, coal samples were collected from portals on the gravimetric feeders of unit 1 (moderate-high-sulfur coal) and unit 3 (low-sulfur coal) (Fig. B1). For the first four samplings (July - October 1994), 5 to 7 kg of coal was collected in a single collection. Beginning in November 1994 samples consisted of 4 feed-coal splits from each unit, collected over a period of 5 to 6 hours. Each split is processed separately with a composite prepared by mixing equal amounts of the four splits. The four feed-coal splits were intended to provide information on the variability in feed coal composition during the sample period.

The sampling scheme used to collect the coal samples does not conform to ASTM standards. Although ASTM does not have a test method specific to sampling coal fed into a power plant, they do have one for the collection of a gross sample of coal (D-2234). If followed, the test method would require collection of a 15 pound sample of coal, a minimum of 35 times, for each unit (70 samples total). This translates into collecting 1,050 pounds of coal (15 pounds of coal collected every 8.5 minutes over a period of 5 hours) per visit. Logistically, this is impractical.

Fly Ash

Fly ash is composed mainly of small particles of noncombustible constituents of the coal. These particles are transported in the exhaust gas that leaves the furnace following combustion. At the power plant sampled, approximately 90% of the fly ash is removed from the exhaust gas by electrostatic precipitators. The electrostatic precipitators at unit 3 remove the fly ash before the exhaust gas passes through the heat exchangers. The heat exchangers transfer heat from the exhaust gas to the air blown into the furnace with the pulverized coal. Precipitators upstream of the heat exchangers are referred to as "hot-side" collectors; those downstream are identified as "cold-side" collectors. These designations are based on the relative temperature of the exhaust gas which is typically 800° F for host-side and near 250° F for cold-side collectors.

Two samples of fly ash are collected at unit 3. These are designated as "coarse-side" and "fine-side" and are collected from two parallel banks of hoppers underneath the electrostatic precipitators. The coarse-side is a bank of 8 hoppers closest to the flue gas entry point. The fine-side hopper bank of 8 hoppers is separated from the coarse-side by about 10 feet. As the exhaust gas passes through the electrostatic precipitators larger particles drop out first and are collected in the first bank of collectors. Farther along the path through the precipitators smaller particles are collected and drop down into the second bank of hoppers. Separate samples of fly ash were collected from each bank of the hoppers.

Unit 1 has a different configuration with respect to the electrostatic precipitator. The electrostatic precipitator on unit 1 is a cold-side collector. Fly ash in Unit 1 was collected in a single bank of hoppers.

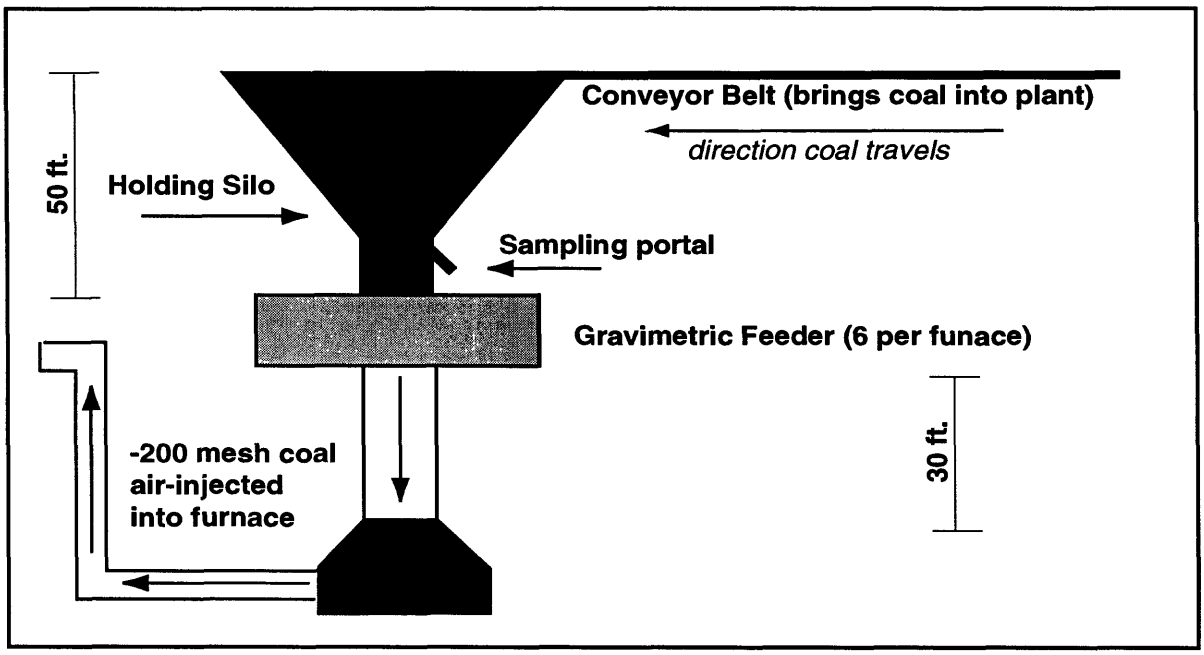

Figure B1. Schematic of coal movement and sampling point at the power plant.

Bottom Ash

Some noncombustible components of the coal fall to the bottom of the furnace where they are collected as bottom ash. Bottom ash is removed from the furnace once a shift (every 8 hours), which involves crushing the solids to about 4 mesh (<5 mm), and sending it out to the ash pond on a water train. The bottom ash collected in this study was gathered from the water train. Although interaction with the water may modify the ash, the water train offered the only accessible sampling point. To collect the bottom ash, we use a bucket with the bottom cut out, and a nylon mesh screen secured over the top. Bottom ash for many of the monthly collections was collected from unit 4 instead of unit 3 because a valve required for sampling unit 3 was not functioning. Unit 4 was chosen as an alternative for bottom ash sampling because the coal used in this furnace and its combustion design are identical to that of unit 3. Typically, 5 to 10 Kg of bottom ash are collected from each unit.

Limestone and Flue-Gas Desulfurization Sludge Samples

During November 1994 a wet limestone flue-gas desulfurization (FGD) circuit began operation on unit 1. Limestone for the scrubber is stockpiled in an open-air mound. We collected the limestone by scraping away the weathered surface material at four to five locations on the mound. In the power plant, the limestone is ground and mixed with water to create a slurry that is mixed with the flue gas in large reaction tanks. Four quarts of the raw limestone slurry are collected monthly along with two quarts of the FGD sludge from each of two functioning reaction tanks. The samples are filtered in the laboratory to separate the limestone and FGD solids from the liquid.

Pond Slurry

In March 1995, samples of a waste pond slurry were collected. This material was collected from the active slurry pond that is used to collect solid wastes from the plant. A shovel was used to clear off the upper few centimeters of the slurry material then several kilograms of material was collected into plastic pails.

Sample Numbering Scheme

The sample numbering scheme used in this report has the following form: **1G1FC10**
The first number (**1**) refers to the sample set. Number 1 is for the first sample set collected in July 1994. Number 2 would represent the second sample set collected in August 1994, etc. The next two characters (**G1**) denote the power plant and unit. G1 represents unit 1 (the unit using high-sulfur coal). G3 represents unit 3 (the unit burning low-sulfur coal). The next two characters (**FC**) denote the sample type. FC stands for feed coal, BA for bottom ash, and FA for fly ash. The final characters (**10**) denote mesh size of the sample fraction. In this case, 10 stands for 10 mesh, 20 would stand for 20 mesh.

C. KENTUCKY GEOLOGICAL SURVEY PRELIMINARY ANALYTICAL RESULTS ON FEED COAL, FLY ASH AND BOTTOM ASH

by Cortland F. Eble, Kentucky Geological Survey, Lexington, Kentucky

Samples collected from the power plant were analyzed in the laboratories of the Kentucky Geological Survey. Measured parameters include proximal and ultimate analysis of the coal, sulfur in all materials, and x-ray fluorescence to determine contents of major and minor inorganic constituents. A summary of the analytical results is presented below.

Raw Coal

Results of standard methods of coal analysis on samples collected from July 1994 through April 1995, are shown in Tables C1 and C2. There are no unit 1 samples for September 1994 and April 1995 because the unit was off-line to perform routine maintenance. Likewise, samples were collected from unit 4 during April 1995 because unit 3 was off-line. Unit 4 is identical in design and in the source of coal. Analytical results indicate that the composition of the feed coal was relatively constant during the study period; this is especially true for unit 3.

Selection of coal for combustion is commonly dependent on several characteristics including calorific value, sulfur content and ash fusion temperature. Calorific values for unit 1 feed coal vary between 12,272 and 13,989 BTU/lb. This variability is attributed to the multiple sources of coal used in unit 1. Unit 3 feed coal has a small range of heating values from 13,263 to 13,904 BTU/lb, with an average of 13,603 BTU/lb. Total sulfur contents for unit 3 vary between 0.66% and 0.92% averaging 0.74%. Unit 1 sulfur contents average 2.97% and are a bit more variable, ranging from 2.53 to 3.51%. This reflects the higher pounds SO_2 / million BTU limit of unit 1 (5.67 lbs SO_2 / MM BTU), compared to units 3 and 4, which have limits of 1.2 lbs SO_2 / MM BTU.

Consistent with the differing sulfur contents of the feed coals, compliance sulfur values, (which are derived by the formula, total sulfur content times 19,500 / BTU) are more variable for unit 1 than unit 3. Compliance sulfur for unit 1 varies between 3.52 and 5.48 lbs SO_2 / MM BTU (average 4.4 lbs SO_2 / MM BTU), whereas compliance sulfur for unit 1 varies only between 0.96 and 1.34 lbs SO_2 / MM BTU (average 1.05 lbs SO_2 / MM BTU). These data are most likely a function of unit 1 being able to burn moderate to high-sulfur coal from both the Appalachian Basin (higher rank), and the Illinois Basin (lower rank). Units 3 and 4, in contrast, are exclusively burning low-sulfur, high-rank Appalachian Basin coal.

Final ash fusion temperatures for unit 1 average 2335° F, with a range of 2146 to 2532 ° F, whereas unit 3 has an average final ash fusion temperature of 2928° F, and this temperature is more tightly constrained (range of 2810 and 3000° F). These numbers reflect the higher iron concentrations in unit 1 coal. High iron tends to lower the ash fusion temperature.

Coal Ash

Prior to analysis by x-ray fluorescence, coal samples were ashed. Results of the x-ray fluorescence analysis of coal ash are presented in Tables C3 and C4. Silicon and aluminum are the most abundant constituents of the ash from both units. Components that are more abundant in the unit 1 coal ash, relative to the unit 3 coal ash, include CaO, Fe_2O_3, MgO, SO_3, Na_2O and Mn. Element oxides that are more abundant in the unit 3 coal ash, relative to the unit 1 coal ash include SiO_2, Al_2O_3, K_2O and TiO_2.

Table C1. Summary of standard analytical parameters for unit 1 feed coal (n = 8). (Vol. Mat - volatile matter; F. Carbon - fixed carbon; Comp S - compliance sulfur)

	Moisture (wt.%)	Vol. Mat (wt.%)	Ash (wt.%)	F. Carbon (wt.%)	Sulfur (wt.%)	Calorific Value BTU/lb	Comp S lbs/MM BTU
Average	2.89	37.87	9.5	52.6	2.97	13,235	4.40
Maximum	7.89	40.25	11.8	55.1	3.51	13,989	5.48
Minimum	0.83	36.76	7.9	50.5	2.53	12,272	3.53

Table C2. Summary of standard analytical parameters for unit 3 feed coal (n = 10). (Vol. Mat - volatile matter; F. Carbon - fixed carbon; Comp S - compliance sulfur)

	Moisture (wt.%)	Vol. Mat (wt.%)	Ash (wt.%)	F. Carbon (wt.%)	Sulfur (wt.%)	Calorific Value BTU/lb	Comp S lbs/MM BTU
Average	1.94	34.96	8.6	56.5	0.75	13,603	1.05
Maximum	2.91	36.54	10.1	58.1	0.92	13,904	1.34
Minimum	0.64	32.83	7.2	55.2	0.66	13,263	0.96

Table C3. Summary of x-ray fluorescence data for unit 1 feed coal ash (n = 8). Element abundances are reported as weight percent on an ash basis, except for Mn, which is reported as parts per million. (Avg., average; Max., maximum; Min., minimum).

	Al_2O_3	SiO_2	P_2O_5	K_2O	CaO	Na_2O	TiO_2	Fe_2O_3	MgO	SO_3	Mn	SrO
Avg.	21.8	45.5	0.27	1.78	3.57	0.45	1.07	19.7	0.86	3.62	288	0.14
Max.	24.9	47.6	0.63	2.28	6.46	0.88	1.16	24.2	0.95	6.05	491	0.18
Min.	19.4	42.8	0.09	1.3	0.83	0.06	0.86	15.6	0.57	0.91	188	0.11

Table C4. Summary of x-ray fluorescence data for unit 3 feed coal ash (n = 10). Element abundances are reported as weight percent on an ash basis, except for Mn, which is reported as parts per million. (Avg., average; Max., maximum; Min., minimum).

	Al_2O_3	SiO_2	P_2O_5	K_2O	CaO	Na_2O	TiO_2	Fe_2O_3	MgO	SO_3	Mn	SrO
Avg.	30.4	58.3	0.22	2.53	1.39	0.28	1.58	4.5	1.01	1.23	152	0.14
Max.	32.8	61.7	0.39	3.11	1.8	0.35	1.98	6.19	1.27	1.89	201	0.16
Min.	28.7	54.6	0.12	1.86	0.87	0.22	1.3	2.57	0.61	0.55	63	0.1

Fly Ash

The total carbon and total sulfur contents of fly ash are summarized in Table C5. Both fly ashes from unit 1 and 3 are low in total carbon and total sulfur. Xx-ray fluorescence results are summarized in Tables C6 and C7. Components that are more abundant in unit 1 fly ash relative to the unit 3 fly ash, include CaO, Fe_2O_3, Na_2O, SO_3, and Mn. Element oxides that are more abundant in the unit 3 coal ash, relative to the unit 1 coal ash, include Al_2O_3, SiO_2, K_2O and TiO_2. Overall, the differences in the composition of the fly ash are similar to differences detected in the feed coal ash.

Table C5. Summary of total carbon and total sulfur content of fly ash.

	Unit 1		Unit 3	
	Total Carbon wt.%	Total Sulfur wt.%	Total Carbon wt.%	Total Sulfur wt.%
Average	1.52	0.39	2.74	0.25
Maximum	3.09	0.48	4.85	0.92
Minimum	0.78	0.29	0.42	0.07

Table C6. Summary of x-ray fluorescence data for unit 1 fly ash (n = 8). Element abundances are reported as weight percent on an ash basis, except for Mn, which is reported as parts per million. (Avg., average; Max., maximum; Min., minimum).

	Al_2O_3	SiO_2	P_2O_5	K_2O	CaO	Na_2O	TiO_2	Fe_2O_3	MgO	SO_3	Mn	SrO
Avg.	22.4	47.5	0.27	1.93	3.66	0.31	1.11	19.4	1.01	0.75	302	0.11
Max.	23.1	49.3	0.37	2.16	4.22	0.51	1.16	21.5	1.27	0.96	401	0.11
Min.	21.6	45.9	0.17	1.58	2.81	0.1	1.06	17.5	0.61	0.43	203	0.11

Table C7. Summary of X-ray fluorescence data for unit 3 fly ash (n = 10). Element abundances are reported as weight percent on an ash basis, except for Mn, which is reported as parts per million. (Avg., average; Max., maximum; Min., minimum).

	Al_2O_3	SiO_2	P_2O_5	K_2O	CaO	Na_2O	TiO_2	Fe_2O_3	MgO	SO_3	Mn	SrO
Avg.	30.05	57.86	0.21	2.63	1.27	0.28	1.57	4.3	0.92	0.13	209	0.16
Max.	31.43	61.1	0.32	3.11	1.6	0.3	1.72	5.01	1.14	0.33	332	0.16
Min.	28.8	55.5	0.12	2.03	0.82	0.26	1.44	2.96	0.6	0.05	136	0.16

Bottom Ash

A summary of the total carbon and total sulfur contents of bottom ash samples are shown in Table C8. Compared to the fly ash, there is more variability in total carbon and total sulfur in the bottom ash samples. As it is doubtful that much carbon and pyrite survive in the combustion furnace, the occasional high carbon and sulfur values may be a function of pulverizer reject material from the pyrite storage tanks being introduced into the ash slurry line "upstream" from where we collect the bottom ash. Visual examination of the bottom ash detected pyrite. The presence of pyrite must be considered when evaluating the

composition of bottom ash in the context of the original feed coal. Not all of the material in the bottom ash is a residue of furnace conditions.

Summary x-ray fluorescence results for the bottom ash samples are shown in Tables C9 and C10. Like the coal ash and fly ash samples, the bottom ash from units 1 and 3 composed mainly of Al_2O_3 and SiO_2. CaO and Fe_2O_3 are more abundant in unit 1 bottom ash than bottom ash from unit 3 and 4. Conversely, K_2O, TiO_2 and Mn are more abundant in the unit 3 bottom ash

Table C8. Summary of total carbon and total sulfur content of bottom ash.

	Unit 1		Unit 3	
	Total Carbon wt.%	Total Sulfur wt.%	Total Carbon wt.%	Total Sulfur wt.%
Average	2.22	0.07	3.79	0.82
Maximum	6.9	0.15	16.8	3.02
Minimum	0.5	0.01	0.29	0.01

Table C9. Summary of x-ray fluorescence data for unit 1 bottom ash (n = 8). Element abundances are reported as weight percent on an ash basis, except for Mn, which is reported as parts per million. (Avg., average; Max., maximum; Min., minimum)

.

	Al_2O_3	SiO_2	P_2O_5	K_2O	CaO	Na_2O	TiO_2	Fe_2O_3	MgO	SO_3	Mn	SrO
Avg.	20.9	45.1	019	1.68	3.85	0.23	1.01	24.6	0.81	0.18	354	0.12
Max.	23.0	46.2	0.24	1.85	4.98	0.46	1.06	27.4	0.93	0.43	477	0.12
Min.	19.5	43.3	0.16	1.56	2.95	0	0.91	21.9	0.66	0.06	186	0.12

Table C10. Summary of x-ray fluorescence data for unit 3 bottom ash (n = 10). Element abundances are reported as weight percent on an ash basis, except for Mn, which is reported as parts per million. (Avg., average; Max., maximum; Min., minimum)

	Al_2O_3	SiO_2	P_2O_5	K_2O	CaO	Na_2O	TiO_2	Fe_2O_3	MgO	SO_3	Mn	SrO
Avg.	26.3	56.1	0.13	2.18	1.2	0.27	1.32	10.5	0.8	0.19	483	0.09
Max.	28.3	61.2	0.2	2.63	2.08	0.32	1.53	25.3	0.96	0.55	716	0.09
Min.	23.1	44.8	0.07	1.8	0.08	0.21	0.92	3.87	0.59	0	333	0.09

D. THE CHEMICAL COMPOSITION OF FEED COAL, FLY ASH AND BOTTOM ASH

by Ronald H. Affolter, U.S. Geological Survey, Denver, Colorado

This section summarizes the major-, minor-, and trace-element contents of samples taken as part of the study of the coal-burning power plant between July 1994 and October 1995. The material analyzed includes feed coal from units 1 (high-moderate sulfur unit) and 3 (low-sulfur unit), fly ash from unit 1, fine-side and coarse-side fly ash from unit 3, and bottom ash from units 1 and 3.

Ash yields and the content of major-, minor-, and trace-elements of samples from the power plant were determined by the U.S. Geological Survey (Denver, Colorado laboratories). Feed coal samples were ashed at 525 °C prior to analysis. Most elements were determined by inductively coupled plasma mass spectroscopy (ICP-MS) or inductively coupled plasma atomic emission spectroscopy (ICP-AES). Selenium concentrations were determined by instrumental neutron activation analysis (INAA) and mercury concentrations were determined by cold vapor atomic absorption spectrophotometry (CV-AAS). The contents of mercury and selenium on feed coal were determined on sample splits that were not ashed prior to analysis. Forms-of-sulfur were determined by a commercial laboratory (Geochemical Testing, Inc.) and are reported on a dry-basis.

Included in each of the summary tables (Tables D1 to D16) are the number of samples, range of values for each of the measured components, arithmetic means, and standard deviation. Tables D17 to D20 present a comparison of mean values between feed coal, fly ash, and bottom ash for selected elements. The element contents are reported to two significant figures and the forms-of-sulfur data are reported to two decimal places. Element contents for the feed coal samples are calculated to a whole-coal and ash (as-determined) basis. Data for the fly ash and bottom ash samples are reported on an as-determined basis. Figures D1 to D6 show the variation of selected elements in the feed coal, fly ash, and bottom ash over a fifteen month period.

Some samples have element concentrations that are below the limits of analytical detection. This results in a censored distribution. To compute unbiased estimates of censored data for the summary statistics we reduced all values that are less than the analytical detection limit to be equal to 50% of that limit.

Two bottom ash samples contain high contents of Pb (> 1000 ppm) , and Mn (>1 wt.%). These are probably the result of pulverizer discards that bypass the furnace and are added to the bottom ash samples. These discards probably include pyrite, siderite and galena, as well as small bolts, gears, nails, etc.

This summary of the data is considered preliminary. An analysis and interpretation of the data will be prepared upon analysis of the remaining sample sets.

Table D1. Number of samples, range, arithmetic mean, and standard deviation of ash and 60 elements in the feed coal from unit 1 (whole-coal basis). (All analyses are in weight percent or parts per million. L, less than value shown. Leaders (--) indicate statistics could not be calculated owing to an insufficient number of analyses above the lower detection limit.)

	Number of y Sam les	Range		Arithmetic mean	Standard deviation
	y	Minimum	Maximum		
		Wei ht Percent			
Ash	12	8.4	12	10	1
Si	12	1.3	2.3	2	0.32
Al	12	0.89	1.3	1.1	0.13
Ca	12	0.16	0.35	0.26	0.053
Mg	12	0.035	0.054	0.046	0.0059
Na	12	0.018	0.068	0.045	0.015
K	12	0.084	0.19	0.15	0.028
Fe	12	0.88	2	1.5	0.33
Ti	12	0.05	0.067	0.059	0.0049
		Parts per million			
Ag	10	0.16L	0.36	0.16	0.1
As	10	6.6	26	12	6.1
Au	–	–	–	–	–
B	12	56	130	86	21
Ba	12	39	78	55	11
Be	12	0.76	2.5	1.5	0.55
Bi	–	–	–	–	–
Cd	10	0.068L	1.1	0.36	0.36
Ce	2	13	21	17	5.6
Co	12	2.4	8.9	4.6	1.8
Cr	12	12	21	15	2.6
Cs	10	0.5	1.2	0.84	0.2
Cu	12	6	21	10	4.6
Dy	2	1.4	1.7	1.5	0.18
Er	2	0.7	0.77	0.74	0.049
Eu	2	0.3	0.44	0.37	0.099
Ga	10	3.4	4.9	4.2	0.62
Gd	2	1	2.2	1.6	0.85
Ge	10	2.5	15	7.9	4
Hf	2	0.6	0.66	0.63	0.042
Hg	12	0.02L	0.18	0.068	0.057
Ho	2	0.2	0.33	0.27	0.092
La	2	7	11	9	2.8
Li	12	7.8	18	12	2.8
Mn	12	12	34	25	6.3
Mo	10	0.73	5.7	3.2	1.8
Nb	10	1.7	2.7	2.2	0.33
Nd	2	6	8.8	7.4	2
Ni	12	7.2	42	18	10
P	12	53	230	120	57
Pb	10	4.1	33	11	8.6
Pr	2	1.6	2.4	2	0.58
Rb	10	6	16	9.9	3.4

Table D1. (Continued)

	Number of Samples	Range		Arithmetic mean	Standard deviation
		Minimum	Maximum		
Sb	10	0.22	1.9	0.87	0.55
Sc	12	2.4	4.3	3.3	0.51
Se	12	1.7	3.7	2.5	0.62
Sm	2	1.5	2.1	1.8	0.42
Sn	10	0.84L	3.3	1.3	1.1
Sr	12	34	120	74	28
Ta	2	0.2	0.22	0.21	0.014
Tb	2	0.2	0.22	0.21	0.014
Te	–	–	–	–	–
Th	12	1.6	2.4	2	0.24
Tl	10	0.17	1.4	0.8	0.38
Tm	2	0.1	0.11	0.11	0.0071
U	10	0.48	5	1.6	1.3
V	12	18	63	30	12
W	2	0.6	1.1	0.85	0.35
Y	12	3.6	6.7	4.9	0.82
Yb	2	0.6	0.77	0.69	0.12
Zn	12	6.7	85	34	29
Zr	12	14	39	24	7.6

Table D2. Number of samples, range, arithmetic mean, and standard deviation of total sulfur and forms-of-sulfur in the feed coal from unit 1. (All analyses are in weight percent and are reported on a dry basis.)

	Number of Samples	Range		Arithmetic mean	Standard deviation
		Minimum	Maximum		
Sulfur	4	2.47	3.03	2.81	0.24
Sulfate	4	0.08	0.49	0.30	0.21
Pyritic	4	0.86	1.27	1.07	0.19
Organic	4	1.29	1.54	1.44	0.11

Table D3. Number of samples, range, arithmetic mean, and standard deviation of ash and 60 elements in the feed coal from unit 1 (as-determined basis). (All analyses are in weight percent or parts per million. Hg and Se were determined on whole coal, all other elements on ashed coal. L, less than value shown. Leaders (--) indicate statistics could not be calculated owing to an insufficient number of analyses above the lower detection limit.)

	Number of Samples	Range		Arithmetic mean	Standard deviation
		Minimum	Maximum		
Weight Percent					
Ash	12	8.4	11.8	10	1
SiO_2	12	33	46	42	4.1
Al_2O_3	12	18	22	21	1.2
CaO	12	2.1	4.8	3.6	0.72
MgO	12	0.64	0.86	0.76	0.068
Na_2O	12	0.22	1.1	0.61	0.24
K_2O	12	1.2	2.2	1.8	0.26
Fe_2O_3	12	15	27	21	3.7
TiO_2	12	0.86	1.1	0.98	0.068
P_2O_5	12	0.12	0.52	0.26	0.12
Parts per million					
Ag	10	2L	3.5	2	0.96
As	10	62	240	120	58
Au	–	–	–	–	–
B	12	520	1500	870	260
Ba	12	420	860	560	150
Be	12	7	23	15	5.4
Bi	–	–	–	–	–
Cd	10	0.8L	11	3.6	3.6
Ce	2	130	190	160	42
Co	12	29	81	45	17
Cr	12	130	210	150	21
Cs	10	6	11	8.4	1.5
Cu	12	56	190	100	41
Dy	2	14	15	15	0.71
Er	2	7	7	7	0
Eu	2	3	4	3.5	0.71
Ga	10	35	48	42	4
Gd	2	10	20	15	7.1
Ge	10	30	140	80	38
Hf	2	6	6	6	0
Hg	12	0.02L	0.18	0.068	0.057
Ho	2	2	3	2.5	0.71
La	2	70	–	85	21
Li	12	72	160	120	30
Mn	12	140	330	250	57
Mo	10	6.8	57	32	18
Nb	10	20	30	22	4.2
Nd	2	60	80	70	14
Ni	12	73	380	170	97
Pb	10	48	300	110	77
Pr	2	16	22	19	4.2
Rb	10	71	160	99	31

Table D3. (Continued).

	Number of y Sam les	Range		Arithmetic mean	Standard deviation
		Minimum	Maximum		
Sb	10	2	17	8.7	5.2
Sc	12	28	39	32	3.3
Se	12	1.7	3.7	2.5	0.62
Sm	2	15	19	17	2.8
Sn	10	10L	30	13	10
Sr	12	390	1300	730	290
Ta	2	2	2	2	0
Tb	2	2	2	2	0
Te	–	–	–	–	--
Th	12	17	22	20	1.5
Tl	10	2	13	8	3.7
Tm	2	1	1	1	0
U	10	5.7	50	16	13
V	12	190	630	300	120
W	2	6	10	8	2.8
Y	12	39	61	48	7.5
Yb	2	6	7	6.5	0.71
Zn	12	80	770	340	280
Zr	12	170	360	240	64

Table D4. Number of samples, range, arithmetic mean, and standard deviation of ash and 60 elements in the feed coal from unit 3 (whole-coal basis). (All analyses are in weight percent or parts per million. L, less than value shown. Leaders (--) indicate statistics could not be calculated owing to an insufficient number of analyses above the lower detection limit.)

	Number of Samples	Range		Arithmetic mean	Standard deviation
		Minimum	Maximum		
		Weight Percent			
Ash	14	7.7	10	9.1	0.69
Si	14	1.7	3.1	2.3	0.37
Al	14	1.2	1.8	1.4	0.15
Ca	14	0.049	0.11	0.083	0.019
Mg	14	0.036	0.061	0.047	0.0074
Na	14	0.016	0.047	0.028	0.0069
K	14	0.13	0.19	0.16	0.02
Fe	14	0.18	0.38	0.28	0.057
Ti	14	0.065	0.1	0.086	0.01
		Parts per million			
Ag	12	0.15L	0.34	0.15	0.091
As	12	2.5	4.7	3.3	0.73
Au	12	0.15	0.8	0.45	0.14
B	14	11	33	23	7.3
Ba	14	62	140	90	22
Be	14	1.8	3	2.4	0.35
Bi	12	0.18L	0.26	0.18	0.048
Cd	12	0.068L	0.11	0.068	0.029
Ce	3	15	27	21	5.9
Co	14	7.2	14	11	2.2
Cr	14	13	24	19	3.1
Cs	12	0.68	1.1	0.83	0.13
Cu	14	16	25	20	2.6
Dy	3	1.5	2.5	1.9	0.53
Er	3	0.84	1.4	1.1	0.29
Eu	3	0.34	0.44	0.4	0.059
Ga	12	5	7.8	6.3	0.88
Gd	3	1.7	2.6	2	0.52
Ge	12	1.5	3	2.1	0.47
Hf	3	0.59	0.88	0.78	0.17
Hg	14	0.02L	0.13	0.034	0.04
Ho	3	0.25	0.44	0.35	0.092
La	3	8.4	14	11	2.8
Li	14	14	24	19	3.2
Mn	14	6.4	20	14	3.9
Mo	12	1.2	2.1	1.6	0.28
Nb	12	2.3	3.5	2.9	0.39
Nd	3	5.9	11	8.4	2.7
Ni	14	12	21	17	2.5
P	14	38	120	71	23
Pb	12	9.2	12	11	0.84
Pr	3	1.8	3.1	2.4	0.69
Rb	12	7.2	18	10	3

Table D4. (Continued).

	Number of Samples	Range		Arithmetic mean	Standard deviation
		Minimum	Maximum		
Sb	12	0.59	0.81	0.71	0.07
Sc	14	2.8	4	3.5	0.39
Se	14	3.2	8.7	5.6	1.8
Sm	3	1.4	2.5	1.9	0.56
Sn	12	0.78L	4.1	1.4	1.3
Sr	14	51	97	72	14
Ta	3	0.17	0.26	0.23	0.055
Tb	3	0.25	0.35	0.29	0.052
Te	–	–	–	–	–
Th	14	2	3.7	2.9	0.49
Tl	12	0.27	0.45	0.38	0.047
Tm	3	0.084	0.18	0.14	0.053
U	12	1.1	2.3	1.4	0.32
V	14	22	40	32	5.4
W	3	0.67	0.87	0.78	0.1
Y	14	6.9	11	8.7	0.91
Yb	3	0.76	1.3	0.98	0.29
Zn	14	8.7	16	12	2.6
Zr	14	17	35	25	6.5

Table D5. Number of samples, range, arithmetic mean, and standard deviation of total sulfur and forms-of-sulfur in the feed coal from unit 3. (All analyses are in weight percent and are reported on a dry basis.)

	Number of Samples	Range		Arithmetic mean	Standard deviation
		Minimum	Maximum		
Sulfur	5	0.64	0.83	0.72	0.07
Sulfate	5	0.01	0.03	0.02	0.01
Pyritic	5	0.05	0.13	0.08	0.03
Organic	5	0.54	0.69	0.62	0.06

Table D6. Number of samples, range, arithmetic mean, and standard deviation of ash and 60 elements in the feed coal from unit 3 (as-determined basis). (All analyses are in weight percent or parts per million. Hg and Se were determined on whole coal, all other elements on ashed coal. L, less than value shown. Leaders (--) indicate statistics could not be calculated owing to an insufficient number of analyses above the lower detection limit.)

	Number of Samples	Range		Arithmetic mean	Standard deviation
		Minimum	Maximum		
Weight Percent					
Ash	14	7.7	10.3	9.1	0.69
SiO_2	14	38	64	53	6.7
Al_2O_3	14	27	33	30	1.6
CaO	14	0.76	1.7	1.3	0.3
MgO	14	0.68	1.2	0.85	0.16
Na_2O	14	0.24	0.61	0.41	0.092
K_2O	14	1.8	2.7	2.1	0.27
Fe_2O_3	14	2.9	6.4	4.4	1
TiO_2	14	1.3	1.8	1.6	0.14
P_2O_5	14	0.09	0.37	0.18	0.069
Parts per million					
Ag	12	2L	3.5	2	0.98
As	12	30	57	37	8.8
Au	–	–	–	–	–
B	14	110	380	250	83
Ba	14	700	1500	990	260
Be	14	21	33	27	3.7
Bi	12	2L	3	2	0.58
Cd	12	0.8L	1.1	0.8	0.32
Ce	3	180	310	240	66
Co	14	86	160	120	23
Cr	14	160	250	210	26
Cs	12	7.5	12	9.2	1.4
Cu	14	170	260	220	27
Dy	3	18	29	22	5.9
Er	3	10	16	12	3.2
Eu	3	4	5	4.7	0.58
Ga	12	58	80	70	8
Gd	3	20	30	23	5.8
Ge	12	17	31	24	5.1
Hf	3	7	10	9	1.7
Hg	14	0.02L	0.13	0.034	0.04
Ho	3	3	5	4	1
La	3	100	160	130	31
Li	14	140	260	210	35
Mn	14	73	240	150	45
Mo	12	14	22	18	2.7
Nb	12	30	40	32	4
Nd	3	70	130	97	31
Ni	14	140	230	190	26
Pb	12	97	130	120	11
Pr	3	21	36	28	7.6
Rb	12	84	180	120	31

Table D6. (Continued).

	Number of Samples	Range		Arithmetic mean	Standard deviation
		Minimum	Maximum		
Sb	12	6.4	9.2	7.9	0.98
Sc	14	34	46	39	4
Se	14	3.2	8.7	5.6	1.8
Sm	3	17	29	22	6.2
Sn	12	10L	42	16	14
Sr	14	540	1100	790	190
Ta	3	2	3	2.7	0.58
Tb	3	3	4	3.3	0.58
Te	–	–	–	–	–
Th	14	24	42	32	5.6
Tl	12	3	5.8	4.2	0.67
Tm	3	1	2	1.7	0.58
U	12	12	26	16	3.9
V	14	260	420	350	58
W	3	8	10	9	1
Y	14	82	130	95	12
Yb	3	9	15	11	3.2
Zn	14	98	170	130	28
Zr	14	180	400	270	65

Table D7. Number of samples, range, arithmetic mean, and standard deviation of ash and 60 elements in the fly ash from unit 1 (as-determined basis). (All analyses are in weight percent or parts per million. L, less than value shown. Leaders (--) indicate statistics could not be calculated owing to an insufficient number of analyses above the lower detection limit.)

	Number of Samples	Range		Arithmetic mean	Standard deviation
		Minimum	Maximum		
		Percent			
Ash	4	99.3	99.7	99	0.2
SiO_2	12	43	51	47	2.2
Al_2O_3	12	21	23	22	0.78
CaO	12	2.8	4.5	3.6	0.54
MgO	12	0.73	0.92	0.83	0.063
Na_2O	12	0.32	1.1	0.66	0.21
K_2O	12	1.3	2.2	1.9	0.27
Fe_2O_3	12	13	25	19	3.8
TiO_2	12	0.91	1.1	1	0.069
P_2O_5	12	0.13	0.38	0.25	0.086
		Parts per million			
Ag	10	2L	3.9	2	1.1
As	10	100	330	170	67
Au	–	–	–	–	–
B	12	300	890	610	200
Ba	12	450	930	600	160
Be	12	10	32	19	6.7
Bi	–	–	–	–	–
Cd	10	0.9	9.5	5.5	3.1
Ce	3	130	180	150	25
Co	12	32	94	59	20
Cr	12	150	190	170	12
Cs	10	8	13	11	1.6
Cu	12	71	180	130	42
Dy	3	10	19	14	4.5
Er	3	6	10	8	2
Eu	3	3	5	4	1
Ga	10	35	62	47	7.8
Gd	3	10	20	17	5.8
Ge	10	38	200	130	55
Hf	3	7	7	7	0
Hg	12	0.02L	0.11	0.039	0.03
Ho	3	2	4	3	1
La	3	60	90	77	15
Li	12	83	170	130	24
Mn	12	160	400	270	63
Mo	10	19	87	50	22
Nb	10	20	30	27	4.8
Nd	3	50	80	67	15
Ni	12	88	390	220	110
Pb	10	51	230	150	67
Pr	3	14	22	18	4
Rb	10	99	180	150	28

Table D7. (Continued)

	Number of Samples	Range		Arithmetic mean	Standard deviation
		Minimum	Maximum		
Sb	10	4.4	23	13	5.9
Sc	12	29	47	38	5.3
Se	12	2.7	19.1	8.9	4.4
Sm	3	11	20	16	4.6
Sn	10	10L	10	10	2.1
Sr	12	270	1300	780	300
Ta	3	2	2	2	0
Tb	3	1	3	2	1
Te	–	–	–	–	–
Th	12	17	28	22	3.1
Tl	10	3	14	10	3.7
Tm	3	0.9	2	1.3	0.61
U	10	7	33	19	8.1
V	12	220	390	320	58
W	3	4	7	5.3	1.5
Y	12	55	99	72	15
Yb	3	5	9	7	2
Zn	12	81	1200	520	360
Zr	12	200	350	240	53

Table D8. Number of samples, range, arithmetic mean, and standard deviation of total sulfur and forms-of-sulfur in the fly ash from unit 1. (All analyses are in weight percent and are reported on a dry basis. Leaders (---) indicate statistics could not be calculated owing to an insufficient number of analyses above the lower detection limit.)

	Number of Samp les	Range		Arithmetic mean	Standard deviation
		Minimum	Maximum		
Sulfur	4	0.29	0.82	0.47	0.24
Sulfate	4	0.29	0.44	0.35	0.07
Pyritic	2	0.01	0.49	0.25	0.34
Organic	---	---	---	---	---

Table D9. Number of samples, range, arithmetic mean, and standard deviation of ash and 59 elements in the fine-side fly ash from unit 3 (as-determined basis). (All analyses are in percent or parts per million. L, less than value shown. Leaders (--) indicate statistics could not be calculated owing to an insufficient number of analyses above the lower detection limit.)

	Number of Samples	Range		Arithmetic mean	Standard deviation
		Minimum	Maximum		
Weight Percent					
Ash	5	95	99.3	98	1.7
SiO_2	11	46	59	55	3.8
Al_2O_3	11	28	32	30	1.3
CaO	11	1.1	1.6	1.4	0.16
MgO	11	0.99	1.3	1.1	0.11
Na_2O	11	0.33	0.51	0.41	0.06
K_2O	11	2.3	3.2	2.6	0.3
Fe_2O_3	11	4.5	5.6	4.9	0.4
TiO_2	11	1.5	1.9	1.6	0.13
P_2O_5	11	0.16	0.37	0.28	0.063
Parts per million					
Ag	9	2L	3	2	1.1
As	9	52	110	91	19
Au	–	–	–	–	–
B	11	93	220	140	40
Ba	11	990	1400	1200	130
Be	11	20	34	27	4.3
Bi	9	2	5.9	3.8	1.1
Cd	9	0.8L	2	1	0.41
Ce	4	200	230	210	13
Co	11	94	200	150	37
Cr	11	180	250	230	22
Cs	9	12	17	14	1.8
Cu	11	180	340	270	45
Dy	4	18	22	19	1.9
Er	4	10	12	11	1
Eu	4	4	5	4.3	0.5
Ga	9	71	140	110	24
Gd	4	20	20	20	0
Ge	9	26	54	42	11
Hf	4	8	10	9.3	0.96
Hg	11	0.02L	0.02	0.02	0.0047
Ho	4	3	4	3.3	0.5
La	4	100	120	110	8.2
Li	11	170	250	210	26
Mn	11	190	300	230	36
Mo	9	17	36	30	7
Nb	9	40	46	43	2.5
Nd	4	80	100	88	9.6
Ni	11	150	290	220	42
Pb	9	130	240	170	33
Pr	4	23	27	25	1.7
Rb	9	160	240	200	25

Table D9. (Continued)

	Number of Samples	Range		Arithmetic mean	Standard deviation
		Minimum	Maximum		
Sb	9	9.4	21	15	3.4
Sc	11	40	49	44	2.9
Se	11	0.1L	5.1	1.1	1.7
Sm	4	18	23	20	2.2
Sn	9	10	30	22	6.7
Sr	11	750	1100	880	100
Ta	4	3	3	3	0
Tb	4	3	3	3	0
Te	–	–	–	–	–
Th	11	27	36	31	2.9
Tl	9	4.5	13	6.7	2.5
Tm	4	1	2	1.3	0.5
U	9	16	30	21	4.1
V	11	280	490	400	60
W	4	8	10	9.5	1
Y	11	97	120	110	8.7
Yb	4	9	10	9.3	0.5
Zn	11	130	310	240	55
Zr	11	170	310	250	38

Table D10. Number of samples, range, arithmetic mean, and standard deviation of total sulfur and forms-of-sulfur in the fine-side fly ash from unit 3. (All analyses are in weight percent and are reported on a dry basis. Leaders (---) indicate statistics could not be calculated owing to an insufficient number of analyses above the lower detection limit.)

	Number of Samples	Range		Arithmetic mean	Standard deviation
		Minimum	Maximum		
Sulfur	4	0.19	1.17	0.60	0.41
Sulfate	4	0.13	0.95	0.52	0.34
Pyritic	3	0.05	0.15	0.09	0.06
Organic	---	---	---	---	---

Table D11. Number of samples, range, arithmetic mean, and standard deviation of ash and 59 elements in the coarse-side fly ash from unit 3 (as-determined basis). (All analyses are in percent or parts per million. L, less than value shown. Leaders (--) indicate statistics could not be calculated owing to an insufficient number of analyses above the lower detection limit.)

	Number of Samples	Range		Arithmetic mean	Standard deviation
		Minimum	Maximum		
		Weight Percent			
Ash	4	97	100	98	1.4
SiO_2	12	53	64	58	3.3
Al_2O_3	12	27	32	30	1.4
CaO	12	0.67	1.6	1.2	0.29
MgO	12	0.73	1.2	0.97	0.16
Na_2O	12	0.23	0.44	0.37	0.067
K_2O	12	1.8	3.3	2.5	0.46
Fe_2O_3	12	3.2	5.4	4.2	0.71
TiO_2	12	1.4	1.9	1.5	0.15
P_2O_5	12	0.08	0.32	0.18	0.069
		Parts per million			
Ag	11	2L	3	2	0.82
As	11	30	100	54	20
Au	–	–	–	–	–
B	12	37	150	96	28
Ba	12	710	1300	1000	180
Be	12	16	26	22	4.1
Bi	11	2L	2	2	0.5
Cd	11	0.8L	1	0.8	0.22
Ce	4	180	270	210	40
Co	12	55	140	97	24
Cr	12	140	240	190	26
Cs	11	9.9	16	13	2.1
Cu	12	89	230	180	36
Dy	4	17	26	20	4.3
Er	4	9	14	11	2.2
Eu	4	4	5	4.3	0.5
Ga	11	49	86	67	12
Gd	4	20	20	20	0
Ge	11	16	31	24	5.3
Hf	4	9	10	9.5	0.58
Hg	12	0.02L	0.02	0.02	0.0045
Ho	4	3	5	3.8	0.96
La	4	90	150	110	26
Li	12	100	220	190	33
Mn	12	100	320	210	69
Mo	11	12	24	17	3.8
Nb	11	40	46	42	2.4
Nd	4	70	120	88	22
Ni	12	130	220	160	32
Pb	11	70	120	100	16
Pr	4	20	32	25	5.3
Rb	11	140	240	190	33

Table D11. (Continued).

	Number of Samples	Range		Arithmetic mean	Standard deviation
		Minimum	Maximum		
Sb	11	6.3	12	8.9	1.7
Sc	12	34	45	41	2.9
Se	12	0.1L	4	0.82	1.4
Sm	4	16	26	20	4.5
Sn	11	10L	20	10	4.2
Sr	12	560	1200	860	200
Ta	4	2	3	2.5	0.58
Tb	4	2	4	3	0.82
Te	–	–	–	–	–
Th	12	17	39	30	5.5
Tl	11	3	6.1	4	0.99
Tm	4	1	2	1.5	0.58
U	11	11	24	15	3.4
V	12	220	350	290	41
W	4	6	8	7.3	0.96
Y	12	64	160	100	22
Yb	4	8	13	10	2.2
Zn	12	72	290	140	55
Zr	12	200	350	250	40

Table D12. Number of samples, range, arithmetic mean, and standard deviation of total sulfur and forms-of-sulfur in the coarse-side fly ash from unit 3. (All analyses are in weight percent and are reported on a dry basis. Leaders (---) indicate statistics could not be calculated owing to an insufficient number of analyses above the lower detection limit.)

	Number of Samples	Range		Arithmetic mean	Standard deviation
		Minimum	Maximum		
Sulfur	4	0.07	0.11	0.10	0.02
Sulfate	4	0.06	0.11	0.09	0.02
Pyritic	---	---	---	---	---
Organic	---	---	---	---	---

Table D13. Number of samples, range, arithmetic mean, and standard deviation of ash and 59 elements in the bottom ash from unit 1 (as-determined basis). (All analyses are in weight percent or parts per million. L, less than value shown. Leaders (--) indicate statistics could not be calculated owing to an insufficient number of analyses above the lower detection limit.)

	Number of Samples	Range		Arithmetic mean	Standard deviation
		Minimum	Maximum		
		Weight Percent			
Ash	5	74	100	93	11
SiO_2	11	40	48	44	2.7
Al_2O_3	11	16	22	20	1.7
CaO	11	3	4.5	3.8	0.63
MgO	11	0.53	0.78	0.71	0.077
Na_2O	11	0.28	0.97	0.58	0.21
K_2O	11	1.2	1.8	1.5	0.21
Fe_2O_3	11	16	35	24	5.1
TiO_2	11	0.63	1	0.85	0.11
P_2O_5	11	0.09	0.21	0.16	0.041
		Parts per million			
Ag	–	–	–	–	–
As	10	5L	20	11	5
Au	–	–	–	–	–
B	11	150	410	260	89
Ba	11	360	770	540	140
Be	11	7	25	14	5
Bi	–	–	–	–	–
Cd	10	0.8L	1	0.8	0.25
Ce	3	120	180	150	31
Co	11	30	77	49	16
Cr	11	120	170	150	12
Cs	10	0.4L	9	7.5	2.6
Cu	11	55	130	88	26
Dy	3	9	17	13	4
Er	3	5	9	7	2
Eu	3	2	4	3	1
Ga	10	10L	28	21	6.6
Gd	3	10	20	13	5.8
Ge	10	2L	56	36	18
Hf	3	6	7	6.7	0.58
Hg	11	0.02L	0.04	0.02	0.01
Ho	3	2	3	2.3	0.58
La	3	60	90	73	15
Li	11	70	150	120	24
Mn	11	200	430	330	63
Mo	10	2L	15	9.5	4.4
Nb	10	8L	25	19	5.5
Nd	3	50	80	63	15
Ni	11	100	340	210	92
Pb	10	8L	70	46	21
Pr	3	14	21	17	3.5
Rb	10	3L	150	110	41

Table D13. (Continued).

	Number of Samples	Range		Arithmetic mean	Standard deviation
		Minimum	Maximum		
Sb	10	2L	5.5	3.5	1.6
Sc	11	25	39	32	4.6
Se	11	0.1L	2.1	0.59	0.76
Sm	3	10	18	14	4
Sn	10	10L	20	10	5.7
Sr	11	360	1100	750	260
Ta	3	1	2	1.7	0.58
Tb	3	2	3	2.3	0.58
Te	–	–	–	–	–
Th	11	17	25	21	2.2
Tl	–	–	–	–	–
Tm	3	0.8	1	0.93	0.12
U	10	1	24	14	7.3
V	11	190	320	250	45
W	3	30	40	37	5.8
Y	11	48	92	65	16
Yb	3	5	8	6.3	1.5
Zn	11	41	530	210	150
Zr	11	190	360	230	48

Table D14. Number of samples, range, arithmetic mean, and standard deviation of total sulfur and forms-of-sulfur in the bottom ash from unit 1. (All analyses are in weight percent and are reported on a dry basis. Leaders (---) indicate statistics could not be calculated owing to an insufficient number of analyses above the lower detection limit.)

	Number of Samples	Range		Arithmetic mean	Standard deviation
		Minimum	Maximum		
Sulfur	4	0.02	0.19	0.08	0.08
Sulfate	4	0.01	0.03	0.02	0.01
Pyritic	3	0.01	0.18	0.08	0.09
Organic	---	---	---	---	---

Table D15. Number of samples, range, arithmetic mean, and standard deviation of ash and 59 elements in the bottom ash from unit 3 (as-determined basis). (All analyses are in weight percent or parts per million. L, less than value shown. Leaders (--) indicate statistics could not be calculated owing to an insufficient number of analyses above the lower detection limit.)

	Number of Samples	Range		Arithmetic mean	Standard deviation
		Minimum	Maximum		
		Weight Percent			
Ash	7	83	99.7	97	6.2
SiO_2	13	48	64	57	5.2
Al_2O_3	13	20	29	26	2.9
CaO	13	0.6	1.7	1.1	0.37
MgO	13	0.62	1	0.81	0.14
Na_2O	13	0.21	0.63	0.32	0.1
K_2O	13	1.7	2.9	2.1	0.37
Fe_2O_3	13	4.2	14	8.2	3.3
TiO_2	13	1	1.8	1.4	0.22
P_2O_5	13	0.04	0.2	0.11	0.045
		Parts per million			
Ag	11	2L	3.5	2	0.8
As	11	4L	150	54	62
Au	–	–	–	–	–
B	13	25	100	49	20
Ba	13	560	1200	790	170
Be	13	11	21	16	2.5
Bi	–	–	–	–	–
Cd	–	–	–	–	–
Ce	4	170	260	210	39
Co	13	47	78	61	9.2
Cr	13	160	360	200	64
Cs	11	8.6	14	11	1.7
Cu	13	69	4200	770	1200
Dy	4	14	21	17	2.9
Er	4	7	12	9.5	2.1
Eu	4	3	4	3.8	0.5
Ga	11	9.1	32	22	6.7
Gd	4	10	20	18	5
Ge	11	2L	8.3	5.2	2.2
Hf	4	8	10	9.5	1
Hg	13	0.02L	0.75	0.24	0.3
Ho	4	2	4	3	0.82
La	4	90	140	110	22
Li	13	130	190	170	19
Mn	13	140	1000	480	320
Mo	11	3	15	5.8	3.6
Nb	11	30	41	35	5.1
Nd	4	60	100	80	16
Ni	13	100	180	140	25
Pb	11	10	3000	380	920
Pr	4	18	29	23	4.6
Rb	11	120	220	160	27

Table D15. (Continued).

	Number of Samples	Range		Arithmetic mean	Standard deviation
		Minimum	Maximum		
Sb	11	2L	75	10	23
Sc	13	31	41	35	3
Se	13	0.1L	3.8	1.7	1.5
Sm	4	14	23	18	3.8
Sn	11	10L	40	12	11
Sr	13	450	800	620	110
Ta	4	2	3	2.8	0.5
Tb	4	2	3	2.5	0.58
Te	–	–	–	–	–
Th	13	24	35	29	2.9
Tl	11	0.7L	14	3.1	3.9
Tm	4	1	2	1.3	0.5
U	11	7.4	17	10	2.7
V	13	190	230	200	13
W	4	50	110	65	30
Y	13	71	120	93	14
Yb	4	7	10	8.3	1.3
Zn	13	4	120	39	28
Zr	13	230	370	270	39

Table D16. Number of samples, range, arithmetic mean, and standard deviation of total sulfur and forms-of-sulfur in the bottom ash from unit 3. (All analyses are in weight percent and are reported on a dry basis. Leaders (---) indicate statistics could not be calculated owing to an insufficient number of analyses above the lower detection limit.)

	Number of Samples	Range		Arithmetic mean	Standard deviation
		Minimum	Maximum		
Sulfur	4	0.01	2.80	0.95	1.31
Sulfate	4	0.01	0.09	0.04	0.04
Pyritic	2	0.92	2.71	1.82	1.27
Organic	—	—	—	—	—

Table D17. Comparison of concentrations of selected elements in unit 1 feed coal, fly ash, and bottom ash. (All elements are in parts per million and are presented on the whole coal and as-determined ash basis for the feed coal, and on an as-determined basis for the fly ash and bottom ash.

Element	Feed Coal Mean (whole coal)	Feed Coal Mean (ash basis)	Fly Ash Mean	Bottom Ash Mean
As	12	120	170	11
Be	1.5	15	19	14
Cd	0.36	3.6	5.5	0.8
Co	4.6	45	59	49
Cr	15	150	170	150
Hg	0.068	0.068	0.39	0.02
Mn	25	250	270	330
Ni	18	170	220	210
Pb	11	110	150	46
Sb	0.87	8.7	13	3.5
Se	2.5	2.5	8.9	0.59
Th	2	20	22	21
U	1.6	16	19	14

Table D18. Comparison of total sulfur content and forms-of-sulfur in unit 1 feed coal, fly ash, and bottom ash. (All values are in weight percent on a dry basis. Leaders (---) indicate statistics could not be calculated owing to an insufficient number of analyses above the lower detection limit.)

	Feed Coal Mean	Fly Ash Mean	Bottom Ash Mean
Sulfur	2.81	0.47	0.08
Sulfate	0.30	0.35	0.02
Pyritic	1.07	0.25	0.08
Organic	1.44	---	---

Table D19. Comparison of the concentrations of selected elements in unit 3 feed coal, fly ash, and bottom ash. (All elements are in parts per million and are presented on the whole coal and as-determined basis for the feed coal, and on an as-determined basis for the fly ash and bottom ash. Leaders (--) indicate statistics could not be calculated owing to an insufficient number of analyses above the lower detection limit.)

Element	Feed Coal Mean (whole coal)	Feed Coal Mean (ash basis)	Fly Ash fine side Mean	Fly Ash coarse side Mean	Bottom Ash Mean
As	3.3	37	91	54	54
Be	2.4	27	27	22	16
Cd	0.068	0.8	1	0.8	–
Co	11	120	150	97	61
Cr	19	210	230	190	200
Hg	0.034	0.034	0.02	0.02	0.24
Mn	14	150	230	210	480
Ni	17	190	220	160	140
Pb	11	120	170	100	380
Sb	0.71	7.9	15	8.9	10
Se	5.6	5.6	1.1	0.82	1.7
Th	2.9	32	31	30	29
U	1.4	16	21	15	10

Table D20. Comparison of total sulfur content and forms-of-sulfur in unit 3 feed coal, fly ash (fine and coarse sides), and bottom ash. (All values are in percent on a dry basis. Leaders (---) indicate statistics could not be calculated owing to an insufficient number of analyses above the lower detection limit.)

	Feed Coal Mean	Fly Ash fine side Mean	Fly Ash coarse side Mean	Bottom Ash Mean
Sulfur	0.72	0.60	0.10	0.95
Sulfate	0.02	0.52	0.09	0.04
Pyritic	0.08	0.09	---	1.82
Organic	0.62	---	---	---

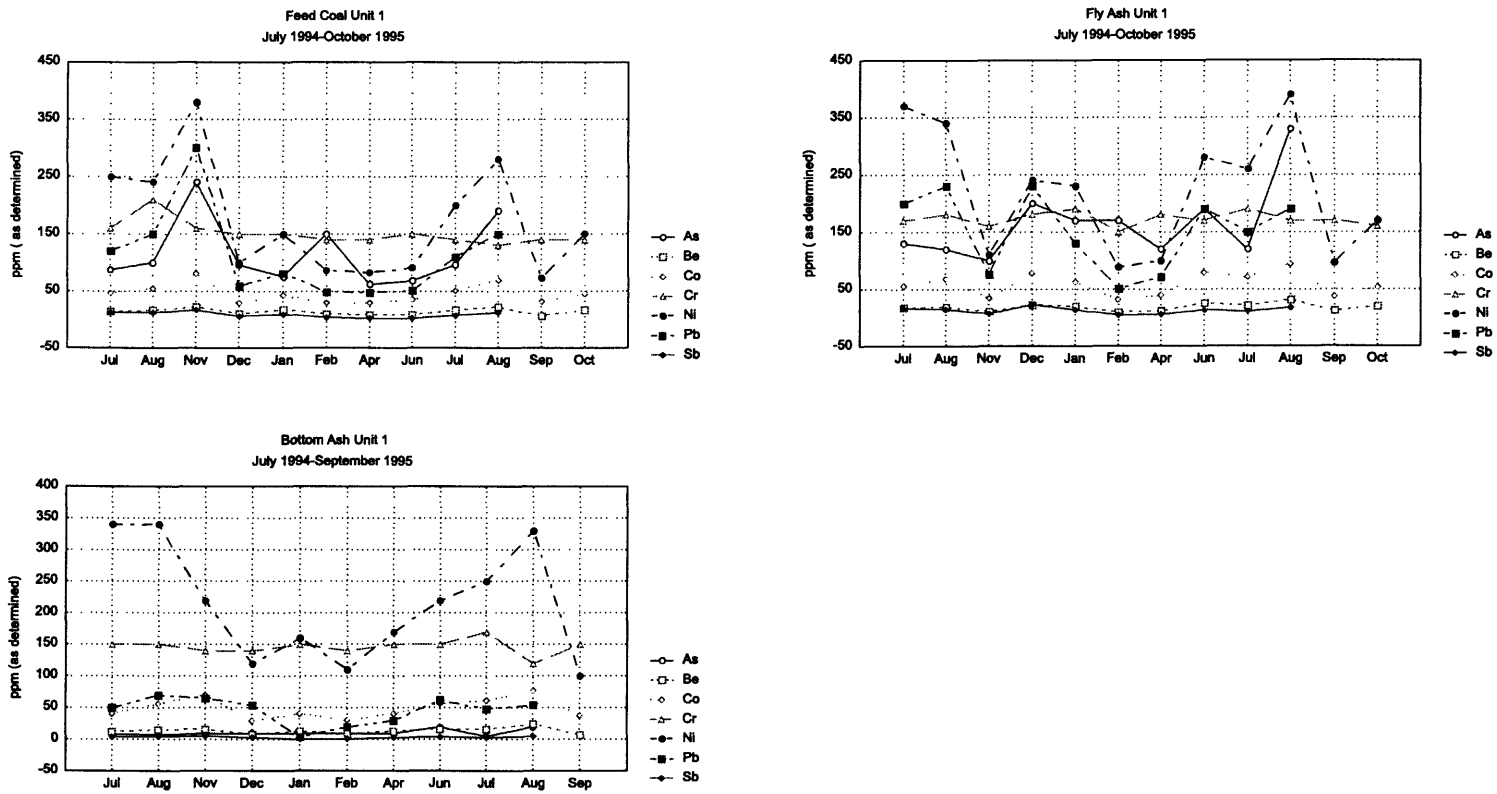

Figure D1. Variation in As, Be, Co, Cr, Ni, Pb, and Sb contents of feed coal, fly ash, and bottom ash from unit 1 (high-sulfur unit) for samples collected from July 1994 to October 1995.

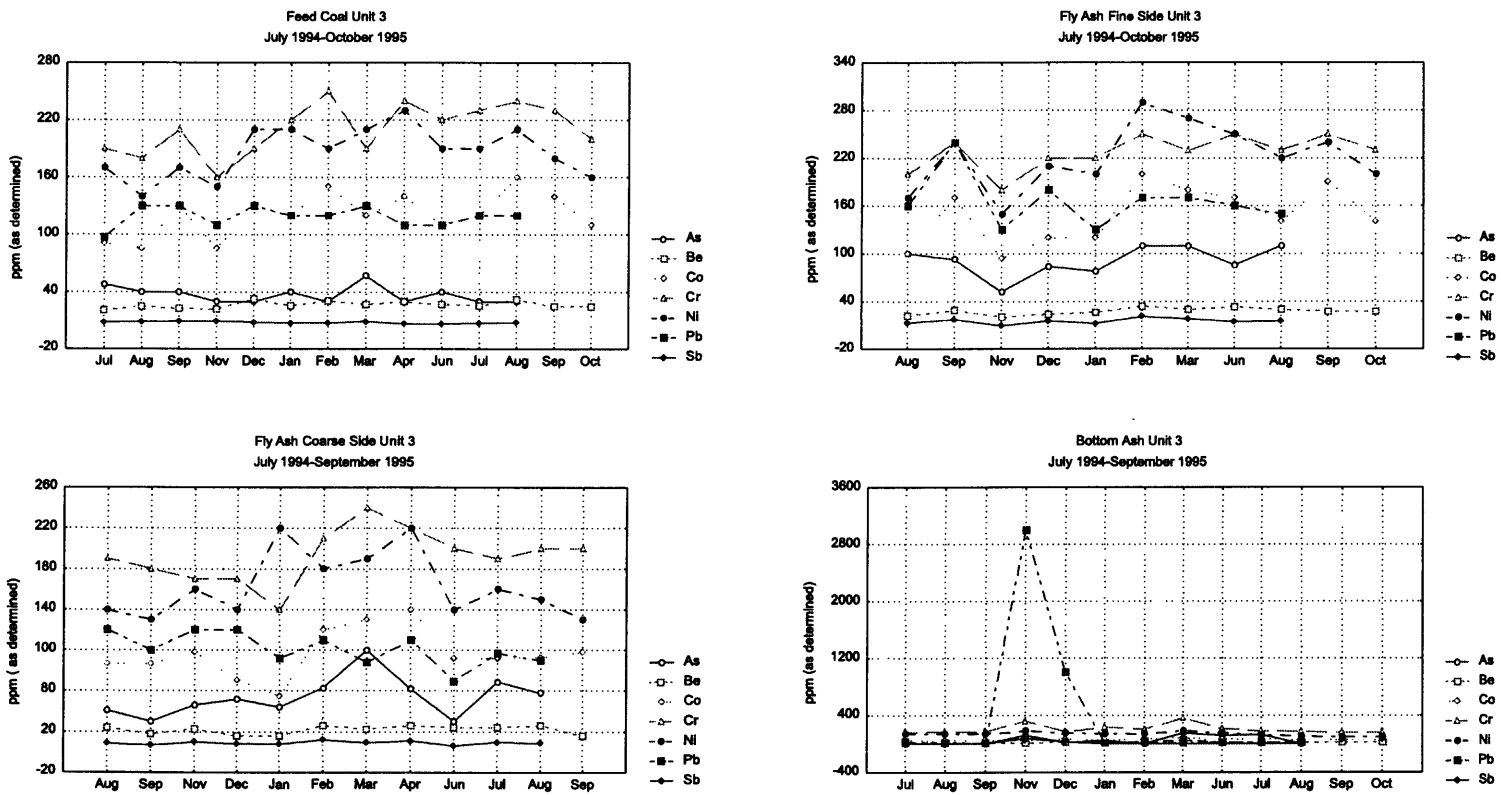

Figure D2. Variation of As, Be, Co, Cr, Ni, Pb, and Sb contents of feed coal, fly ash (coarse and fine sides) and bottom ash from unit 3 for samples collected between July 1994 and October 1995.

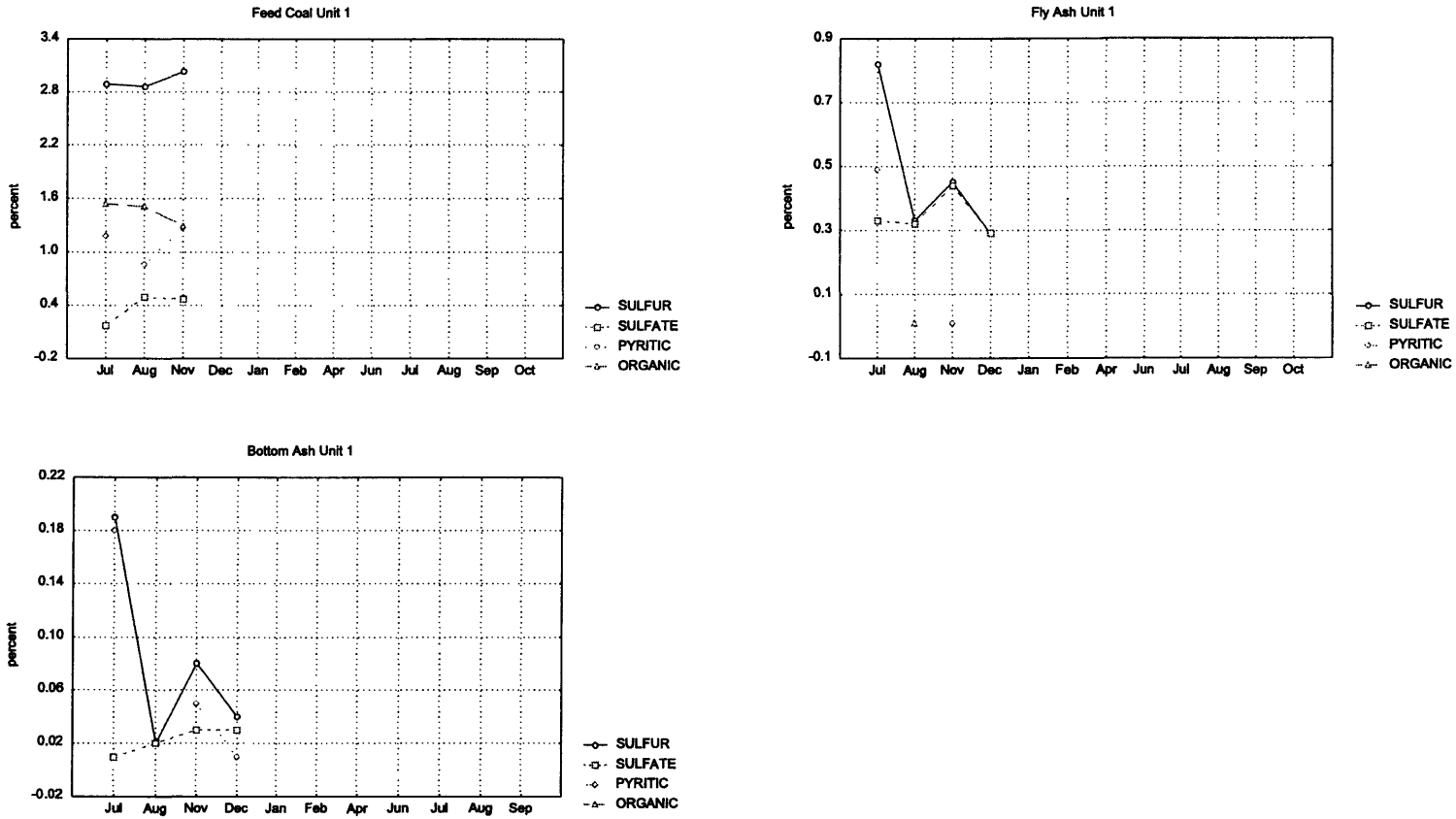

Figure D3. Variation of total sulfur and forms-of-sulfur in feed coal, fly ash and bottom ash from unit 1 (high-sulfur unit) for samples collected from July 1994 until December 1994.

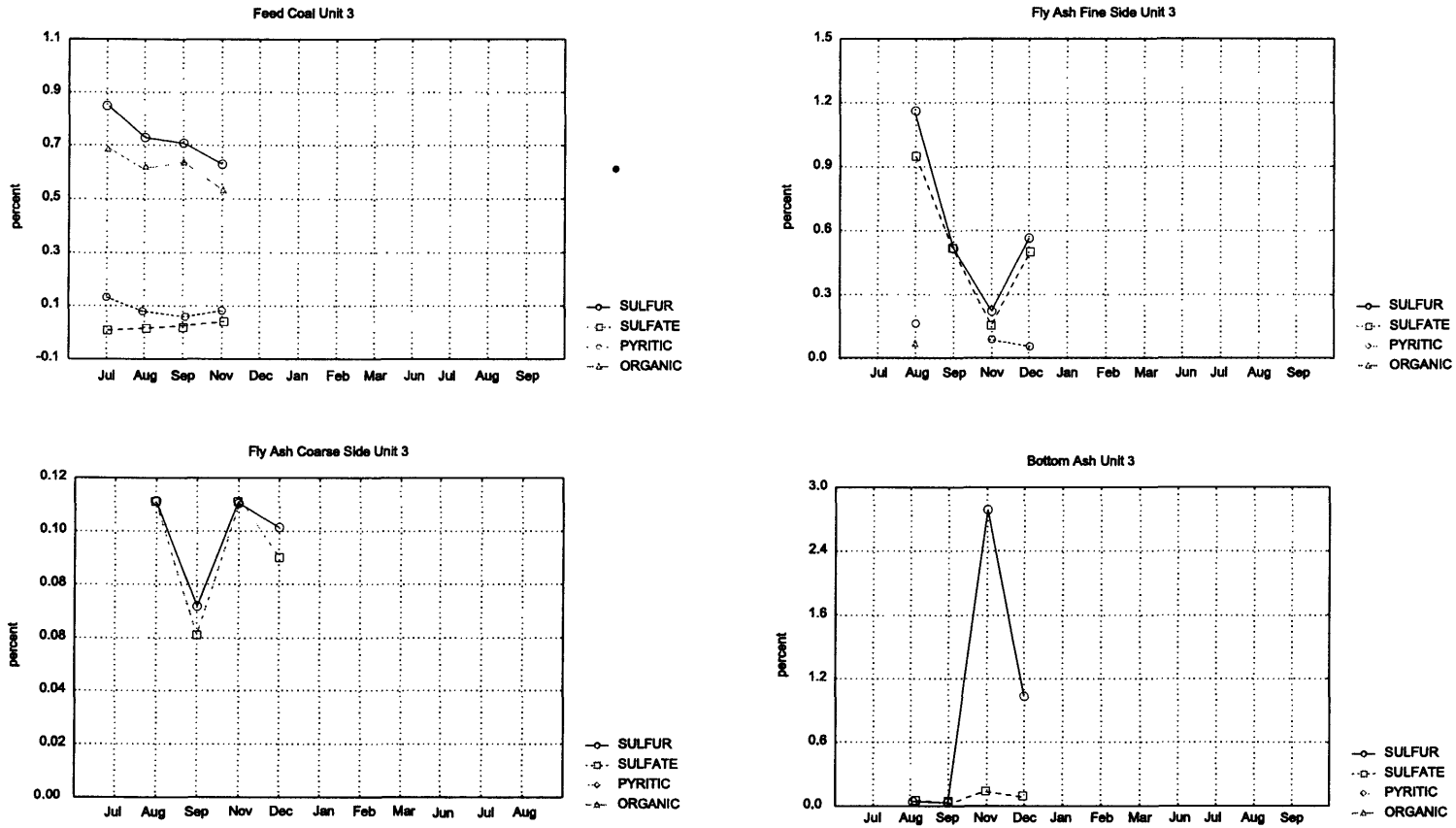

Figure D4. Variation of total sulfur and forms-of-sulfur in feed coal, fly ash (fine and coarse sides) and bottom ash from unit 3 (low-sulfur unit) for samples collected from July 1994 until December 1994.

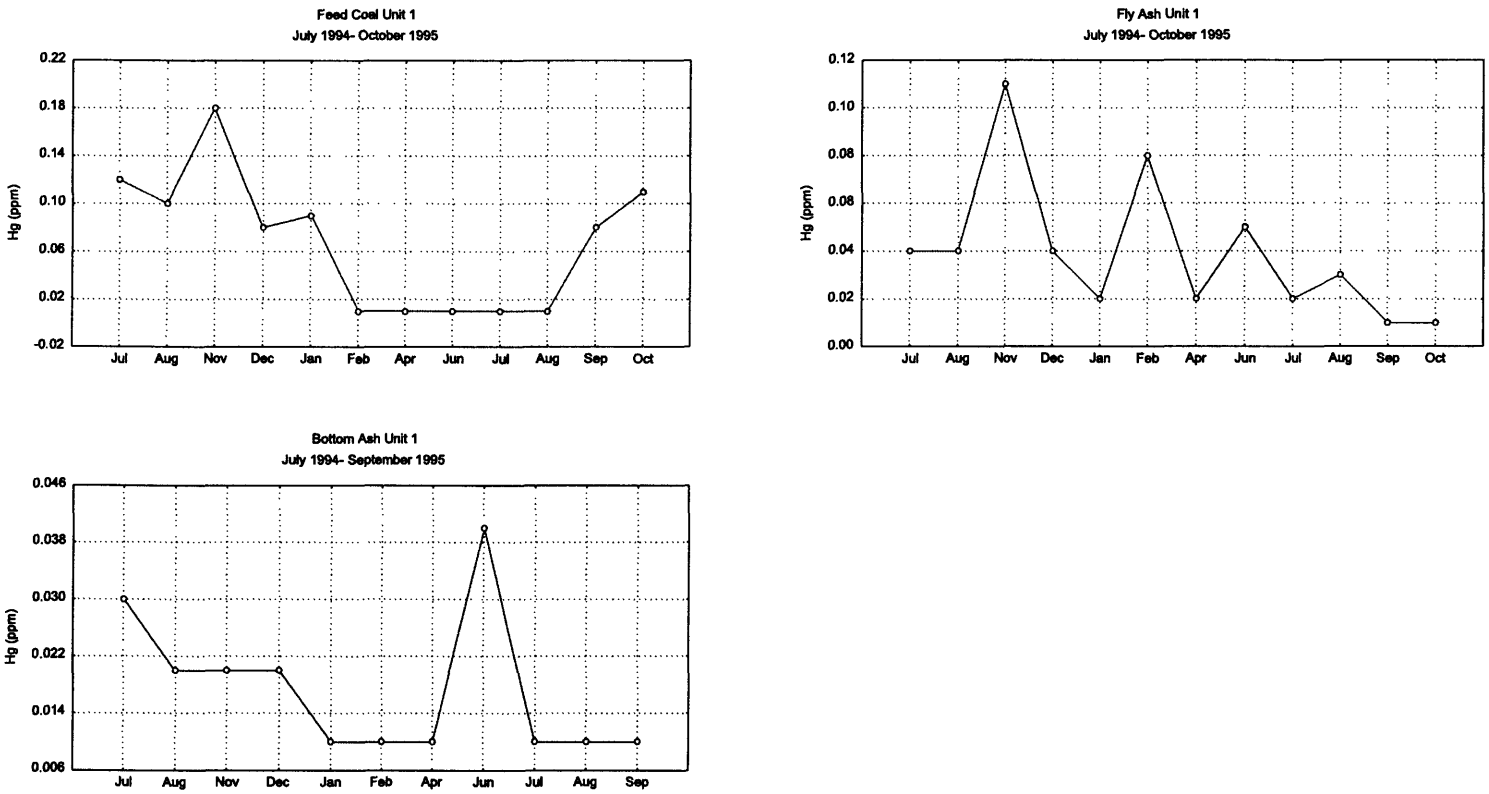

Figure D5. Variation in mercury content of feed coal, fly ash, and bottom ash from unit 1 (high-sulfur unit) for samples collected from July 1994 to October 1995.

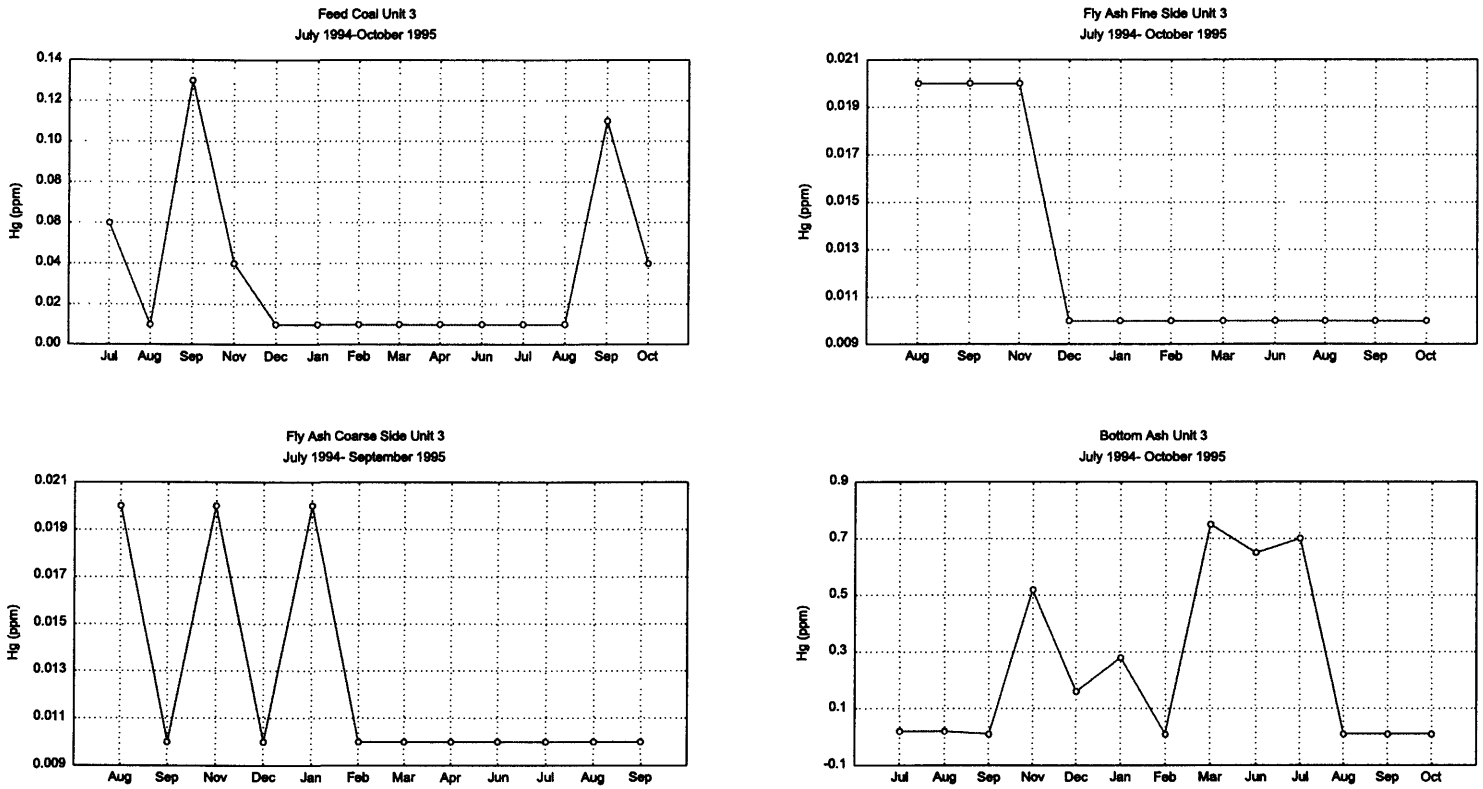

Figure D6. Variation in mercury content of feed coal, fly ash (fine and coarse sides), and bottom ash from unit 3 (low-sulfur unit) for samples collected from July 1994 to October 1995.

E. CHARACTERIZATION OF HAZARDOUS TRACE ELEMENTS IN SOLID WASTE PRODUCTS FROM A COAL-BURNING POWER PLANT IN KENTUCKY

by Sharon S. Crowley, Robert B. Finkelman, and Curtis A. Palmer, U.S. Geological Survey Reston , Virginia, **and**
Cortland F. Eble, Kentucky Geological Survey, Lexington, Kentucky

This section presents a detailed analysis of the chemical composition of feed coal and the solid combustion wastes from the first set of samples collected at the power plant. A particular focus is on the distribution and mode of occurrence of elements in the fly ash and bottom ash samples relative to the feed coal. The intent is to evaluate the volatility of elements during combustion and therefore predict their distribution among the waste products. In general, the results are similar to the patterns of volatility established by previous researchers.

Methods

ASTM standard proximate and ultimate analyses and sulfur-form analysis of the coal, fly ash, and bottom ash samples were performed by the Kentucky Geological Survey (Eble, this volume). Major and trace element abundance using inductively coupled plasma atomic emission spectroscopy (ICPAES), ICP mass spectroscopy (ICPMS), and instrumental neutron activation analysis (INAA). Analytical errors for INAA analyses range from 2 to 18% (As = 4%; cobalt = 2-4%; Cr = 3-6%, Ni = 9-14%; Sb = 2-5%; Se = 10-18%; U = 6-7%.) Analytical errors for ICP-MS analyses (Cd, Pb) and ICP-AES analyses (Mn, Be) range from 5 to 10%. In this paper, INAA, ICP-MS and ICP-AES analyses on a coal ash basis are used for examination of the distribution of inorganic hazardous air polluting substances (HAPS) in fly ash, bottom ash, and magnetic separates from the high-sulfur and low-sulfur units of the power plant (Table E1). INAA analyses were calculated on an ash basis. Magnetic separates were produced using a hand magnet. Sample mineralogy was determined by using x-ray diffraction (XRD), Mossbauer spectroscopy, and optical microscopy.

In order to assess trace-element modes of occurrence, selective leaching was conducted using ammonium acetate ($NH_4C_2H_3O_2$), hydrochloric acid (HCl), hydrofluoric acid (HF), and nitric acid (HNO_3) (Palmer and others, 1995). Electron microprobe and scanning electron microscopy-energy dispersive analyses were also performed to determine the mode of occurrence of selected elements.

Mass-balance calculations were used as a means of identifying volatile elements and assessing the quality of the analytical data. Mass balance was calculated using the following formula:

$$C_{ESW} = aC_{EFA} + (1-a)C_{EBA}$$

Where C_{ESW} is the total content of the element in the solid waste products, C_{EFA} is the concentration of the element in the fly ash, C_{EBA} is the concentration of the element in the bottom ash, and a is the fraction of solid wastes that the fly ash constitutes. The power plant operator estimates that 75 wt.% of their solid combustion products is fly ash and 25 wt. % is bottom ash (oral commun., company personnel); therefore a is equal to 0.75 for this power plant. Results of these mass balance calculations (C_{ESW}) are presented in column 2 of Table E2. C_{ESW} should equal the measured concentration of the element in the feed coal ash (C_{EFC}) if there is no loss of volatile elements in the flue gas. The ratio C_{ESW}/C_{EFC} is given in column 3 of Table E2.

Results

Mass-balance calculations

Calculated (C_{ESW}) and measured concentrations (C_{EFC}) of each of the HAPS elements measured in the feed coal are probably within the analytical error, with the exceptions of selenium and manganese from unit 3 and lead from the unit 1 (Table E2). The greatest difference between measured and calculated concentrations occurs for selenium. Previous studies indicate that selenium is a highly volatile element that escapes with flue gas (Germani and Zoller, 1988). The loss of selenium through the smokestack can account for the very large difference between calculated and measured concentrations. Calculated concentrations of arsenic in the feed coal are in close agreement with the measured concentrations of arsenic in feed coal, even though arsenic is also reported to be a volatile element (Clarke and Sloss, 1992). Perhaps the close agreement between calculated and measured concentrations of arsenic can be explained by vaporization during combustion followed by condensation onto particle surfaces in the flue gas stream during cooling (Palmer and others, 1995). This model could explain why arsenic does not apparently leave the plant with the flue gas that discharges through the smokestack.

Mass balance calculations (Table E2) indicate that the HAPS elements are retained (within analytical error) in the solid waste products, with the exception of selenium. From 70 to 90% of the selenium was not accounted for in the solid waste products and presumably was released into the atmosphere. Results for mercury are not presented because the analytical data are incomplete; previous work has shown that mercury is also highly volatile and is released through the smokestack (Germani and Zoller, 1988).

A comparison of ratios of element contents in fly ash to bottom ash is another parameter useful for determining the level of volatilization of each of the elements (Table E3). Ratios less than 1 indicate enrichment of the element in bottom ash; ratios greater than 1 signify enrichment of the element in the fly ash. The distribution of trace elements among the fly ash and bottom ash is related on the volatility of the elements studied; the more volatile the element (as reported by Clarke and Sloss, 1992), the greater its relative concentration in the fly ash. Ratios of element contents of fly ash to bottom ash are greater than 1 for arsenic, beryllium, cadmium, cobalt, lead, and antimony, which indicates enrichment of the element in the fly ash. The fly ash / bottom ash ratios for chromium, nickel, and perhaps uranium are near 1 and indicate no differentiation during combustion. The ratio for manganese is less than 1 and indicates enrichment in the bottom ash. Ratios of elements are similar for high-sulfur (unit 1) and low-sulfur units (unit 3); this similarity indicates that there is no substantial difference in distribution of elements in the solid combustion wastes between the units.

Summary of analytical work for each of the HAPS elements

The following discussion summarizes our observations on each of the HAPS elements studied on the basis of: (1) the distribution of the elements in feed coal, fly ash, bottom ash, and magnetic fractions (Table E1) and (2) behavior of the elements during leaching experiments (Palmer and others, 1995). McGee (this volume) reports preliminary results of microprobe analyses for arsenic. Although scanning electron microscopy has been used in preliminary studies, it has not been a useful method for detection of the HAPs elements due to their low concentrations.

The concentration of arsenic is greater in samples of feed coals from unit 1 than in corresponding samples from unit 3 (Table E1). The association of arsenic with pyrite in coal has been established in previous studies (Finkelman, 1994; Minkin and others, 1984). Leaching experiments indicate that 80 percent of arsenic was leached from fly ash with HCl (Palmer and others, 1995). The leaching behavior could indicate that arsenic was volatilized during combustion and condensed as arsenates on the surface of the particles during cooling in the stack (Palmer and others, 1995). However, preliminary microprobe analyses of the fly ash do not support the occurrence of As on the surface of particles; analyses of selected glassy fly ash

spheres indicate that arsenic is uniformly distributed (McGee and others, 1995). There is no clear differentiation of arsenic between magnetic and nonmagnetic fractions. Arsenic is very strongly concentrated in the fly ash compared to the bottom ash.

The concentration of antimony is greater in samples of feed coals from the high-sulfur unit than in corresponding samples from the low-sulfur unit (Table E1). In coal, antimony has been found in solid solution in pyrite and as minute accessory sulfides (Finkelman, 1994). Experimental data on the fly ash and bottom ash show that antimony is leached by HCl, although not to the degree that arsenic is leached (Palmer and others, 1995). There is no apparent differentiation of antimony between magnetic and nonmagnetic fractions. Antimony is strongly concentrated in the fly ash compared to the bottom ash.

The concentration of cobalt is greater in samples of feed coal from unit 3 than in corresponding samples from unit 1 (Table E1). These observations contrast with previous studies that suggest the association of cobalt with sulfide minerals in coal (Finkelman, 1994). Cobalt also shows enrichment in the magnetic fractions, particularly for the low-sulfur samples. Differences in concentrations of cobalt for magnetic fractions from unit 1 and unit 3 may be attributed to incomplete separations of magnetic components in the high-sulfur samples (unit 1). Cobalt is strongly concentrated in the fly ash compared to the bottom ash.

High-sulfur (unit 1) and low-sulfur (unit 3) samples of feed coals contain similar concentrations of chromium (Table E1). Like cobalt, chromium is enriched in the magnetic fractions of fly ash, particularly in the low-sulfur sample. However, there is no differentiation of chromium between the magnetic and non-magnetic fractions of bottom ash in the high-sulfur samples. HF leaching experiments on fly ash and bottom ash with HF indicate that chromium is concentrated in the glassy or crystalline silicates (Palmer and others, 1995). Chromium is slightly more concentrated in the fly ash than in the bottom ash.

The concentration of nickel is greater in samples of the high-sulfur (unit 1) feed coal than in samples of the low-sulfur (unit 3) feed coal. There is a strong enrichment of nickel in magnetic splits of fly ash for both the low-sulfur (unit 3) and high-sulfur (unit 1) samples; bottom-ash samples from unit 1 also show enrichment in the magnetic fraction. Appreciable nickel is concentrated in the glassy or crystalline silicates, as indicated in leaching experiments using HF (Palmer and others, 1995), in addition to the iron oxide phases as previously suggested. Nickel concentrations are essentially the same in the fly ash and bottom ash.

Uranium has similar concentrations in both the high-sulfur (unit 1) and low-sulfur (unit 3) samples of feed coal. There is no apparent differentiation of uranium among magnetic and nonmagnetic splits, with the exception of slightly higher levels of uranium in the magnetic fly ash from the low-sulfur unit (unit 3). Leaching experiments on the fly ash and bottom ash indicate that uranium is leachable only to a small degree by HCl, HF, or HNO_3, perhaps as a result of the association of uranium with resistate minerals such as zircon (Palmer and others, 1995). Uranium is slightly enriched in the fly ash compared to the bottom ash.

The concentration of selenium is greater in samples of unit 3 feed coal than in samples from unit 1 (Table E1). Data are not available on the leaching characteristics of selenium, and there is no apparent differentiation of selenium among the magnetic and nonmagnetic fractions of fly or bottom ash. Selenium is enriched in the fly ash compared to the bottom ash of the high-sulfur unit (unit 1). However, its concentration is greater in the bottom ash than in the fly ash of the low-sulfur unit.

There are no data on magnetic fractions for the following elements in the present study; these data will be available in future work. Cadmium is greater in samples of feed coals from the high-sulfur unit (unit 1) than in samples from the low-sulfur unit (unit 3) (Table E1). Cadmium is

also highly enriched in the fly ash compared to the bottom ash of unit 1. Lead has a higher concentration in samples of feed coal from the high-sulfur unit than corresponding samples from the low-sulfur unit (unit 3). Lead is also highly enriched in the fly ash in contrast to the bottom ash. Manganese is greater in samples of feed coals from the high-sulfur unit (unit 1) than in samples from the low-sulfur unit. Manganese is the only HAPS element that is preferentially concentrated in the bottom ash. There is no apparent differentiation of beryllium in the feed coal or magnetic samples.

Several of the HAPS elements (nickel, cobalt, and chromium) are enriched in the magnetic relative to the non-magnetic fractions. Magnetite can readily incorporate chromium, manganese, and nickel. Maghemite, a common alteration product of magnetite, also can contain these elements. X-ray diffraction data indicate substantial amounts of maghemite and lesser amounts of hematite in the fly ash and bottom ash of the high-sulfur unit (unit 1). Minor amounts of these minerals are found in the fly ash and bottom ash of the low-sulfur unit (unit 3). These findings are consistent with optical petrography and Mossbauer spectroscopy.

Conclusions

The distributions of 11 potentially hazardous trace elements in feed coal, fly ash, and bottom ash samples are useful in defining general tendencies of trace elements in the combustion wastes. (1) Mass-balance calculations indicate that most of the HAPS elements monitored are retained in the solid waste products. Selenium is a notable exception; and mercury could not be evaluated. 75 to 90% of the selenium is not accounted for in the solid waste products and presumably was released into the atmosphere. (2) Ranking of the ratios of element contents in fly ash to bottom ash are similar to the order of volatility reported by Clarke and Sloss (1992). (3) Nickel, chromium, and cobalt show substantial enrichment in the magnetic fractions of the fly ash from the low-sulfur unit (unit 3). In the bottom-ash samples, nickel shows a strong concentration in the magnetic split from the high-sulfur unit (unit 1). Maghemite, a common alteration product of magnetite, can contain these elements.

Table E1. Distribution of environmentally sensitive trace elements in feed coal, fly ash, bottom ash, magnetic and nonmagnetic samples from high-sulfur (unit 1) and low-sulfur (unit 3) units of the power plant. All values are in ppm, on an ash basis. (mag. = magnetic; nonmag. = nonmagnetic; Bot. ash = bottom ash; n.d. = no data available).

	Arsenic		Berylium		Cadmium		Cobalt		Chromium		Manganese	
	Unit 1	Unit 3	Unit 1	Unit 3	Unit 1	Unit 3	Unit 1	Unit 3	Unit 1	Unit 3	Unit 1	Unit 3
Feed coal	68.3	29.2	15	21	7.2	1	44.6	70.3	162	160	310	170
Fly ash	90.	35.	18	19	7.8	<0.8	53.1	79.2	161	169	300	180
Bottom ash	5.7	1.7	12	14	0.8	<0.8	39.3	48.6	141	150	360	360
Fly ash mag.	64.0	16.4	n.d.	n.d.	n.d.	n.d.	60.	214.	181	200	n.d.	n.d.
Fly ash - nonmag.	72.2	8.6	n.d.	n.d.	n.d.	n.d.	40.7	30.2	158	124	n.d.	n.d.
Bot. ash - mag.	3.1	26.3	n.d.	n.d.	n.d.	n.d.	45.0	50.3	137	142	n.d.	n.d.
Bot. ash - nonmag.	7.2	n.d.	n.d.	n.d.	n.d.	n.d.	41.0	n.d.	139	n.d.	n.d.	n.d.

	Nickel		Lead		Antinony		Selenium		Uranium	
	Unit 1	Unit 3	Unit 1	Unit 3	Unit 1	Unit 3	Unit 1	Unit 3	Unit 1	Unit 3
Feed coal	264	161	120	97	12.9	6.8	20.4	33.7	12.7	12.8
Fly ash	300	152	200	100	15.0	7.9	6.8	3.0	14.1	11.4
Bottom ash	288	139	50	30	4.4	2.4	2.1	3.8	12.7	8.2
Fly ash mag.	380	410	n.d.	n.d.	11.6	4.6	<8	<5	15.1	11.6
Fly ash - nonmag.	190	<150	n.d.	n.d.	11.3	2.0	7.5	<4	15.3	6.7
Bot. ash - mag.	490	<130	n.d.	n.d.	3.7	4.9	<4	<3	13.7	12.8
Bot. ash - nonmag.	200	n.d.	n.d.	n.d.	5.4	n.d.	<4	14.1	n.d.	n.d.

Table E2. Mass-balance calculations for solid waste products based on the production of 75 wt. % fly ash and 25 wt. % bottom ash from the power plant. (1, unit 1 (high-sulfur unit); 3, unit 3 (low-sulfur unit). All values are in ppm.

Element	Unit	Measured element content in feed coal ash, (C_{EFC})	Calculated element content in solid wastes (C_{ESW})	Material Balance ($C_{ESW}/C_{EFC}*100$)
Arsenic	1	68.3	68.9	100
	3	29.2	26.9	90
Beryllium	1	15	16.5	110
	3	21	17.8	80
Cadmium	1	7.2	6.1	80
	3	1	<0.8	<80
Cobalt	1	44.6	49.6	110
	3	70.3	71.6	100
Chromium	1	162	156	100
	3	160	164.3	100
Manganese	1	310	315	100
	3	170	225	130
Nickel	1	264	297	110
	3	161	148.8	90
Lead	1	120	162.5	140
	3	97	82.5	90
Antimony	1	12.9	12.4	100
	3	6.8	6.5	100
Selenium	1	20.4	5.6	30
	3	33.7	3.2	10
Uranium	1	12.7	13.8	110
	3	12,8	10.6	80

Table E3. Ratios of element contents of fly ash (FA) to bottom ash (BA) for high-sulfur (unit 1) and low-sulfur units (unit 3). Se is not included because it does not have a mass balance calculation approaching 100% (see Table E2). (--, data insufficient for calculation).

Element	High-Sulfur Unit FA/BA	Low-Sulfur Unit FA/BA
Arsenic	15.8	20.6
Cadmium	9.8	–
Lead	4.0	3.3
Antimony	3.4	3.3
Beryllium	1.5	1.4
Cobalt	1.4	1.6
Chromium	1.1	1.1
Nickel	1.0	1.1
Uranium	1.1	1.4
Manganese	0.8	0.5

F. LABORATORY LEACHING BEHAVIOR OF ENVIRONMENTALLY SENSITIVE TRACE ELEMENTS FROM FLY ASH AND BOTTOM ASH SAMPLES

by Curtis Palmer, Robert B. Finkelman, and Martha R. Krasnow, U.S. Geological Survey, Reston , Virginia, **and Cortland F Eble,** Kentucky Geological Survey, Lexington, Kentucky.

Introduction

The distribution of trace elements in coal combustion residues such as fly ash and bottom ash has received considerable attention (Keefer and Sajwan, 1993; Eary and others, 1993). Several studies of fly ash have concentrated on relationships of trace elements to fly ash particle size (Davidson and others, 1974; Hansen and others, 1984; Furuya and others, 1987). Studies of etching (Heulett and Weinberger, 1980) mineralogical transformation during combustion (Chinchon and others, 1991) and leaching have also been reported. Dudas (1981) conducted long-term leachability studies. Grisafe and others (1988) examined leachability of fly ash as a source of selenium contamination. Fernandez-Turiel and others (1994) examined the mobility of heavy metals from coal fly ash. The objectives of these studies are primarily to understand potential problems associated with the storage or disposal. To meet these objectives, the solvents used in these studies were chosen to emulate conditions in nature.

The leaching study presented in this paper differs from previous leaching studies (e.g. Palmer and others, 1993) because the primary objective is to obtain information on modes of occurrence of trace elements in the fly ash and bottom ash rather than on whole-coal samples. Although preliminary data for 29 elements in the fly ash and bottom ash are available at this time, only results for environmentally sensitive trace elements and other associated elements will be discussed in this paper. The elements investigated include several of those identified in 1990 Clean Air Act Amendments: cobalt, chromium, nickel, antimony, and radionuclides (thorium and uranium). Iron was also studied because of its importance to coal cleaning and sulfur removal, and zinc because of its relationship to cadmium. Zinc and cadmium are known to occur in sphalerite that has been detected in coal.

Experimental

Samples were collected from an electric utility power plant having furnaces burning high-sulfur (3.3 weight percent total sulfur) and low-sulfur (0.9 weight percent total sulfur) coal. Approximately 10 grams of each of two fly ash samples and two corresponding bottom ash samples were subjected to sequential leaching. In this procedure, the sample was combined separately with each leachate solution then shaken automatically for 18 hours, centrifuged, and the leachate separated by filtration. The samples were first leached with 1N ammonium acetate ($NH_4C_2H_3O_2$). A representative 0.5 gram split of each of the leached samples was reserved for analysis by instrumental neutron activation analysis (INAA). This procedure was repeated in subsequent leaching steps using 2N hydrochloric acid (HCl), concentrated (48 to 51 %) hydrofluoric acid (HF), and 1.5 N nitric acid (HNO_3). A representative 0.5 gram split was obtained for INAA from the material leached by each solvent.

Representative samples and all resulting splits of the original material were irradiated for 8 hours at a neutron flux of about 2×10^{12} neutrons/cm^2sec^{-1} using INAA procedures similar to those of Palmer (1990). The data were calculated using the SPECTRA program (Baedecker and Grossman, 1994). The amount of each element extracted by the solvents was determined by comparing the element abundance and mass of each the split before and after treatment with each solvent.

Results and Discussion

The relative amount of an element leached by a specific solvent is an indicator of the elements' mode of occurrence. In contrast to coal, which is primarily an organic matrix not leachable to a significant extent by most inorganic solvents, the bottom ash and fly ash consist mainly of silicates that are leachable to a large degree by inorganic solvents, particularly by HF. In addition, because of the high temperature of combustion (~1500 °C), mineral phases present in the coal such as clays, carbonates, and sulfides are transformed to silicates and oxides. Table F1 shows the percent of the material leached by each of the solvents used in this study. The total amount of material leached ranged from 78 to 99 percent, with 97 percent or more leached from the fly ashes. Seventy to seventy-nine percent of each sample dissolved in HF. Clearly, a large percentage of the fly ash and bottom ash are in silicates. Generally less than 5 percent of the fly ash and bottom ash is ammonium acetate soluble (probably water soluble as well). Less than 5 percent of the bottom ash and fly ash is HCl soluble. About 5 to 15 percent of the ash was leached by nitric acid. Because sulfides are not likely to be present in the fly ash (as discussed above) it is not clear which mineral forms are leached by nitric acid. It is possible that species soluble in the nitric acid, unleached by HF, and encased in the silicates during combustion could have been leached following the destruction of the silicates. It should be noted that the fly ash is generally more soluble in the solvents used in this study than is the bottom ash. This trend may be explained in part by the presence of a larger proportion of unburned carbon in the bottom ash than the fly ash. Preliminary results from carbon-hydrogen-nitrogen analyses and ash determinations showed that up to 18 percent unburned carbon was found in the bottom ash in BA3.

Table F1. Weight percentage of material leached by solvents used in this study.

Solvents	BA1	BA3	FA1	FA3
$NH_4C_2H_3O_2$	1	1	5	3
HCl	2	1	5	3
HF	70	71	78	79
HNO_3	14	5	10	13
Total	86	78	98	98

The relative amount of some environmentally important elements leached differed among the samples (weight % of all elements leached) indicating that the elements are not uniformly distributed through the ash. More than 80 percent of the arsenic in the fly ash samples and about 45 percent of the arsenic in one bottom ash sample were leached with HCl (Fig. F1). Davidson and others (1974) suggest that arsenic, as well as some other elements, may be volatilized during combustion and recondensed on the surface of the particles as they cool in the stack. Turner (1981) and EPRI (1994) suggest that arsenic in fly ash may be present as a metal arsenate, such as $Ca_3(AsO_4)_2$ or $Ba_3(AsO_4)_2$. These phases are consistent with the large relative percentage of arsenic leached by HCl. The behavior of arsenic in BA3 is different than the other bottom ash sample and the fly ash samples. Condensation of volatile species such as arsenic is unlikely to occur in bottom ash samples.

As much as 25% of the antimony (Fig. F2) in the two fly ash samples, are leached by HCl . The amount extracted by HCl is not as large as the relative amount of arsenic extracted. Results from a comparison of magnetic and non-magnetic fractions (Palmer and others, unpublished data) show similarities in behavior between antimony and arsenic. The results of this study however, suggest that antimony and arsenic are extracted to different degrees.

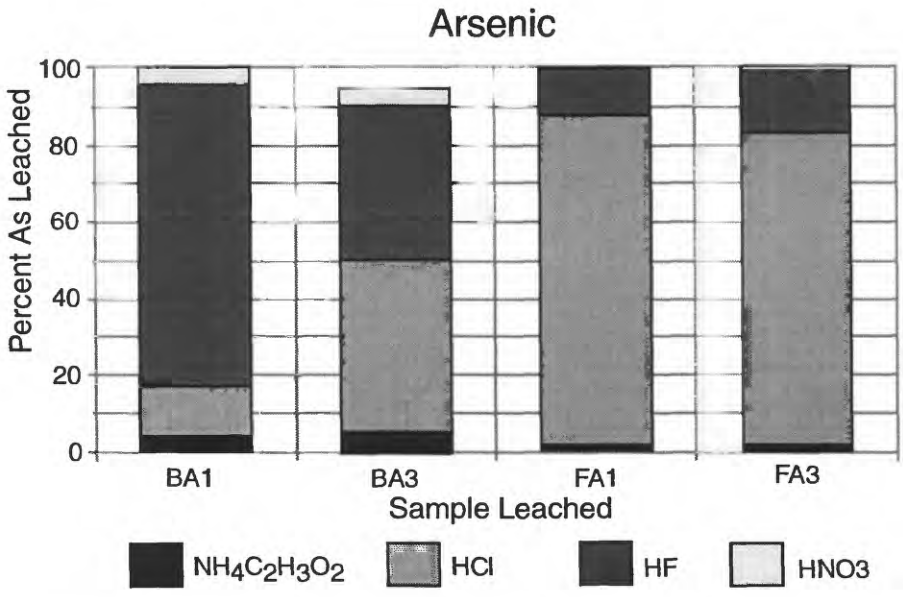

Figure F1. Percent of arsenic leached from bottom ash samples (BA1 and BA3) and fly ash samples (FA1 and FA3) by solvents used in this study.

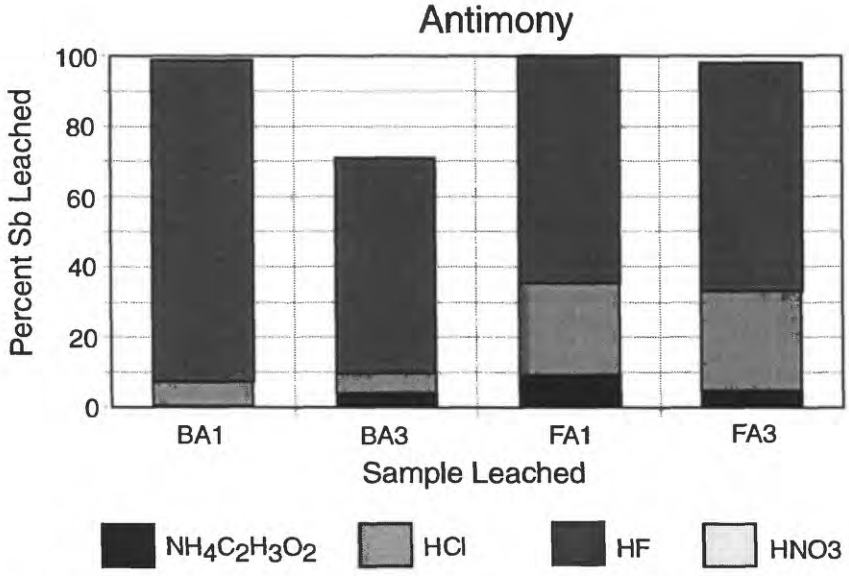

Figure F2. Percent of antimony leached from bottom ash (BA1 and BA3) and fly ash samples (FA1 and FA3) by solvents used in this study.

Elements such as uranium and thorium are leached only to a small degree (as little as 20 percent leached by all solvents). This behavior may be due to their association with minerals such as zircon which are inert and are not significantly altered by either combustion or leaching. These elements are significantly more soluble in fly ash (especially FA1) than in the bottom ash, and uranium is more soluble than thorium. The data for uranium in fly ash suggests that it may exist in several forms because there is roughly equal leaching by HCl and HF in both fly ash samples, and

equal leaching by HNO_3 in FA1. Figure F3 shows the percentage of uranium and thorium leached by each solvent.

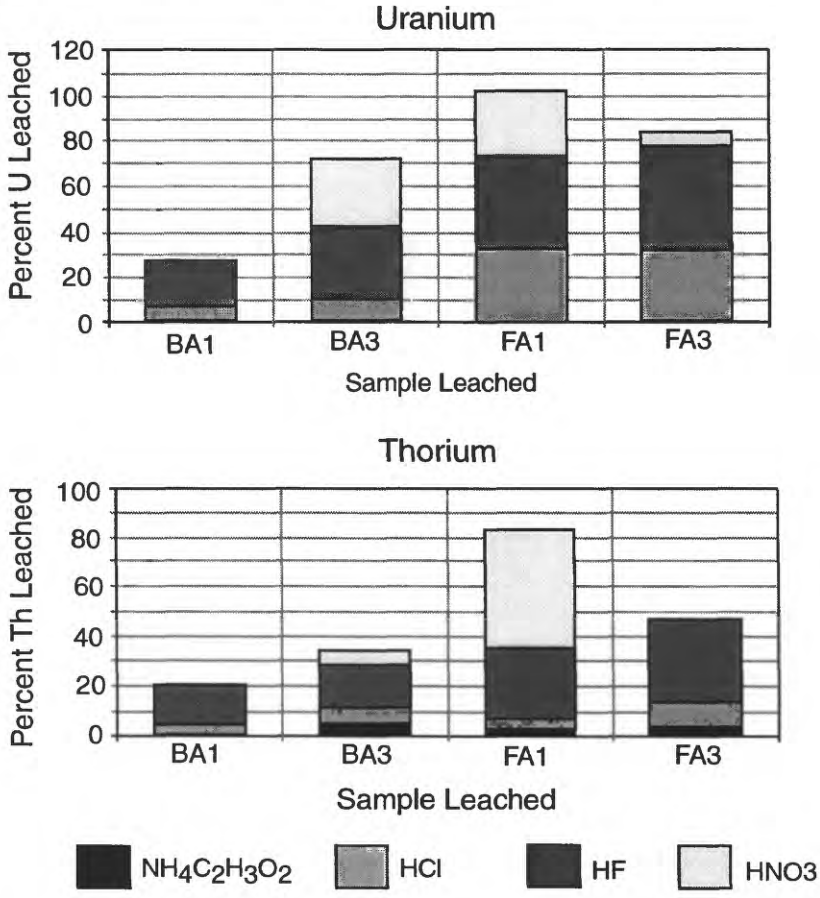

Figure F3. Percent of uranium and thorium leached from bottom ash (BA1 and BA3) and fly ash samples (FA1 and FA3) by solvents used in this study.

Most of the other elements studied show leaching behavior similar to the bulk material. Fig. F4 shows the percentage leached for iron, nickel, cobalt, and chromium in the bottom ash and the fly ash. In all cases, the majority of these elements are leached by HF, which is interpreted to indicate accumulation of these elements in silicates and iron oxides. Most of these elements show a small amount (<20 percent) of material leached by HCl. Any oxides present are probably locked in the matrix and not exposed until HF dissolves the silicates.

Figure F5 shows the percent zinc leached (likely an indicator of Cd behavior). The leaching behavior of zinc is similar to the leaching behavior of the bulk material (Table F1). However, there is a significant fraction of zinc leached by HCl in sample FA3. In addition, about 20 percent zinc was leached by ammonium acetate in sample BA3.

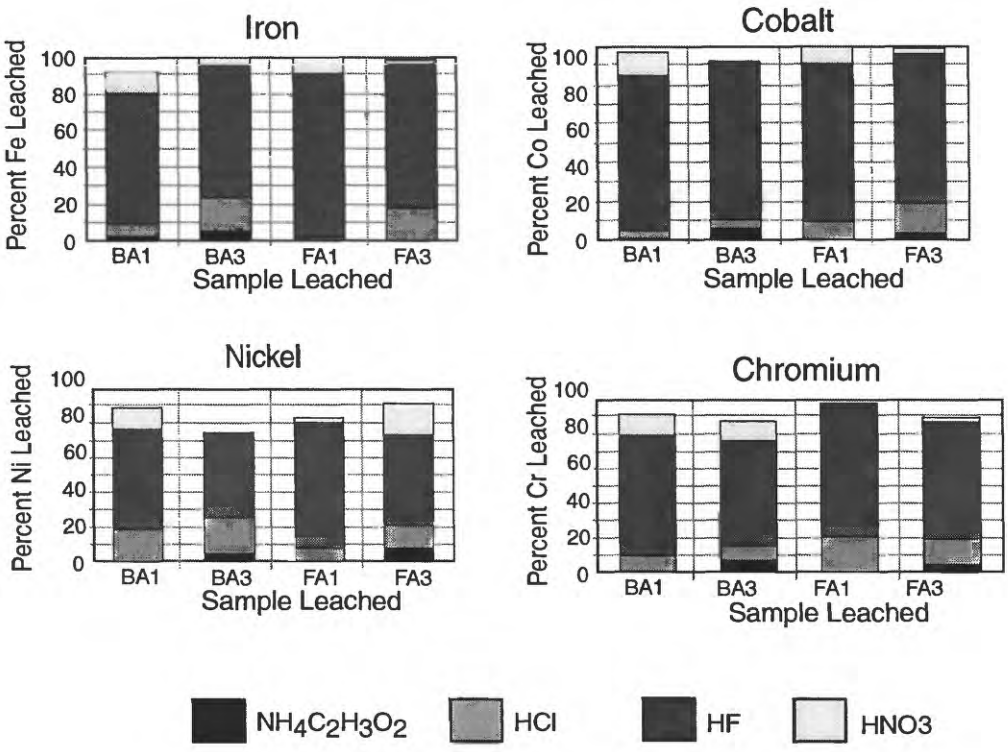

Figure F4. Percent of iron, cobalt, nickel, and chromium leached from the two bottom ash and the two fly ash samples by solvents used in this study.

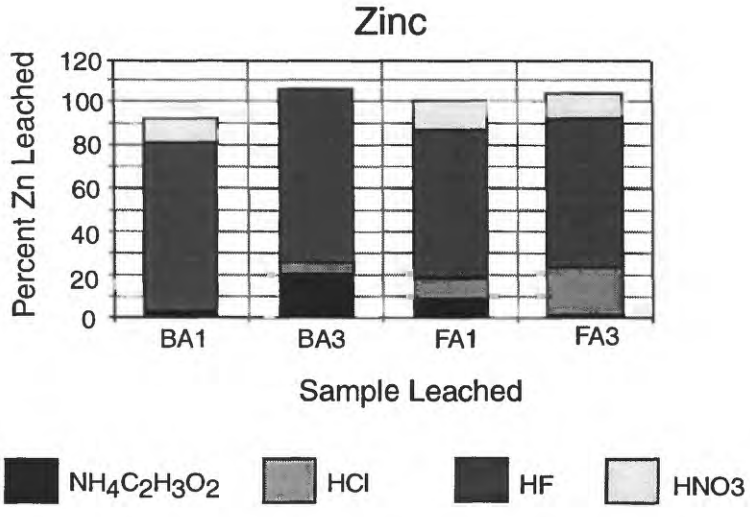

Figure F5. Percent of zinc leached from bottom ash samples (BA1 and BA3) and fly ash samples (FA1 and FA3) by solvents used in this study.

Summary

In summary, most, but not all, elements studied are extracted in proportions similar to the amount of bulk material dissolved by the different solvents. Most elements are probably associated with the glassy or silicate portions of the fly ash and bottom ash. Because arsenic, uranium, thorium and possibly antimony (in the fly ash) display behavior significantly different than that of the bulk sample, it can be inferred that these elements are associated with different minerals or chemical forms than the major elements. Other minor differences in the leaching behavior may indicate that small amounts of that element are associated with minor phases in the ash. Some of these minor phases may be material that has not been completely combusted.

MAGNETIC STUDIES OF FLY ASH AND BOTTOM ASH

by Richard L. Reynolds, Frances E. Gay, Joseph G. Rosenbaum, and Michael E. Brownfield U.S. Geological Survey, Denver, Colorado,

Introduction

Magnetic iron oxide minerals are reported in most mineralogic studies of ash produced by coal combustion (Mattigod and others, 1990). Although these minerals occur in small amounts, generally commensurate with the pyrite content in the feed coal (Lauf and others, 1982), they may have important bearing on issues of waste disposal of the combustion products and on other aspects of coal combustion. First, iron oxide minerals may concentrate certain metals, especially those having ionic radii close to that of divalent or trivalent iron (Cr, Co, Ni, Mn, Mg, Zn, Cu, Al, and V). These elements are thus likely to substitute for iron in the crystal lattice. (Substitution of a divalent metal for divalent iron, as in magnetite, $Fe^{2+}Fe_2^{3+}O_4$, creates ferrimagnetic oxides with the spinel structure; these and other magnetic oxides containing iron as a major metallic component are known as ferrites [see Smit and Wijn, 1959]). Knowing the chemical and physical conditions of iron oxide stability, it should be possible to predict the potential for release or retention of such elements under different disposal conditions.

The primary goal of our work is to determine whether elements such as Co, Cr, Ni, Mn, and Zn are concentrated in the magnetic iron oxide minerals. By understanding the residence of these elements in iron oxides and the potential for their release, we may help identify conditions of combustion or disposal that might retard releases of such elements into the environment. A related long-term goal is to evaluate whether magnetic properties can be used to estimate trace-element contents in combustion wastes.

The common iron oxide minerals are indicators of redox conditions during formation and alteration. Monitoring the magnetic minerals produced over time in the same boiler may thus provide useful and inexpensive information on changes in the redox environment of combustion. Finally, magnetic iron oxide minerals produced during coal combustion appear to have diagnostic textures that would be useful for determining the aerial dispersion of particles from combustion units. Such minerals can be easily concentrated from material such as lake sediment and identified using petrographic methods (Puffer and others, 1980).

The magnetic minerals identified as part of coal combustion wastes are strongly magnetic magnetite (Fe_3O_4) and other ferrites, as well as weakly magnetic hematite (Fe_2O_3; e.g., Hulett and others, 1980; Lauf and others, 1982; Eary and others, 1990; Mattigod and others, 1990). The magnetic iron oxide minerals are considered to be derived primarily from the high-temperature oxidation of pyrite (FeS_2) in the feed coals (Lauf and others, 1982; Thorpe and others, 1984). Therefore relatively high amounts of magnetic phases are expected in the combustion waste produced from high-sulfur/high-iron coal and lower amounts in waste from low-sulfur/low-iron coal. Other sources of iron in coal can be naturally occurring iron-bearing carbonates and clays, and magnetite added during beneficiation.

In the few combined magnetic-chemical studies of fly ash, magnetite was found or inferred to concentrate elements that may have been incorporated into the spinel structure during combustion. Dekkers and Pietersen (1992) found that magnetic susceptibility correlated strongly with the sum of certain trace elements (Cu, Zn, Mn, Ni, Co, Cr, V, Pb, and Mo). In addition to Fe, certain elements have been found in magnetic fractions from fly ash. These elements include Al, K, Ni, Mn, Cu, Zn, and V (Hulett and others, 1980) and Zn and Cr (Locke and Bertine, 1986).

Methods

Techniques developed for the study of paleomagnetism and rock magnetism can be used to determine the distribution of magnetic minerals in coal combustion wastes. We are applying such methods, which are rapid and sensitive, to samples of bottom ash and fly ash collected as part of the power plant study. Magnetic properties of feed coal have also been routinely determined; the results, which are not summarized here, indicate the presence of residual magnetite that was used as part of coal beneficiation to remove pyrite. Our bulk-sample measurements, typically made on 5 to 10 grams of material, mainly reflect the absolute amounts of magnetite and hematite, the amount of magnetite relative to magnetic oxides (proportions of magnetite and hematite), and the magnetic grain size of magnetite. The magnetic grain size, or domain state, reflects the physical grain size of magnetite. When discussing bulk magnetic properties in this report we use "magnetite" to include Fe_3O_4 along with closely related magnetic ferrites having the spinel structure.

The determination of the abundance of iron-oxide phases is important because of the possible residence of certain trace metals in these minerals. The determination of the type of magnetic mineral is important because of the possible affinity of certain metals for either magnetite or hematite. Finally, the determination of magnetite grain size is important if the trace-element residence was found to be controlled by adsorption; for example, a population of small iron-oxide grains possess a large surface area compared to the same volume in a population of large grains. Thus, these small grains would be more susceptible to dissolution and leaching than large grains. The magnetic-property measurements are supplemented by compositional and petrographic studies of magnetic particles concentrated from the bulk sample. Magnetic minerals were identified from x-ray diffraction (XRD) results. The limit of detection of XRD is about 2 %. In contrast, the magnetic-property methods are much more sensitive for magnetic minerals, which can be detected in amounts of 0.01 % or less. In addition, thermomagnetic analysis, the measurement of high-field magnetization as a function of temperature, was done to determine Curie temperatures, which reflect magnetic-mineral composition. Magnetite and hematite, as well as minerals intimately intergrown with them, have also been observed in polished section using reflected-light microscopy.

The concentration of magnetite was estimated using magnetic susceptibility (MS) measured at two frequencies, 600 Hz and then at 6000 Hz. Substances other than ferrimagnetic magnetite contribute to MS and include ultrafine grained (superparamagnetic) magnetite, a paramagnetic iron-bearing phase, or diamagnetic coal. Other estimates for magnetic mineral content come from isothermal remanent magnetization (IRM). IRMs are typically imparted in a forward induction of 1.2 Tesla (T) ($IRM_{1.2}$) and a backfield (oppositely directed induction) of 0.3 T ($IRM_{0.3}$) in an impulse magnetizer and then are measured using a magnetometer. Magnetite saturates below 0.3 T, so that $IRM_{0.3}$ is another good measure of magnetite content. The difference in IRM between 0.3 T and 1.2 T is caused by hematite, which can be expressed in the HIRM parameter, $(IRM_{1.2} - IRM_{0.3})/2$. The ratio, $IRM_{0.3}/IRM_{1.2}$, called the S parameter, is a measure of the proportions of magnetite and hematite. High S values indicate large amounts of magnetite relative to hematite (a maximum value of 1) and decreasing values indicate increasing amounts of hematite. Because of the very different magnetic properties of magnetite and hematite, large quantities of hematite in a magnetite-bearing sample will diminish the S value only slightly. Even values of 0.90 indicate large amounts of hematite.

Information about the domain state of magnetite (magnetic grain size) may be obtained from several kinds of measurements. A narrow range of superparamagnetic grain size (about 18-22 nanometers, nm) will be sensed by a difference in MS at the two frequencies. Moreover, ratios of magnetic hysteresis properties (saturation isothermal remanent magnetization to saturation magnetization; coercivity of remanence to coercivity) can be

used to estimate the magnetic domain states of magnetite (Day and others, 1977), provided that hematite does not overwhelm the properties.

X-ray Diffraction Results

X-ray diffraction of the fly and bottom ashes from both units collected in July, 1994 (Table G1), detected the presence of magnetite, ferrites that contain Mg, Cr, and Ni, as well as hematite. Magnetite and hematite are more abundant in the unit 1 ashes (derived from the high-sulfur coal) than in the unit 3 ashes. Hematite is the dominant iron oxide in unit 3 ashes. Metallic iron is identified in both samples of bottom ash. Maghemite, strongly magnetic ferric oxide (γ–Fe_2O_3) having a spinel structure like magnetite, was tentatively identified in samples from unit 1. The magnetic separates contained small amounts of non-magnetic substances such as mullite (trace), quartz, carbonate, and glass, at least some of which probably contain inclusions of magnetic minerals.

Table G1. Minerals identified by x-ray diffraction of magnetic mineral separates.

Unit 1 Fly Ash	Unit 1 Bottom Ash
Magnetite Fe_3O_4	Magnetite
Magnesioferrite $MgFe_2O_4$	Hematite
Hematite α–Fe_2O_3	Magnesioferrite
Donathite $(Fe,Mg)(Cr,Fe)_2O_4$	Donathite, minor
Trevorite $NiFe_2O_4$	Iron
Chromite $FeCr_2O_4$	Trevorite ?
Maghemite γ–Fe_2O_3	Maghemite ?
Mullite $Al_6Si_2O_{13}$	Mullite

Unit 3 Fly Ash	Unit 3 Bottom Ash
Hematite	Hematite
Magnetite	Magnetite ?
Magnesioferrite	Magnesioferrite
Amorphous Fe, Al glass	Iron
Mullite	Mullite
	Ankerite ? $(Ca(Fe,Mg)(CO_3)_2)$
	Quartz

Magnetic-Property Results

Magnetic-property studies reveal (1) the relation between magnetite and hematite, at one sampling and over time; (2) the control of feed-coal chemistry on magnetic properties; (3) relations among trace elements and amounts of magnetite and hematite; and (4) the presence of a large superparamagnetic component in one class of sample.

Magnetite-Hematite Relations

The plot of MS against $IRM_{0.3}$ shows the great difference in magnetization between ashes from the two units (Fig. G1a). The high magnetization of unit 1 ash (open symbols) reflects the abundance of magnetite produced from the high pyrite content of the feed coal. The distribution of points for the November collection was found to be similar for samples from the other monthly collections. The plot of HIRM against $IRM_{0.3}$ (Fig. G1b) does not show a clear correspondence of hematite with magnetite content. Such a lack of correspondence may be related to the formation of hematite (1) directly from pyrite under highly oxidizing conditions or (2) via the high-temperature oxidation of magnetite during

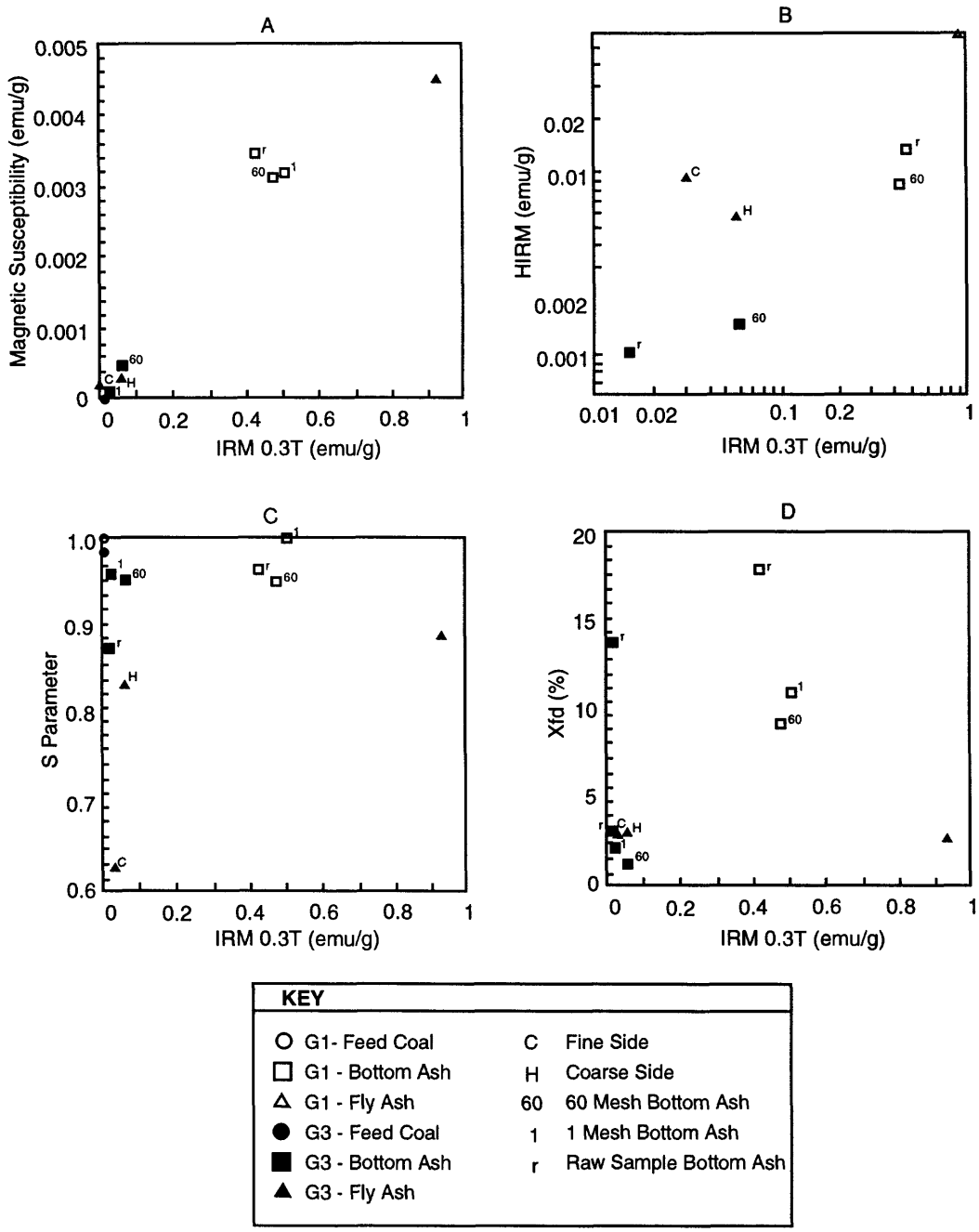

Figure G1. Plots of bulk magnetic properties from November, 1994 samples. A, IRM (isothermal remanent magnetization acquired at 0.3T) against magnetic susceptibility (MS), both in electromagnetic units/gram (emu/g). Both parameters indicate predominantly the concentration of strongly magnetic minerals, mainly magnetite. IRM is a measure of those grains large enough to have a permanent magnetization, whereas MS additionally may respond to large amounts of paramagnetic, superparamagnetic, and diamagnetic minerals. B, hematite content (HIRM) plotted against magnetite content (IRM 0.3T). S parameter expresses proportions of magnetite/hematite, a value of 1 indicating that the entire magnetic-grain population is magnetite. D, Frequency-dependent magnetic susceptibility (Xfd) against magnetite content (IRM 0.3T). Xfd is sensitive to a narrow range of magnetite grain size, around 20 nm, having superparamagnetic behavior.

cooling. The latter possibility is suggested petrographically by hematite rims found commonly on magnetite spheres. Notably, the relatively low-iron fly ash from unit 3 contains nearly as much hematite as does the high-iron bottom ash from unit 1. The relative hematite enrichment in unit 3 fly ash is indicated in the plot of S against $IRM_{0.3}$ (Fig. G1c). The very low S values of about 0.84 for coarse-side and about 0.63 for fine-side fly ash reflect very high amounts of hematite relative to magnetite and thereby indicate substantial oxidation of the fly ash particles, presumably during their transport from the unit 3 boiler. Similarly, hematite content of the unit 1 fly ash (S=0.89) is high relative to its cogenetic bottom ash (S>0.95).

Magnetite Grain Size

For the most part, our dual-frequency MS method yields little evidence for substantial superparamagnetic behavior in any of the samples. Consistently in each collection, bottom ash from unit 1 had frequency-dependent MS (X_{fd}) values greater than 5 % and as much as 18 %, indicating a large concentration of grains about 20 nm in diameter (Fig. 15D). X_{fd} values of about 2-5 % imply the presence, but not abundance, of such ultrafine grains in the other bottom and fly ash samples.

Hysteresis ratios of bulk samples of fly and bottom ash from both units (5G samples; November, 1994) indicate overall pseudosingle-domain (PSD) behavior, characteristic of magnetite in the size range from 0.1 μm to about 10 or 20 μm (Table G2). Although many grains of this size range do occur, as confirmed petrographically for the 2-20 μm sizes, the results may be ambiguous with respect to the range of particle sizes for several reasons. First, large oxide grains may contain smaller subdivided magnetite volumes that give PSD or single-domain (SD; 0.03-0.1 μm) behavior. Second, a mixture of large multidomain (MD; >20 μm) magnetite grains with SD grains would contribute to the overall pseudosingle-domain signature of the bulk samples. Preliminary transmission electron microscopic study reveals magnetite grains in the SD-size range (G. Nord, written communication), and reflected-light microscopy reveals magnetite grains sufficiently large for MD behavior.

Table G2. Summary of hysteresis ratios, 5G Collection, November, 1994. (M_{rs}, saturation remanent magnetization; M_s, saturation magnetization; H_{cr}, coercivity of remanence; H_c, coercivity; PSD, pseudosingle domain.

Sample	M_{rs}/M_s	H_{cr}/H_c
Unit 1 Fly Ash	0.14	2.86
Unit 1 Bottom Ash 60 mesh	0.14	2.79
Unit 3 Fly Ash Fine-Side	0.16	3.44
Unit 3 Fly Ash Coarse-Side	0.15	2.82
Unit 3 Bottom Ash 60 mesh	0.07	3.38
Range for PSD magnetite	0.05-0.5	1.5-4.0

Temporal Changes in Magnetic Properties

We present two examples that illustrate changes in magnetic properties with time. In the first example, pyritic sulfur in feed coals is plotted against MS. The plot of results from both units illustrates that an approximate order of magnitude difference in pyritic sulfur is associated with a similar difference in MS (Fig. G2a). The decrease in pyritic sulfur in unit 1 feed coal over three months (July, August, and September, 1994; collections 1, 2, and 3, respectively) was accompanied by decreases in MS of nearly all samples of the different ash components (Fig. G2b).

In the other example, changes in magnetite and hematite contents are shown through time (Fig. G3). In the fly ash from unit 1 (Fig. G3a) hematite content (HIRM) increased greatly while magnetite content (MS) changed slightly between July and October, 1994. In most samples of both ash types from unit 3 (Fig. G3b), magnetite content varied without strong departures in hematite content. An exception is the September collection, in which large amounts of hematite were produced, perhaps at the expense of magnetite. These changes in the magnetic mineralogy of waste products from the same boiler may reflect changes in conditions of combustion and (or) cooling.

Relations Between Magnetic Minerals and Trace-element Composition

Several types of observations are being made to evaluate magnetic iron oxides as sites for the concentration of hazardous elements. One observation involves a comparison of the trace-element composition (using instrumental neutron activation analysis) of magnetic and nonmagnetic fractions separated from fly and bottom ash. Thus far, the project members have compared only three pairs of samples from the July, 1994, collection: fly ash from both units and bottom ash from unit 1. Nickel is enriched by a factor of two or more in the magnetic fractions; Cr and Co show at most only slight enrichment (a few tens of percent) in the magnetic fraction. Zinc is slightly enriched in the fly-ash magnetic fraction from unit 1 but is relatively depleted in the other samples.

Another type of observation involves comparisons between magnetic properties and trace-element compositions of bulk samples (Fig. G4). High magnetization (reflecting abundant magnetite) fly and bottom ash from unit 1 contains substantially more Zn plus Ni than low magnetization ashes from unit 3 (Fig. G4a). Mass balance calculations are needed to determine whether this relation is caused by the enrichment of these elements in the iron oxides or whether it merely reflects the higher abundance of these elements in the G1 feed coal. Ni+Zn contents for the August, 1994, feed coals (2G samples) are about 18 ppm for unit 3 and 69 ppm for unit 1. Contents of Co+Cr in the unit 3 fly ash samples, however, range from slightly to greatly higher than those contents in the unit 1 ashes (Fig. G4b) and so do not appear to be closely related to bulk-sample magnetite content. Co+Cr contents for the August, 1994, feed coals (2G samples) are about 21 ppm for unit 3 and 25 ppm for unit 1. Neither Ni+Zn nor Co+Cr content consistently corresponds to hematite content (HIRM) (Figs. G4c,d).

A third type of observation comes from the measurement of Curie temperatures of magnetic-mineral concentrates (Figs. G5, G6). In this measurement, very small amounts (typically <1 mg) of the most strongly magnetic grains were measured; for this reason the results do not reveal the range of magnetic substances in the separates. Pure magnetite has a Curie temperature of about 580 °C; the solid-solution addition of most metals (but not Ni) suppresses the Curie temperature. Some examples of Curie temperatures of end-member ferrites include: 440 °C for $MgFe_2O_4$, 520 °C for $CoFe_2O_4$, and 585 °C for $NiFe_2O_4$. Curie temperatures of the magnetic separates from fly ash are between about 570 and 580 °C, indicating pure magnetite, or magnetite in which minor amounts of some other element has substituted for iron (Fig. G5). The nearly reversible paths of heating and cooling

indicate a lack or paucity of maghemite. In contrast, two samples of bottom ashes (one from each unit) have greatly suppressed Curie temperatures indicating that the magnetite is strongly doped in solid solution with one or more other elements (Fig. G6). Further examination using scanning electron microscopy with energy-dispersive analysis, microprobe analysis, or single-crystal x-ray diffraction is needed to determine the elemental composition of these strongly magnetic particles.

Summary

1. Preliminary magnetic, geochemical, and XRD work on the coal combustion waste products from the two units strongly suggests that Ni, as well as Cr and perhaps Zn, are enriched in at least some of the magnetic minerals. It should be possible to predict the potential for release or retention of such elements under different disposal conditions from a knowledge of the conditions of iron oxide stability.

2. Monitoring the magnetic minerals produced over time in the same boiler may provide useful and inexpensive information on changes in the redox environment of combustion or some other factors that reflect combustion efficiency.

3. Future work should proceed with a fuller understanding of the magnetic behavior of spinel-structure ferrites that contain Ni, Mg, Co, Cr, Zn, and Al. In particular, if saturation inductions are found to vary greatly among these species, then we may use IRMs imparted at different inductions to help recognize their presence.

4. Because iron oxide minerals are magnetic, they can readily be removed from the greater nonmagnetic fraction using magnetic or electromagnetic separation techniques. If these minerals contain toxic elements, they may be concentrated and handled separately for disposal or other use.

5. If redox conditions control certain geochemical, mineralogic, or physical properties of recoverable byproducts, then the magnetic properties that reflect redox during combustion and cooling may help determine the suitability of waste products for other uses.

6. Magnetic iron oxide minerals produced during coal combustion appear to have diagnostic textures that would be useful in studies to determine the aerial dispersion of particulates from stacks. Although low in abundance, such minerals can be easily concentrated from material such as lake sediment.

Acknowledgments. Hysteresis measurements were made on a vibrating sample magnetometer at the Institute for Rock Magnetism (IRM), which is funded by the National Science Foundation, the W.M. Keck Foundation, and the University of Minnesota.

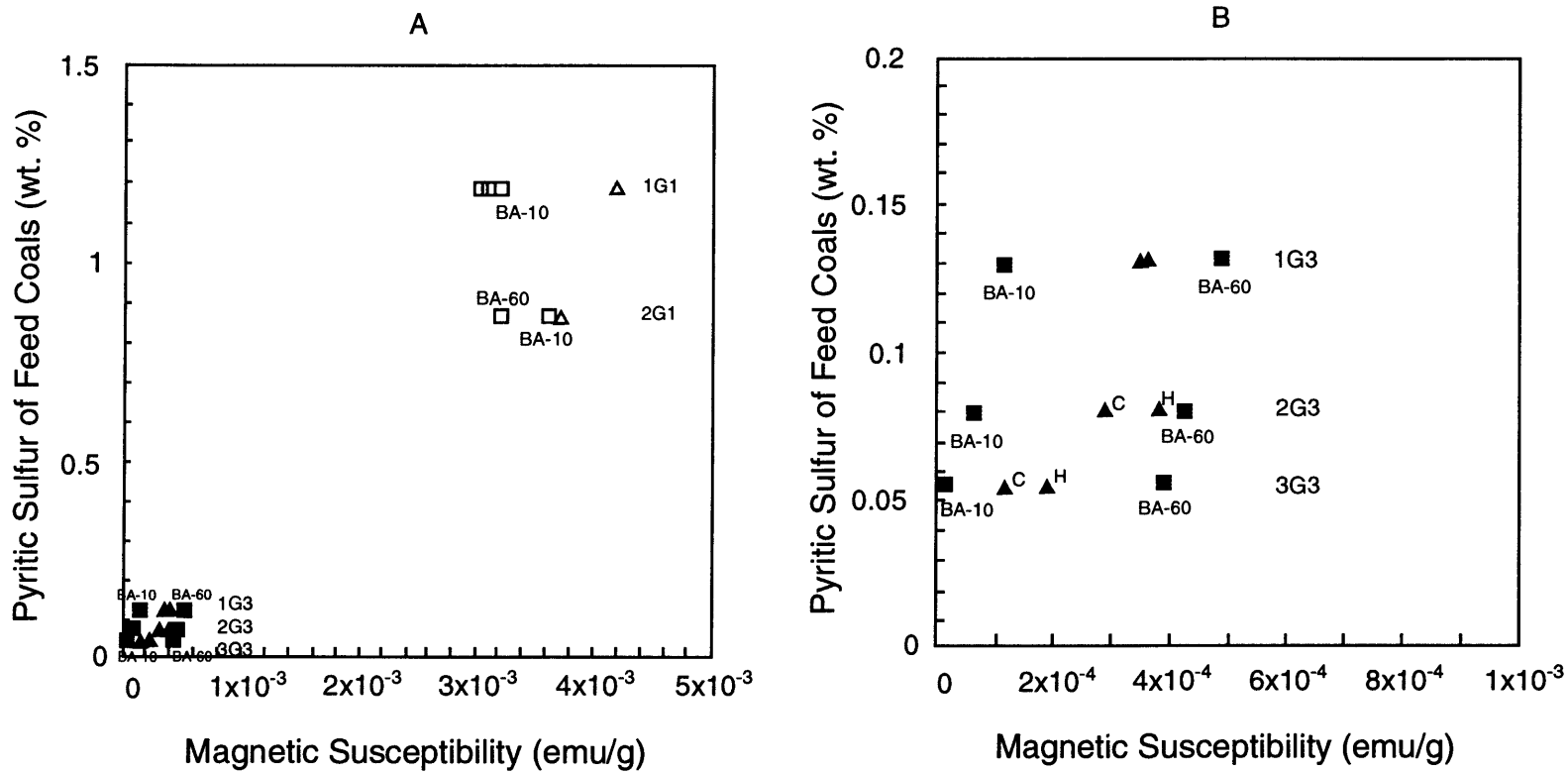

Figure G2. Variations in pyritic sulfur and magnetic susceptibility for the July to September (1994) collections from unit 3 (1G3, 2G3, and 3G3, respectively) and the July and August (1994) collections from unit 1 (1G1 and 2G1, respectively). Bottom ash samples at 10 and 60 mesh are indicated by BA-10 and BA-60, respectively. Fly ash samples from the fine side port are indicated by a "C" and fly ash samples taken from the coarse side port are indicated by an "H".

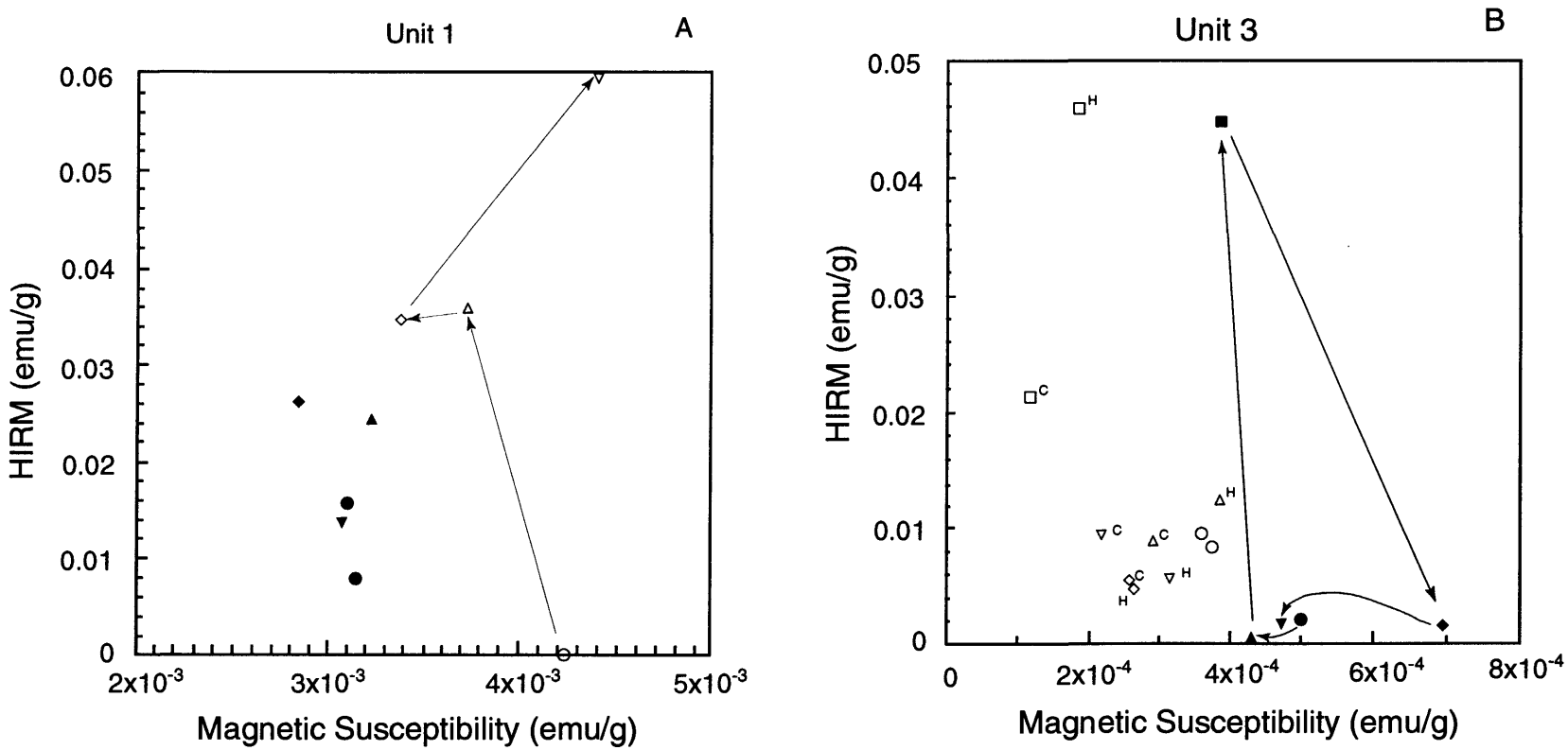

Figure G3. Plots of HIRM against magnetic susceptibility, indicating variations in hematite and magnetite contents, repectively, over time. Fly ash samples from unit 3 included those taked from the fine side (c) and coarse side (H). All bottom ash samples plotted are 60 mesh size. Two bottom ash samples from the unit 1 July (1G) collection are plotted .

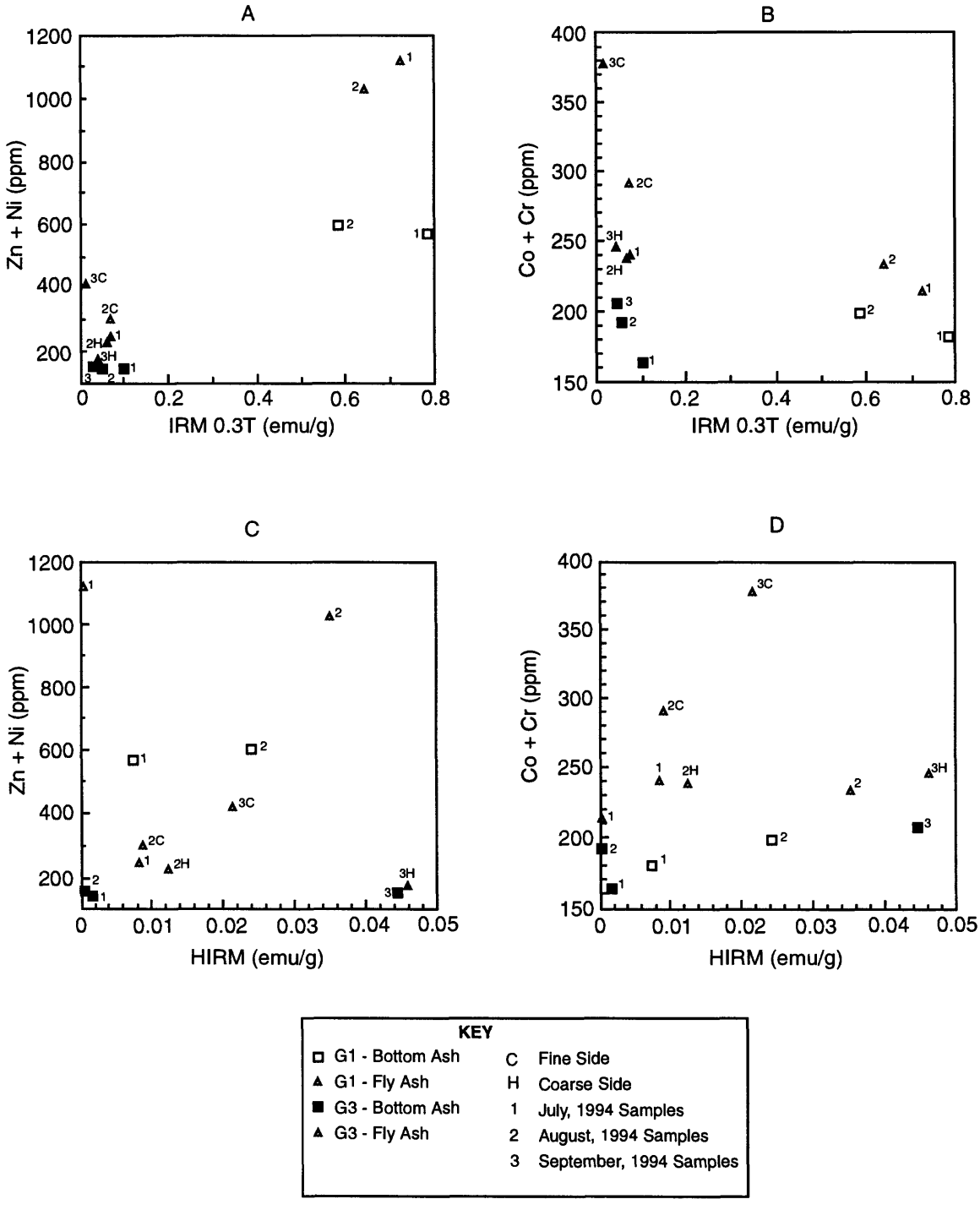

Figure G4. Plots of trace element contents against magnetic properties. A) The sum of Zn and Ni against magnetite content, represented by IRM 0.3T. B) The sum of Co and Cr against magnetite content. C) The sum of Zn and Ni against heamtite content, represented by HIRM. D) The sum of Co and Cr against hematite content.

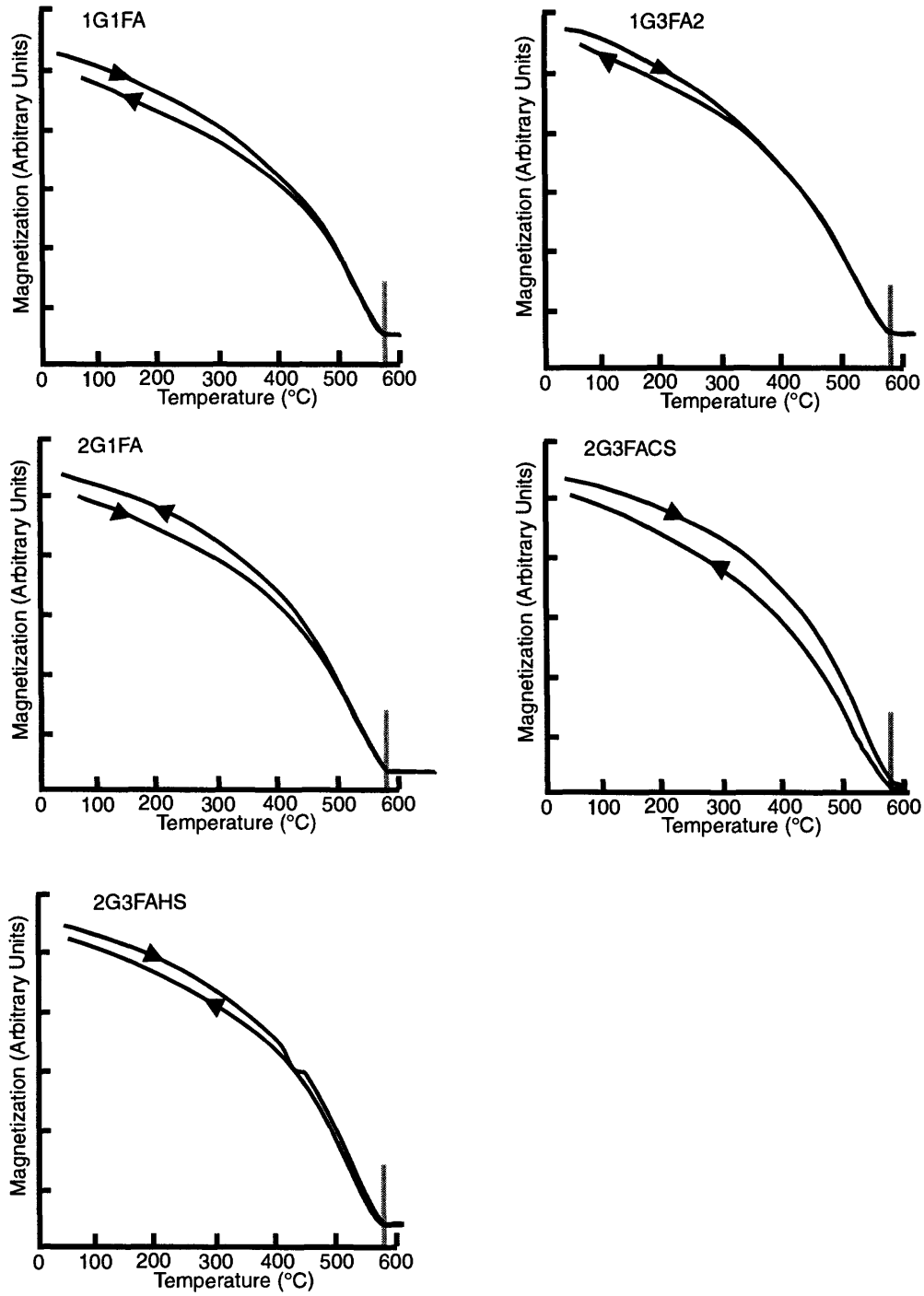

Figure G5. Thermomagnetic curves for samples of fly ash. Heating and cooling curves are represented to the right and left respectively. Light gray line at 580 °C indicates the Curie point of pure magnetite.

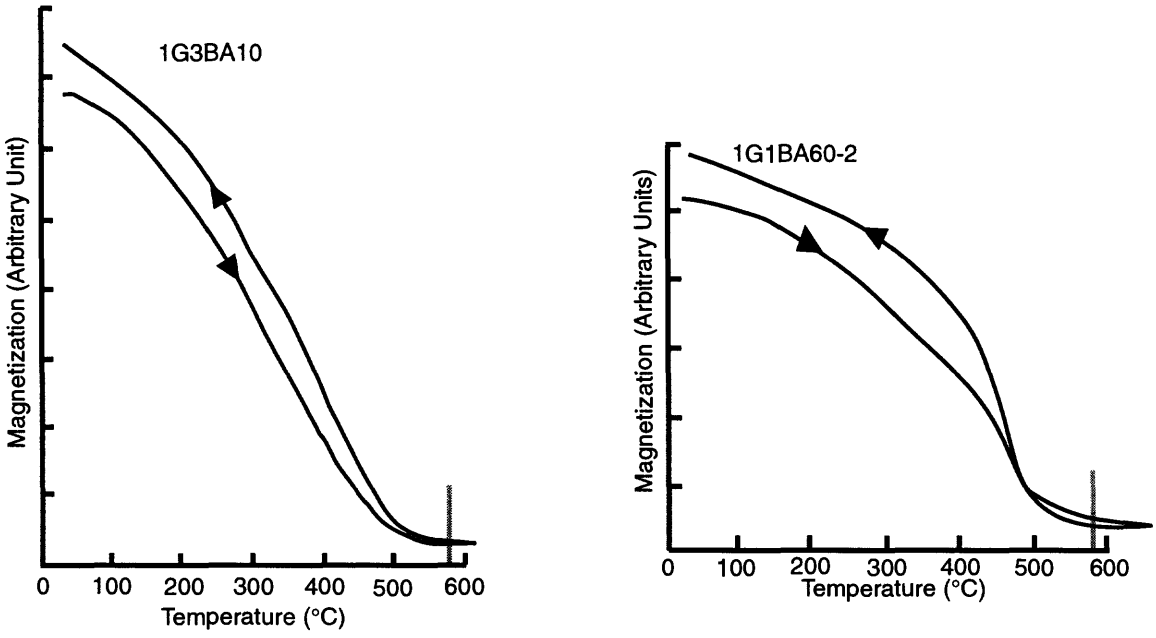

Figure G6. Thermomagnetic curves for samples of bottom ash. Heating and cooling curves are represented by arrows to the right and left, respectively. Light gray line at 580 °C indicates the Curie point of pure magnetite.

H. RADIONUCLIDES IN COAL AND COAL COMBUSTION WASTE PRODUCTS

by Robert A. Zielinski and James R. Budahn, U.S. Geological Survey, Denver, Colorado.

Uranium distribution in ash particles

The distribution of uranium in individual particles of fly ash and bottom ash was directly observed using fission-track radiography. Preliminary results indicate that the technique holds considerable promise for studies of uranium in coal combustion wastes. Particle-based observations provided by fission-track radiography are highly specific for uranium and complement bulk-sample observations of uranium concentration and leachability. The combined results permit more informed prediction of the behavior of uranium during physical or chemical treatment of fly ash, or prolonged environmental exposure. The variety of uranium hosts and uranium distributions observed in ash particles illustrates the complexity that should be expected when other refractory trace elements are investigated by particle-specific techniques.

Polished thin sections of grains of fly ash or bottom ash were irradiated with neutrons in the USGS research reactor to induce fission of ^{235}U in the samples. During irradiation, fission fragments recoil from the surface of the thin section and pass into an overlying sheet of muscovite mica detector material. The passage of fission fragments causes linear paths of damage (tracks) in the mica that are made visible by subsequent etching of the recovered mica in HF. Areas of high fission track density in the mica can be related to areas of high uranium concentration in the original sample. Depending on the angle of incidence, fission-track lengths in the mica are <1 to 5 μm. Very small uraniferous grains or rinds <1 μm thick are magnified by this technique because recorded fission tracks are up to 5 μm long. More subtle gradients in uranium concentration (>2X) can be detected by observing changes in fission-track density across particles of >10 μm diameter.

Dominantly spherical particles from fly ash sample 1G1FA (+250 mesh fraction) and dominantly charred coal particles from sample 1G3FA (+60 mesh fraction) were prepared as grain mounts on polished thin sections. Previous analysis of the as-received samples by a delayed neutron technique indicate bulk uranium contents of approximately 15 and 12 ppm respectively. The resulting fission-track images of cross sections of spheres and other particles revealed interesting variety in the distribution of contained uranium as summarized below.

1. Hollow glassy spheres (cenospheres) show uniform distribution of uranium in glassy rims with no apparent evidence of surface enrichment (Fig. H1). Dark-colored, Fe-enriched glass appear to have higher concentrations of uranium than clear glass and some spheres are a mixture of dark and clear glass.

2. Glass-rimmed spheres filled with a variety of smaller spheres (plerospheres) show the expected variety of uranium concentrations in the fill material but retain a uniform distribution of uranium in glassy rims. Apparent uranium enrichment on the surfaces of some of these spheres could be explained by relatively uraniferous glassy rims.

3. A few rare spherical particles are filled with uranium-rich crystalline material (Fig. H2). Further characterization by SEM-EDS indicate the presence of Ca, Al, Si, Fe and P.

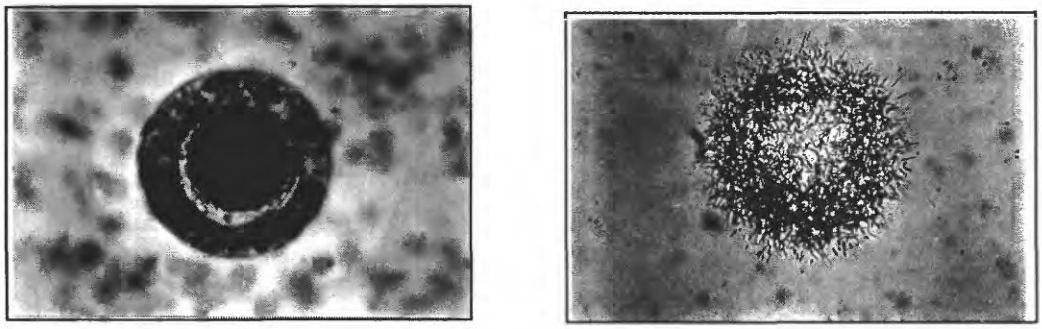

Figure H1. Photomicrograph (left) and corresponding fission-track image (right) of uranium distribution in a hollow glassy sphere from fly ash 1G1FA. 400x magnification. Long axis of photo is 250 μm.

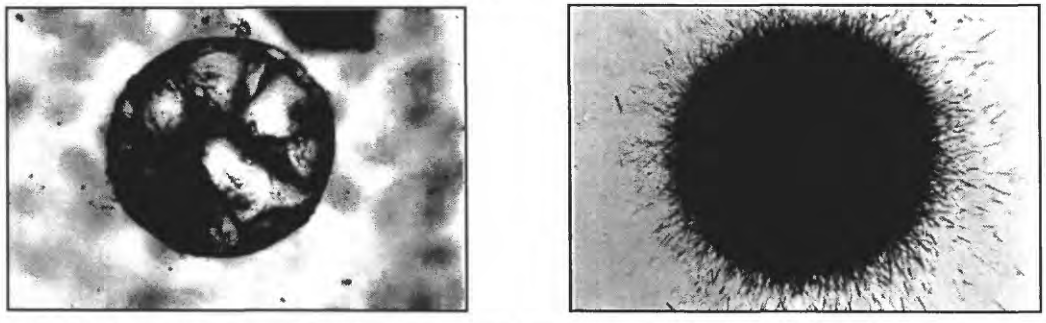

Figure H2. Photomicrograph (left) and corresponding fission-track image (right) of a uraniferous crystalline sphere from fly ash 1G1FA. 400 x magnification. Long axis of photo is 250 μm.

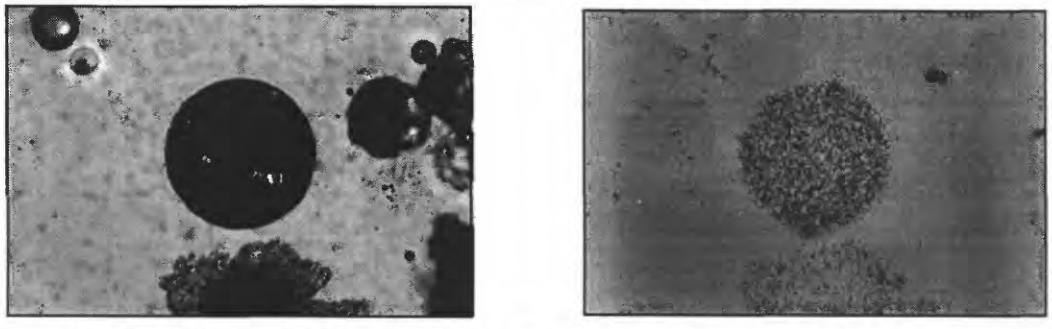

Figure H3. Photomicrograph (left) and corresponding fission-track image (right) of an opaque sphere from fly ash 1G3FA. 100x magnification. Long axis of the photo is 980 μm.

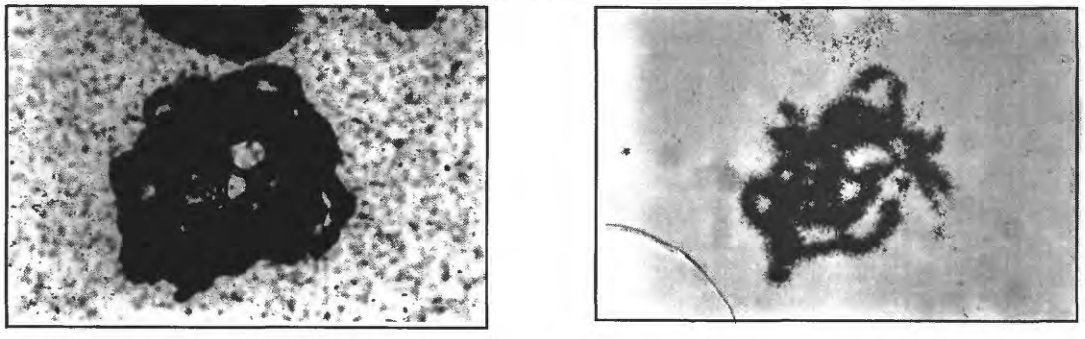

Figure H4. Photomicrograph (left) and corresponding fission-track image (right) of a charred coal fragment with areas of uranium enrichment from fly ash 1G3FA. 100x magnification. Long axis is 980 μm.

4. Spherical opaque grains can contain moderate amounts of uniformly distributed uranium (Fig. H3). The resolution of this technique is insufficient to determine if uranium is in constituent magnetite or in uniformly distributed hematite replacements of magnetite.

5. Other irregularly shaped opaque grains have non-uniform distribution of uranium on the surfaces exposed by the thin section. In some cases this can be attributed to red areas (hematite?) or to composite grains of opaque and glass.

6. Additional rare, irregularly-shaped grains have high uranium contents. Possible phases include Ti-bearing minerals such as sphene quartz grains have very low uranium.

7. Charred coal particles generally have low uranium concentrations and rather uniform uranium distribution. One interesting exception has a markedly higher uranium concentration that followed a sinuous, tortuous pattern (Fig. H4).

Uranium and Decay Products in Coal Combustion Wastes

High precision gamma-ray spectrometry of coal combustion wastes was performed to determine if combustion caused significant fractionation between uranium and its long-lived radioactive decay products ^{226}Ra (half-life =1600 y) and ^{210}Pb (half-life = 22.3 y). Uranium daughter products are significant sources of radioactivity in coal combustion wastes and their geochemical mobility during coal combustion and subsequent management of wastes can be very different from parent uranium. Radioactive isotopes such as ^{210}Pb can also serve as tracers for monitoring the partitioning of elemental lead.

Initial setup included modifications to the gamma counting equipment to reduce background counts and the use of calibrated radioisotope sources to correct for variable attenuation of the measured gamma-ray energies in the 150-250 g sample splits. Samples were sealed for three weeks prior to counting to permit attainment of radioactive equilibrium between ^{226}Ra and its short-lived daughters (through ^{214}Po). Radioactivity of each measured isotope (in disintegrations-per-minute per gram) is directly compared to that of the other measured isotopes. Analytically significant deviations from equal-radioactivities suggest departure from the condition of secular equilibrium expected in the original feed coals. Preliminary results include direct determination of ^{226}Ra as well as a better-determined proxy value for ^{226}Ra based on the activity of its short-lived daughter product ^{214}Pb (half-life = 26.8 min). The latter may be fractionated during coal combustion but re-establishes radioactive equilibrium with ^{226}Ra during the three week period of closed-system storage prior to counting.

Very preliminary results for two samples of fly ash and one bottom ash (Fig. H5) suggest that ^{238}U and ^{226}Ra (or ^{214}Pb proxy) are not significantly fractionated. In contrast, there is some indication of preferential enrichment of ^{210}Pb on one sample of fly ash and depletion in the bottom ash compared to ^{238}U and ^{226}Ra. If this trend is confirmed in subsequent analyses the apparent fractionation of ^{210}Pb relative to ^{238}U and ^{226}Ra may relate to the expected greater volatility of lead during coal combustion.

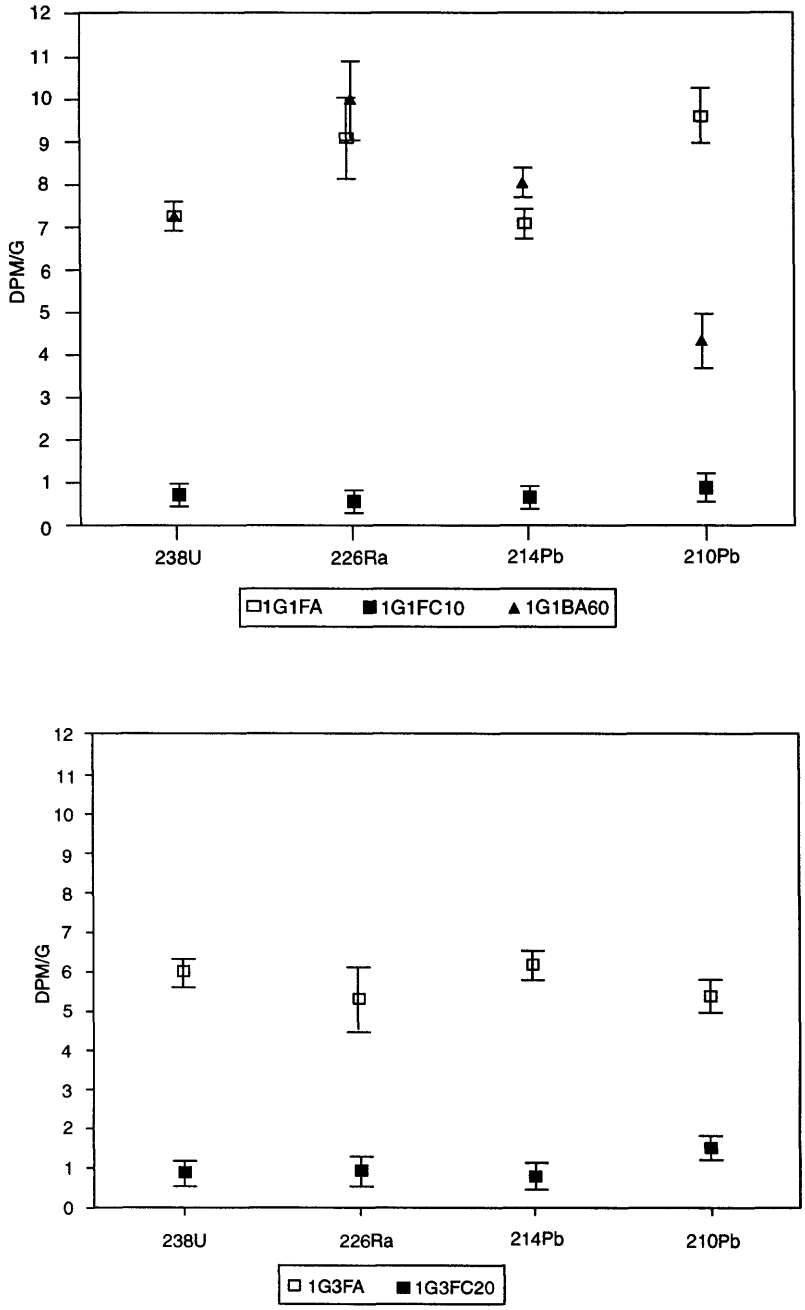

Figure H5. Comparative radioactivity of four ^{238}U decay-series isotopes in samples of feed coal (FC), fly ash (FA), and bottom ash (BA) from the high-sulfur (1G1) and low-sulfur (1G3) units. Error brackets indicate estimated analytical precision of ± one standard deviation.

I. WATER-SOLUBLE ANIONS: IMPLICATIONS FOR SOLUBLE PHASES ON COMBUSTION PRODUCT SURFACES

by George N. Breit and Jerry M. Motooka, U.S. Geological Survey, Denver, Colorado.

Common inorganic anions such as chloride, nitrate, phosphate and sulfate participate in many natural processes at the earth's surfaces. Among these processes are those that impact the mobility and accumulation of some trace elements. As part of the characterization of combustion products of the power plant, anion analyses were conducted on water extracts of selected fly ash, bottom ash and feed coals to provide data relevant to understanding the fate of combustion products. The purpose of these analyses is to complement cation and trace metal analyses (Motooka and others, this volume) by identification of soluble anions. Results of both the anion and cation analyses provided input to computer-based chemical models used by Rice (this volume).

Methods of analysis

Approximately 1 gram of sample and 10 milliliters of water were agitated for 1 hour. The suspension was centrifuged and the solution injected in an ion chromatograph to determine anion concentrations. Thermal gravimetric analysis of selected samples was done on 20 mg samples heated from 25 to 1100 °C at a rate of 10 °C/minute.

Results and Discussion

Results of the water-soluble anion analyses are presented in Table I1. Concentrations are relative to the dry solid. Samples of feed coal have detectable water-soluble chloride and sulfate.

Table I1. Concentrations of water soluble anions in feed coal, fly ash, and bottom ash. (G1, samples from high-sulfur unit; G3, samples from low-sulfur unit; FC feed coal, FA, fly ash; BA, bottom ash; 10, -10 mesh; 60, -60 mesh)

Sample Number	Chloride (ppm)	Sulfate (ppm)	Other Anions Detected
1G1FC60	60	4,000	-
1G1BA60	20	290	phosphate
1G1FA	<5	4,400	-
1G3FC60	100	350	-
1G3BA10	<10	<20	phosphate
2G1BA10	24	320	phosphate
1G3FA	5	3,900	-
2G3BA10	25	120	fluoride, nitrate
2G3BA60	54	230	fluoride, nitrate
2G3FA (fine)	130	33,000	-
2G3FA (coarse)	60	3,800	-
3G3BA10	20	58	fluoride, nitrate
3G3FA (fine)	100	16,000	-

In all materials analyzed sulfate is the most abundant water extractable anion. The sulfate extracted from the coal is attributed to oxidation of sulfide minerals. The markedly higher content of sulfate in 1G1 (high-sulfur coal) relative to 1G3 (low-sulfur coal) is notable and consistent with the composition of the coal (Eble, this volume). Results of the bottom ash analyses are ambiguous because they were collected from a "water train". Suspension of the bottom ash particles in the water likely removed most of the soluble constituents. Anions detected in our analyses likely precipitated from the transport water when the sample was dried. The trace but consistently detectable quantities of fluoride and nitrate in G3BA samples and phosphate in G1BA samples are tentatively attributed to the transport water. Variation in the fly ash composition, particularly between the fine side and coarse side will be the focus of the subsequent discussion.

The fine-side fly ash has soluble sulfate contents 10 times the value for the coarse side for two consecutive samplings. This difference in sulfate is also matched by the lower pH (3.0) and higher water-soluble metal content in the fine-side ash relative to the coarse-side ash as reported by Anderson and Leventhal (this volume). Because the water soluble sulfate is a significant fraction of the solid (2 to 3 wt. %), a thermal gravimetric analysis (TGA) was conducted to identify the sulfate solid. The TGA results do not match any common sulfate compound, but the temperature of maximum weight loss is close to that determined for alunite ($KAl_3(SO_4)_2(OH)_6$). Further work is needed to refine the identification but the results are consistent with the large amounts of potassium and aluminum detected in the water-soluble fraction of the fine-side fly ash (Motooka and others, this volume). An additional factor supporting the presence of aluminum sulfate is the low pH. In near neutral pH dissolved aluminum reacts with water to form aluminum hydroxide. Formation of the aluminum hydroxide lowers pH. Results of equilibrium computer modeling showed that water that reacted with the fine-side fly ash precipitated aluminum hydroxide (Rice, this volume).

Hypothesis

The aluminum sulfate on the fine-side ash probably formed by reaction of sulfur oxide gases, steam and ash particles. Sulfur oxides and water adsorbed on the fly ash particles would etch the surface of the silicate glass and release aluminum and potassium from the matrix. The lower amount of leachable sulfate in the coarse relative to the fine fly ash from unit 3 may be attributed to particle size or temperature of the exhaust gas near the precipitators.

Implications

The contrasting composition of water produced by reaction of fine-side and coarse-side ash reflects the complex composition of the ash and the need for detailed studies. The fine-side ash, because of the low pH and high soluble aluminum content, may be suited for special uses. Precipitation of aluminum from the ash as a hydroxide could trap trace elements by adsorption and coprecipitation, and lead to clay precipitation that would decrease permeability within a disposal site.

J. COAL ASH ENVIRONMENTAL LEACHING: pH

by Tim Anderson and Joel S. Leventhal, U.S. Geological Survey, Denver, Colorado

The mobility of trace elements from fly ash and bottom ash produced during coal combustion is a concern because of the large amount of combustion solids in disposal sites. A major parameter in controlling element mobility is pH. This paper summarizes results of experiments to determine how pH is affected by reactions of feed coal, fly ash and bottom ash with deionized water.

Our first experiment was to put one gram samples of feed coal (FC), fly ash (FA), and bottom ash (BA) in 6 mL of deionized water, shake them and monitor the changes in pH with time (1hr, 2 hr, 6 hr, 24 hr, 96 hrs and 126 hours). This rather simple experiment yielded interesting results for both the high-sulfur (unit 1, 3.3 wt.% S) and low-sulfur (unit 3, 0.9 wt.% S) feed coals (Fig. J1 and J2). Results of leaching of the feed coal are analogous to natural weathering of a coal outcrop and depend on the chemical form of sulfur (organic or pyritic) and physical properties such as surface area, fracture density, and grain size. The high-sulfur coal leachate initially was quite acidic (pH = 3.8) and, with time became less acidic (pH = 5.4). The low-sulfur coal leachate initially had a pH of 7 but within 2 hours became acidic (pH = 5.4) and remained near this pH for the 126 hour duration of this experiment. In contrast, the fly ash leachate for both coals becomes quite alkaline (pH 9 to 11) after a few hours. The bottom ash solution varies with time between pH 5.8 and 8.4 in an irregular fashion, probably as various minerals dissolve. The pH of the bottom ash solution is near neutral (around pH = 7) after 126 hours (Fig. J2).

Experiments (not shown on Figs. J1 and J2) that reacted the "coarse side" and "fine side" fly ash from unit 3 with water resulted in distinctly different solution pHs. The fine-side fly ash decreased the pH of the leach water to a value near 4, while the coarse side raised the pH to 9. This difference in pH for the different ash collection points may be useful in determining a way to blend ash fractions in order to stabilize the solution pH to be near neutral .

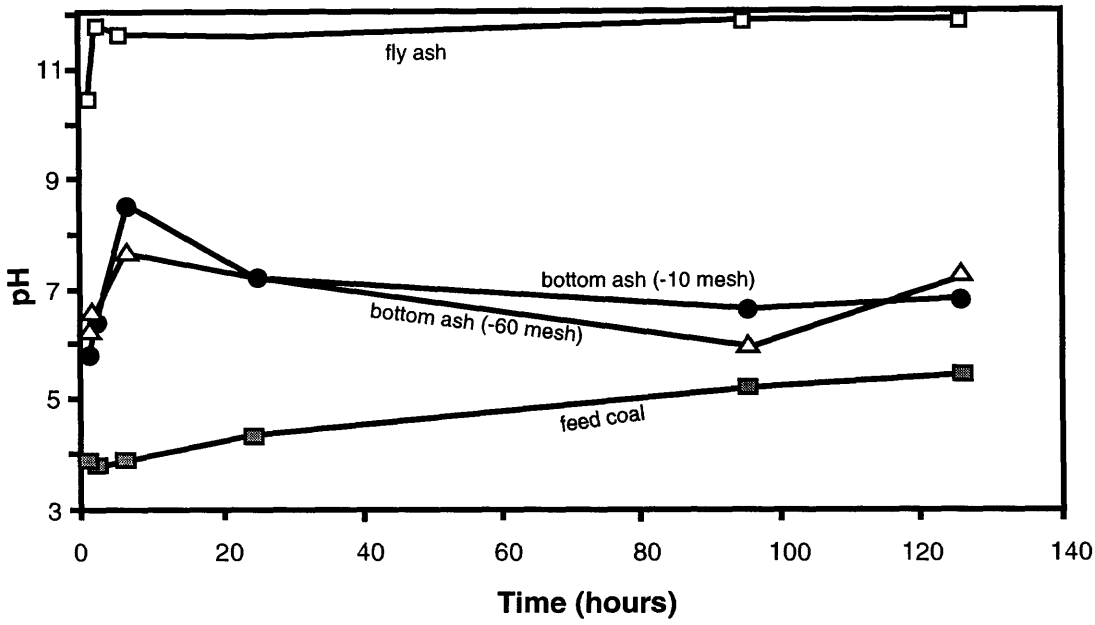

Figure J1. Evolution of pH in distilled water that has reacted with samples of fly ash, bottom ash and feed coal from the high-sulfur unit (unit 1).

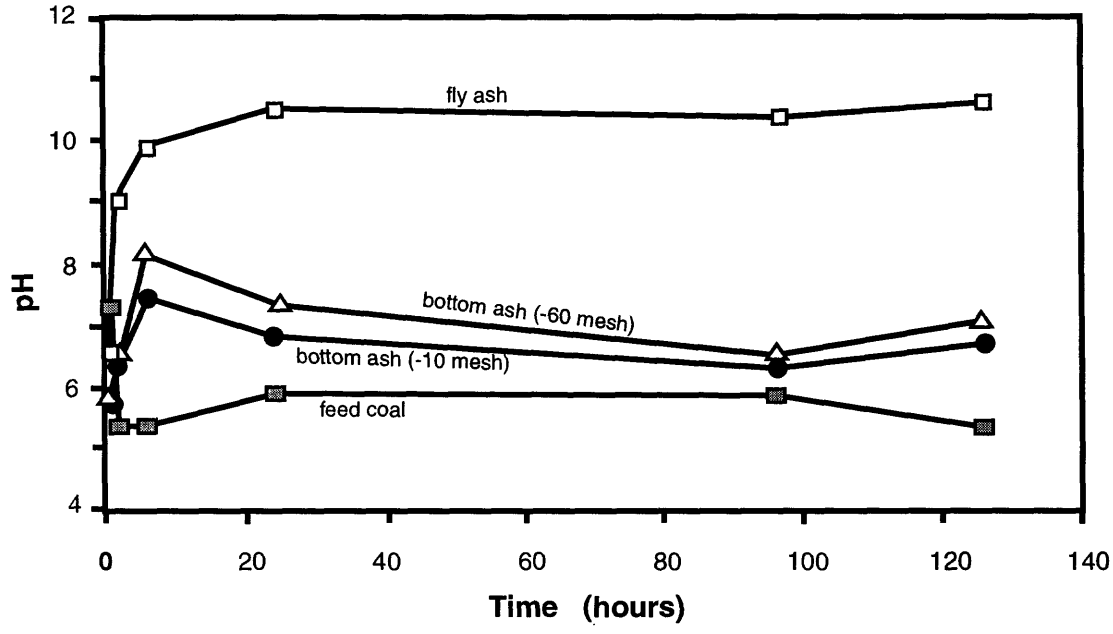

Figure J2. Evolution of pH in distilled water that has reacted with samples of fly ash, bottom ash and feed coal from the low-sulfur unit (unit 3).

K. COAL ASH ENVIRONMENTAL LEACHING: Elemental

by Jerry M. Motooka, Tim Anderson, Allen L. Meier, and Joel S. Leventhal, U.S. Geological Survey, Denver, Colorado

Selective (sequential) leaching of feed coal, fly ash, and bottom ash was investigated to help understand the behavior of these materials in the natural aqueous environment. This was accomplished by a sequential leaching of the solids with water, acetic acid / sodium acetate, and 1N HCl. The intent of the extraction scheme is to dissolve progressively more resistant phases and determine the relative amounts of trace elements dissolved by each extraction.

Subsequent to measuring the pH of the water leachate (Anderson and Leventhal, this volume), the water was analyzed by inductively-coupled plasma atomic emission spectroscopy (ICP-AES) and inductively-coupled plasma mass spectrometry for approximately 30 elements. The second sequential leach solution is similar to USEPA (TCLP 1311) solutions using acetic acid for the alkaline samples and sodium acetate for acid samples. After 20 hours we removed the solution and replaced it with 1N HCl for 24 hours. The ICP results are shown in Figure K1 for samples of bottom ash and fly ash from unit 1 (G1BA and G1FA) for the HCl leach. This plot depicts the ppm (log scale) of the element extracted by the HCl (after the water and acetate extracts), relative to the original ash weight of the sample. Certain elements are more abundant in the fly ash extract (S, Ca, Ti, V, Cr, Mn, Cu, Zn, As, Zr, Mo), whereas a few elements (Fe, Ni, Sn, W) are more abundant in the bottom ash extract. [Note: to convert the ppm to mg/L for a 20 mL extract solution (as in the acetate procedure) divide the ppm by 20.]

Figure K2 shows a log scale plot for the ICP-MS results of the water and acetate extractions plotted with total element present (all in ppm) in a fly ash from unit 3 (G3FA). The water leach has higher amounts of Ga, As, Rb, Mo, Sr, Xe, Sb, Ba, and W than the (next) sequential acetate leach, probably because this water leach is very alkaline. The acetate solution, which was buffered to approximately pH 5, contained a different suite of elements that were leached and or complexed by the acetate. These data are also interesting because generally only 1 to 10% of most elements are extracted by either of these solutions. This suggests that relatively small amounts of these elements are expected to be leached after disposal.

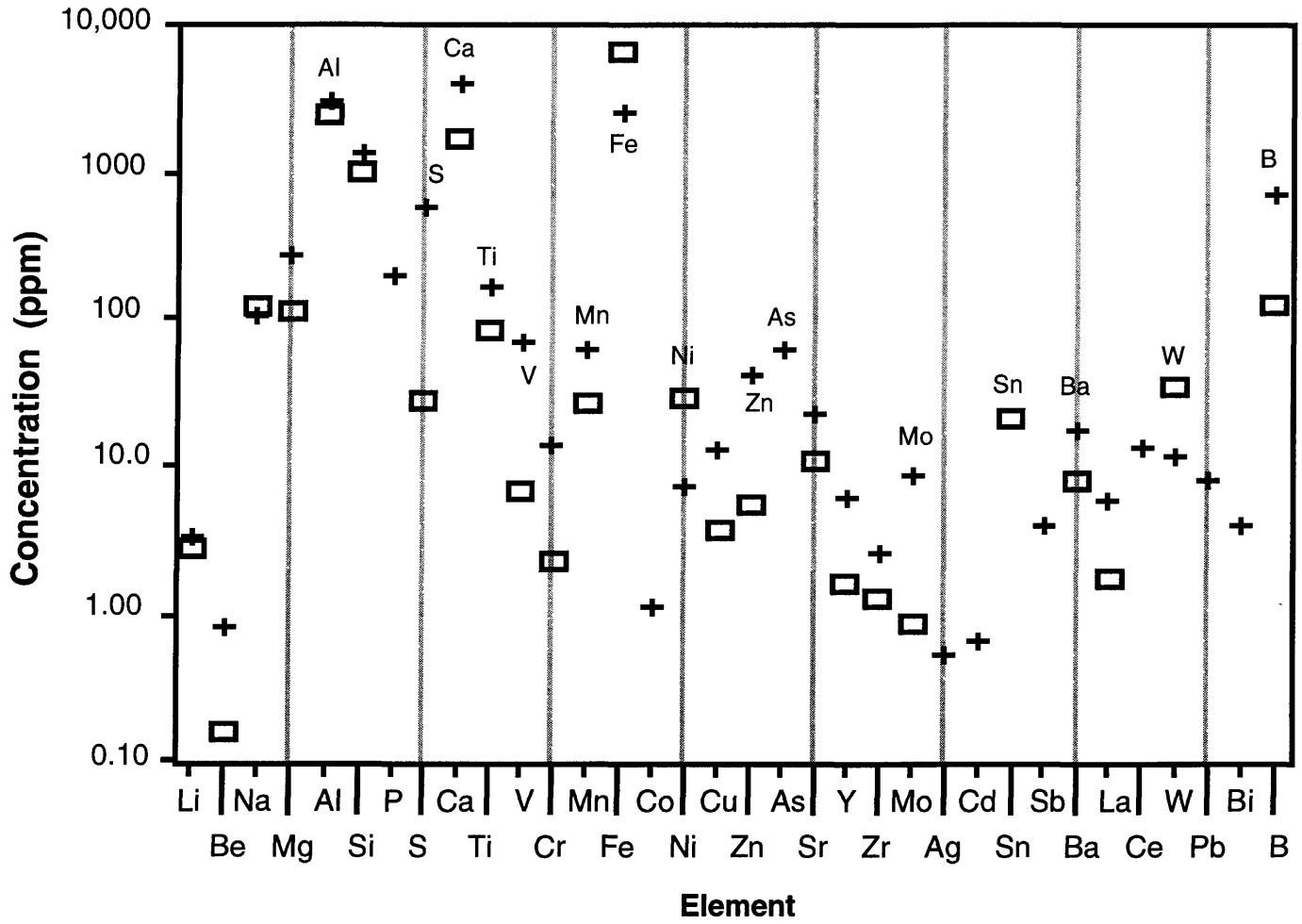

Figure K1. Concentration of selected elements in HCl leach solutions of fly ash and bottom ash from the high-sulfur unit (unit 1). Missing symbols indicate concentrations below the detection limit. (□ , bottom ash; +, fly ash)

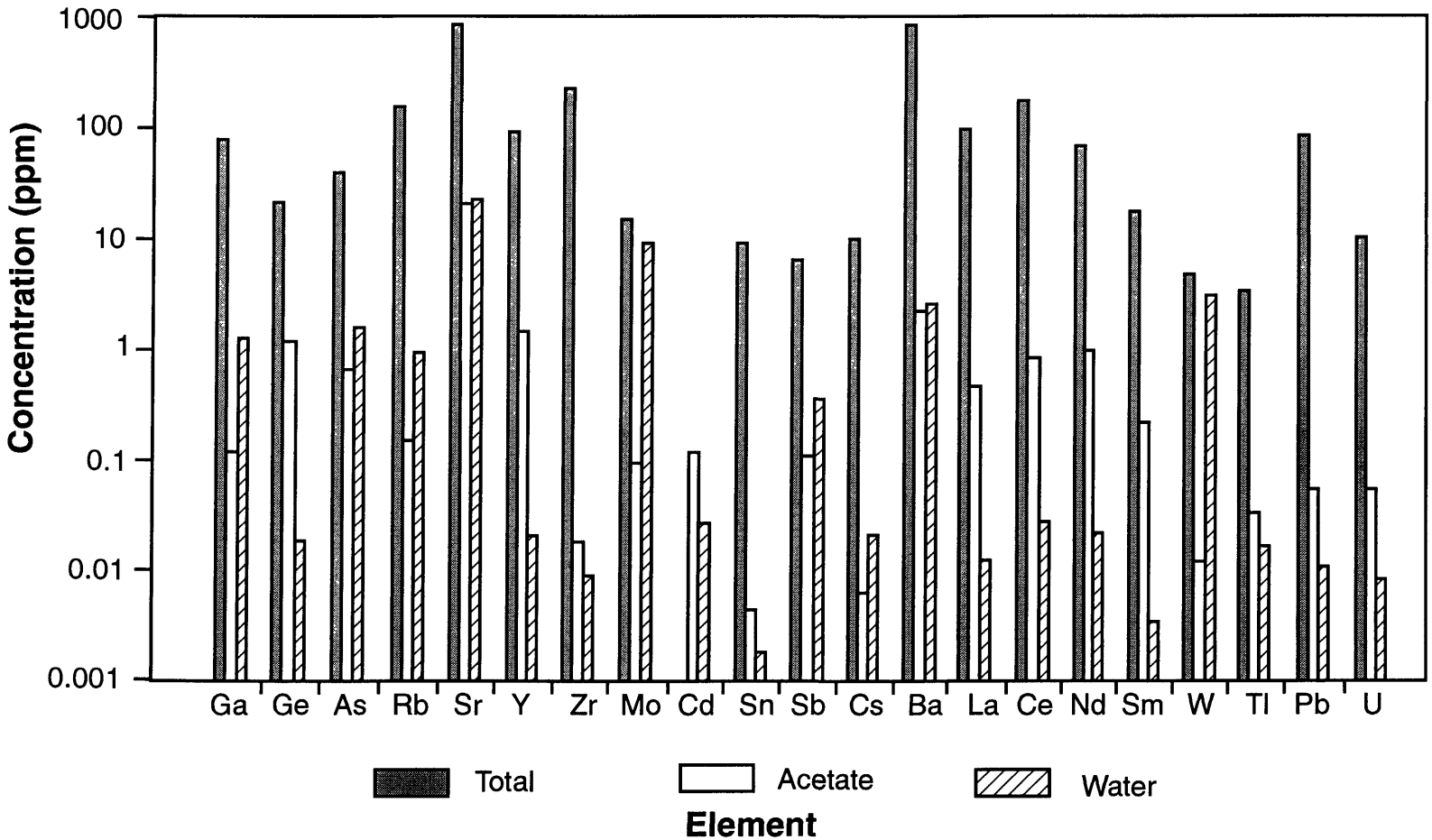

Figure K2. Concentrations of elements leached from the low-sulfur unit (unit 3) fly ash by water and acetate relative to the content in the bulk sample.

L. PRELIMINARY GEOCHEMICAL MODEL RESULTS OF WATER LEACHATES

by Cynthia A. Rice, U.S. Geological Survey, Denver, Colorado

The chemical composition of deionized water leachates of feed coal, bottom ash, and fly ash (Motooka and others, this report) were evaluated by geochemical modeling. The pH range reported by Anderson and Leventhal (this volume) ranges from 2.8 for a feed coal to 11.8 for a fly ash. Major element concentrations reported by Motooka and others (this volume) for feed coal, fly ash and bottom ash are similar within each group with a few notable exceptions. The deionized water leachate from one of the feed coals from the high-sulfur unit (2G1FC), has very low pH values, near 2.8, and correspondingly high values of Mg^{2+}, Al^{3+}, SO_4^{2-}, Ca^{2+}, Fe^{3+}. The pH and dissolved element concentration are consistent with the presence of jarosite, a common weathering product of pyrite. In addition, leachate solutions from fly ash taken from the fine side (FSFA) of the precipitators had much lower pH (pH = 3.9) values than solutions leached from fly ash taken from the coarse side (CSFA) of the precipitators (pH = 9). The CSFA leachates had much higher concentrations of Na^+, Mg^{2+}, Al^{3+} SiO_2, SO_4^{2-}, and Ca^{2+}, than did leachate solutions from HSFA. Geochemical modeling was applied to constrain possible reasons for the contrast in solution composition amoung the materials tested.

Breit and Motooka (this volume) proposed that a potassium-aluminum-sulfate (K-alum) phase formed on the fine-side fly ash of unit 3. This K-alum would be water soluble and account for the low pH values of the water that reacted with the FSFA and higher concentrations of Na^+, Mg^{2+}, Al^{3+}, SiO_2, SO_4^{2-}, Ca^{2+}. Geochemical computer modeling using Geochemists Workbench (Bethke, 1994) calculated that the reaction of a phase of the approximate formula $KAl(SO_4)_2 \cdot 10H_2O$, a potash alum, with water immediately lowers the pH to values observed in leachates of fine-side fly ash (Fig. L1). In addition, the modeling predicts that as the solution pH increases, possibly as a result of hydrolysis of the silicate glass, gibbsite [$Al(OH)_3$] will precipitate. However, because the concentrations of Al^{3+} are much higher in the FSFA leachates than those of the CSFA leachates, the amount of gibbsite that would precipitate from the fine-side leachate solutions is on the order of hundreds of times greater than that from the coarse side (Figs. L2 and L3). The importance of this difference to overall leaching of coal ash that is a mixture of fine and coarse sides needs to be determined. The results of the modeling suggest that water leaching of fly and bottom ash, such as would occur from slurrying the ash to a disposal site or in a disposal site, could potentially produce large amounts of the secondary mineral gibbsite. Aluminum oxyhydroxides and aluminum hydroxides are well-known scavengers of trace elements (Stumm and Morgan, 1981) and their formation through natural leaching of fly and bottom ash could be important in attenuating trace elements which are also released from coal waste. Similar reactions may occur in the bottom ash, but because this material was collected from a water train within the plant they could not be observed.

Preliminary leaching and modeling results raise questions that can be answered in future leaching studies and sample collections. The slurry water from which the bottom ash is collected should also be collected and analyzed to determine the extent of leaching of the bottom ash and whether or not secondary mineral phases can be expected to form from the slurry solution. During longer-leaching experiments, mineral phases are expected to form from the slurry solution . Longer-term, column leaching experiments are planned to determine the effects of water flowing the through fly and bottom ash over time. Studies by Dudas (1981) and Hassett (1993) indicate that long-term leaching results with water differ from very short, acidic leaching protocols used by regulatory agencies, with some trace elements being attenuated in the water-leaching experiments by the formation of secondary mineral phases such as aluminum hydroxide or ettringite. The long-term column leaching experiments planned for this study should allow investigation of secondary mineral formation. Leachate solution collection over the long-term will allow the

progress of the reactions to be monitored and will provide data for modeling the dissolution of condensed or adsorbed phases, as well as amorphous glass, mullite, spinels, calcium oxides, aluminum hydroxides, gypsum, and other mineral phases. Finally, experiments involving mixtures of different types of waste including flue gas desulfurization sludge and fly ash should be conducted to determine the effects of the co-disposal of different types of coal power plant waste. Leaching studies of individual waste components cannot adequately predict the expected behavior of a waste pile where several types of coal waste are mixed.

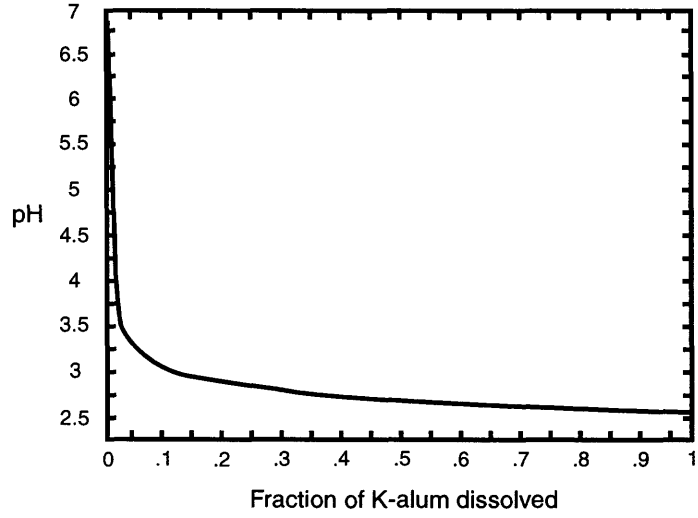

Figure L1. The effect of dissolution of twenty grams of potash alum $KAl(SO_4)_2 \cdot 10H_2O$ in 1 kg of water on the solution pH.

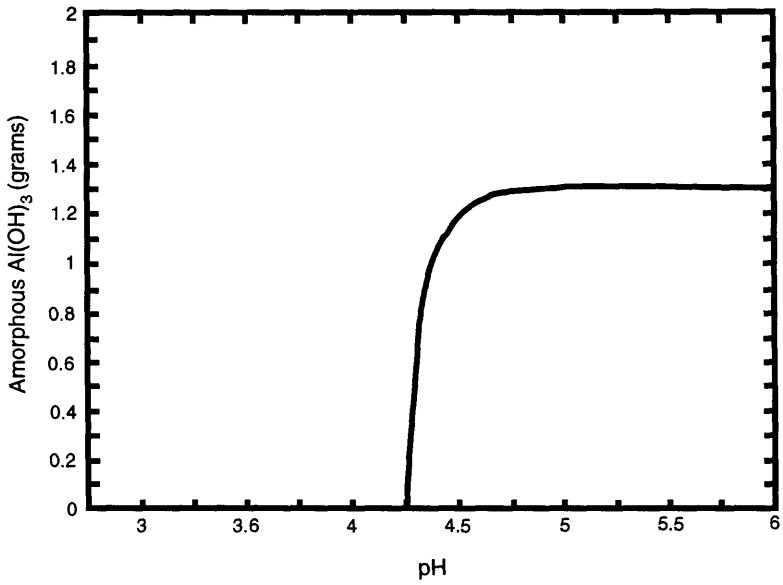

Figure L2. The amount in grams of amorphous $Al(OH)_3$ expected to form from 1 kilogram of water leachate solution of sample 2G3FA-- fine side. The solid to liquid ratio of fly ash to water is 1:6.

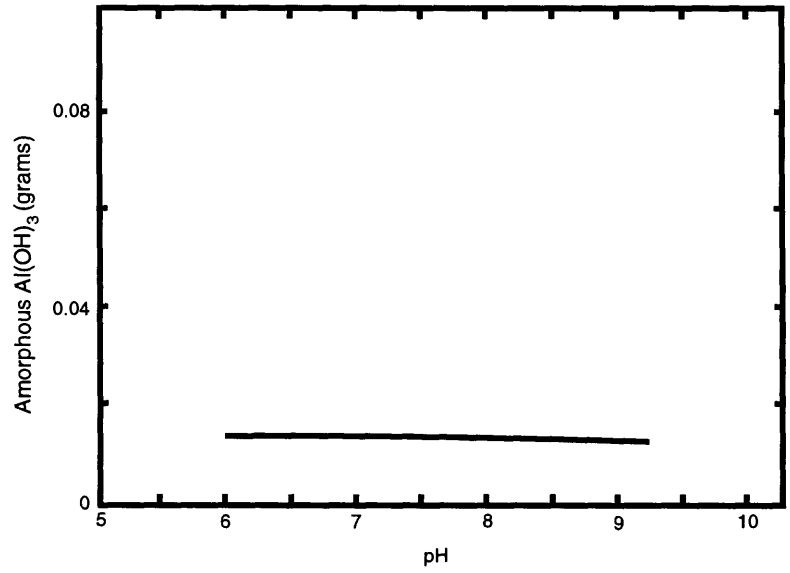

Figure L3. The amount in grams of amorphous $Al(OH)_3$ expected to form from 1 kg of water leachate solution of sample 2G3FA--coarse side. The solid/liquid ratio of fly ash to water is 1:6.

M. ELECTRON MICROPROBE ANALYSIS OF FLY ASH AND BOTTOM ASH

by James J. McGee, U.S. Geological Survey, Reston, Virginia

Introduction

This report summarizes analytical procedures and preliminary electron microprobe data for coal combustion waste products (fly ash and bottom ash). Electron microprobe studies of the ash are being conducted to identify the location and mode of occurrence of some of the potential hazardous air polluting substances (HAPS); data for arsenic, chromium, lead, nickel, manganese and chlorine have been collected. Initial emphasis has been on developing an analytical scheme to reliably detect and measure arsenic in the ash samples. Concurrent with this effort, the major and minor element contents of the ash have been analyzed quantitatively by wavelength dispersive analysis (WDS) and mapped qualitatively by x-ray map analysis. The analytical methodology and preliminary data for the ash samples are summarized below. An abstract describing the preliminary data has been published (McGee and others, 1995).

Methods

The results presented below were collected using a JEOL 8900 electron probe microanalyzer (EPMA). For the ash measurements, the EPMA was operated at 20kV accelerating voltage and probe currents between 20 nanoamps and 100 nanoamps, depending on the particular measurement. Several microprobe sessions were spent developing and refining the analysis procedures for quantitative and element-map measurement of the ash particles. Quantitative data are produced by correcting the sample's element x-ray intensity data for instrument drift, deadtime, and beam/sample interaction due to atomic number, absorption and fluorescence effects (ZAF).

Results

A series of reconnaissance maps were made for the 1-inch polished multi-particle ash mounts of 1G1FA, 1G3FA, and 1G3BA60. Initial element x-ray maps acquired with a relatively coarse resolution (~25 μm) help to locate areas with particles of potential interest. Additional maps at resolutions of ~1μm are obtained to examine in detail and highlight the particles of interest. Particles identified in this way are then analyzed quantitatively by WDS for all major and minor elements detected by qualitative spectral identification, as well as for any additional elements of interest.

For the WDS analyses performed to date the 15 analyzed elements are sodium, potassium, calcium, titanium, iron, magnesium, silicon, aluminum, arsenic, chloride, nickel, lead, chromium, manganese and sulfur. Detection limits for these elements range from ~50 ppm to ~500 ppm, depending on the element, measurement time, and composition of the sample. The preliminary quantitative analyses and distribution of elements are summarized below.

The fly ash consists mostly of solid, glassy, or partly devitrified spheres, vesicular cenospheres (some hollow), or plerospheres. Most particles have diameters between 10 and 50 μm. Some particles appear to be welded agglomerates of one or more of the different sphere types. Quantitative microprobe analyses indicate that these spheres are predominantly aluminosilicate glasses with variable amounts of iron, magnesium, calcium, sodium, titanium and potassium. Compositions of the aluminum-silicate spheres are summarized for the unit 1 fly ash and bottom ash in Table M1. Compositions of iron-rich spheres and the nearly pure silica spheres are presented in Table M2. Iron-rich spheres have a composition near that of magnetite. Some of the particles show detectable, but low, contents of arsenic; preliminary data suggest that some particles, particularly the iron-rich

ones, contain arsenic at concentrations of approximately 1000 ppm. The element x-ray maps indicate that there are no large (>1000 μm), arsenic-rich (>1wt.%) particles present in any of the sample surfaces (each 1-inch polished sample is estimated to have roughly 500,000 particles exposed at the surface). Random sampling of particles <100 μm has not yet located any arsenic-rich particles in this size range, although some mapped particles show detectable but low concentrations of arsenic. One of the iron-aluminum-silicon spheres in fly ash 1G3FA in which the arsenic signal, corrected for background, shows a faint but detectable and uniform distribution in the hollow sphere. Lead and chlorine are generally below detection (~300 and 100 ppm, respectively) in the particles measured to date. Chromium, manganese, and nickel contents of the fly ash particles are low and fairly constant, although the highest nickel contents occur in the iron-rich particles. Sample 1G1FA appears to have more abundant iron-rich spheres than sample 1G3FA consistent with the higher pyrite content of the high-sulfur coal (unit 1). Also, sample 1G1FA appears slightly more calcium-rich than 1G3FA (although this is based on only a very limited data). All grains exhibited edge (surface) increases in the abundance of some elements. One sphere in 1G3FA showed the following variations across the particle: FeO (12 to 37 wt.%; SiO_2 (37 to 52%); Al_2O_3 (19 to 27%).

The bottom ash contains abundant angular fragments, predominantly Al-silicate glasses with compositions similar to those of the fly ash. Aluminum-silicate spheres are present but much less common than in the fly ash. The bottom ash spheres are commonly hollow. Iron-rich particles are less common in the bottom ash than in the fly ash. Minor-element contents in the bottom ash appear to be similar to, but less variable than, those in the fly ash.

Based on the compositional data for these sphere types the silica-spheres, iron-aluminum-silicon spheres, and iron-spheres also have distinct estimated densities of ~2.7, 3.0-4.0, and ~5.2, respectively. We will be looking more closely at the compositional types, both in the unit 1 ash and in subsequent ash samples, to see if the HAPS elements have an affinity for any particular ash compositions. Refined quantitative analysis, optimized for trace element measurements, will also be performed to more accurately determine concentrations of the measured HAPS elements (arsenic, chromium, chlorine, manganese, nickel, and lead) in the ash fragments and spheres.

Table M1. Compositions of iron-aluminum-silicate spheres in fly ash (FA) and bottom ash (BA) from the high- (G1) and low-sulfur (G3) units. All values are in weight percent. (Avg., average; Min., minimum; Max., maximum)

	1G3FA				1G1FA				1G3BA60		
	Avg.	Min.	Max.		Avg.	Min.	Max.		Avg.	Min.	Max.
SiO_2	49.56	36.84	61.33		51.43	36.16	69.02		52.75	38.33	68.17
As_2O_3	0.04	0.00	0.09		0.03	0.00	0.09		0.03	0.00	0.09
FeO	12.43	0.15	37.85		13.59	0.25	37.06		8.66	0.65	33.47
Na_2O	0.31	0.03	1.42		0.36	0.06	0.86		0.22	0.15	0.30
PbO	0.01	0.00	0.06		0.01	0.00	0.06		0.00	0.00	0.04
K_2O	2.56	0.07	6.60		2.23	0.09	9.69		2.27	0.19	4.40
CaO	1.70	0.00	5.89		2.22	0.00	19.26		1.62	0.00	5.45
TiO_2	1.33	0.00	13.22		1.15	0.00	4.58		0.99	0.02	2.71
Cr_2O_3	0.01	0.00	0.04		0.02	0.00	0.07		0.02	0.00	0.12
MnO	0.03	0.00	0.21		0.03	0.00	0.14		0.04	0.00	0.19
S	0.00	0.00	0.03		0.00	0.00	0.02		0.01	0.00	0.05
MgO	1.00	0.03	2.55		0.92	0.00	2.16		0.95	0.17	1.63
Cl	0.00	0.00	0.04		0.00	0.00	0.02		0.00	0.00	0.04
NiO	0.03	0.00	0.16		0.05	0.00	0.15		0.03	0.00	0.13
Al_2O_3	29.06	17.47	44.19		26.40	19.26	41.90		29.44	17.24	39.98
Total	98.10				98.44				97.05		

Table M2. Compositions of silica -spheres and iron-spheres in fly ash (FA) and bottom ash (BA) from the high- (G1) and low-sulfur (G3) units. All values are in weight percent.

	1G1FA	1G1FA	1G3FA	1G3FA	1G3BA60
	Si-rich	Fe-rich	Si-rich	Fe-rich	Si-rich
SiO_2	100.49	1.08	99.74	1.95	100.54
As_2O_3	0.03	0.10	0.04	0.17	0.05
FeO	0.08	90.70	0.15	91.40	0.08
Na_2O	0.00	0.02	0.01	0.00	0.01
PbO	0.00	0.00	0.00	0.00	0.00
K_2O	0.00	0.02	0.03	0.03	0.04
CaO	0.02	0.04	0.00	0.12	0.02
TiO_2	0.02	0.09	0.00	0.08	0.02
Cr_2O_3	0.00	0.00	0.00	0.03	0.00
MnO	0.03	0.00	0.00	0.02	0.01
S	0.00	0.00	0.00	0.00	0.00
MgO	0.01	0.04	0.00	0.06	0.00
Cl	0.00	0.00	0.00	0.00	0.00
NiO	0.00	0.00	0.11	0.21	0.01
Al_2O_3	0.03	1.52	0.06	0.94	0.11
Total	100.71	93.62	100.17	95.01	100.89

N. ANALYTICAL TRANSMISSION ELECTRON MICROSCOPY OF FLY ASH FROM UNIT 1

by Gordon L. Nord Jr., U.S. Geological Survey, Reston, Virginia

Transmission electron microscopy (TEM) was tested as a method of examining the composition and mineralogy of small fly ash particles because of the instrument's ability to resolve and analyze small particles. This contribution reviews preliminary results of an examination of fly ash from the high-sulfur unit (unit 1).

Methods

The <10 μm fraction of the fly ash was suspended in ethanol and dispersed in a sonic cleaner for five minutes. Minute drops of this dispersion were then placed on 3.0 mm (diameter) 200-mesh copper grids that had been coated with a thin film of carbon. Initially, the grids were placed on a mesh having 2.5 mm holes so that surface of the sample-containing copper grid is only in contact with air. This prevented the solution from wetting the carbon film and attaching the sample grid to a supporting surface. After placing the drops of dispersed sample, the grids were dried overnight in a covered dish. In addition to the <10 μm fraction, a 100 μm hollow black sphere from the fly ash was examined. It was crushed between two glass slides and pressed onto a carbon-coated 200 mesh sample grid.

All sample grids were lightly coated with carbon in an automatic coater. The grids were then mounted in a double-tilt beryllium holder. The analyses were performed using a 200B JEOL Scanning Transmission Electron Microscope, which is capable of operating at 200 keV. However, the operating voltage for the x-ray energy dispersive analysis (EDS) is routinely done at 100 keV. This is because the background x-radiation is high at 200 keV and almost zero at 100 keV (Nord, 1982).

Because the fly-ash particles are much larger than the 90 nm spot size used in the scanning mode of the TEM, a normal beam was used for the analyses. Use of the normal beam requires the beam to be converged over the particle. The observer can see the particle at all times until the beam is converged. In this way the exact position of the beam relative to the sample is known. The normal beam is typically too intense for analytical work because the current yields in this mode swamp the electronics. However a small condenser aperture of 20 μm was used with the smallest spot size to yield a current of 0.03 nanoAmperes which reduced the signal to acceptable levels. Detection in this mode results in 3% deadtime and an adequate number of counts are collected in one minute.

The x-ray energy spectra were collected on a Tracor Northern 2000 Multichannel Analyzer and printed out on a 7475A HP Plotter. The nominal resolution of the detector is about 155 eV.

Results

Thin edges of the broken particles are electron transparent and were found to be filled with discrete particles. The size of the particles examined ranged from 30 nm to 100 nm. Many of the precipitates are interconnected. EDS analysis of the area indicates high iron and minor titanium. Thicker areas contain high silicon contents and minor amounts of aluminum and trace potassium. Selected area diffraction indicates the presence of the strong 111 line (d=4.85 Å) from magnetite. Additional reflections are consistent with maghemite. General observations from the EDS and diffraction analysis are presented below.

- The most common fly ash particles observed in the <10 μm size fraction are usually sintered aggregates of smaller particles. Isolated particles are rare but wide spread.

Particle-sizes range from 0.1 μm to about 8 μm. Sintered aggregates are commonly larger. Invariably, all of the particles are spheroidal.

- Most attempts at electron diffraction were unsuccessful because of the thick particles. Even at 200 keV, the thickness of a particle needs to be less than 0.5 μm in order to obtain coherent diffraction (spots).

- 100 particles each less than 4 μm in diameter were analyzed by x-ray energy dispersive spectroscopy in an elemental range from sodium to uranium and a sensitivity of about 500 ppm. The analyses should be considered qualitative, because the activated volume of the particle is unknown. General trends in element concentration were identified as follows.

  - Most of the particles contain, listed in order of decreasing abundance, silicon, aluminum, iron, calcium, potassium and titanium.

  - Individual particles containing only one major element were dominated by either silicon, iron, titanium or calcium. The high silicon particles also appear to be shaped like a football (American Football).

  - Minor elements detected in the particles include phosphorous, sulfur, vanadium, nickel, and zinc.

  - Vanadium contents are highest in high calcium particles (Fig. N1).

  - Zinc contents are greatest in particles with high silicon and iron.

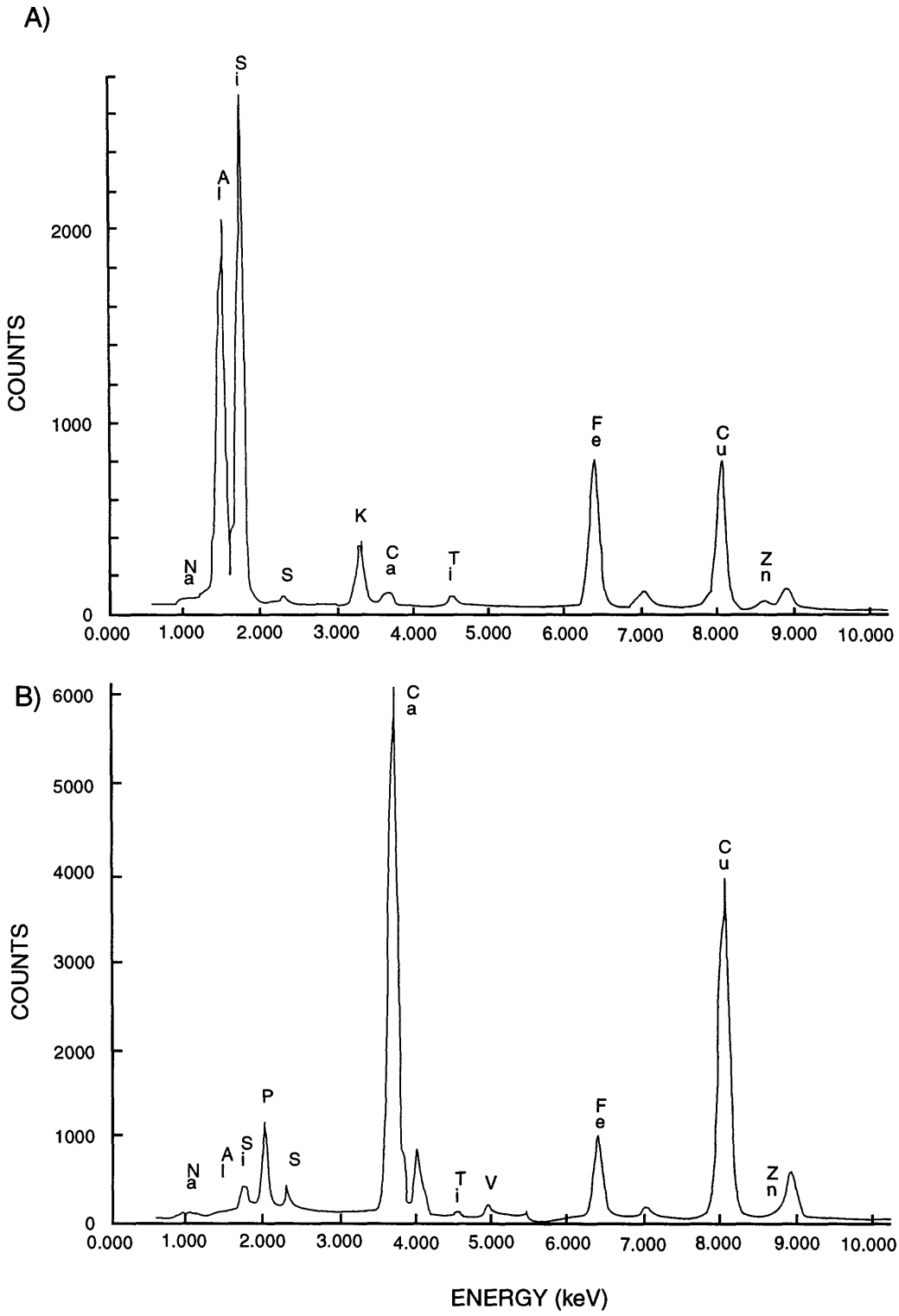

Figure N1. Energy spectrum generated by TEM analysis of fly ash particles. A) A typical spectrum for a Si-Al-Fe particle (see text). B) Spectrum for a Ca-rich particle. The Cu in both spectra is from the supporting Cu grid.

O. PETROGRAPHIC ANALYSIS OF SIZED FRACTIONS OF FLY ASH: NOVEMBER 1994 SAMPLES

by James C. Hower and Alan S. Trimble, Center for Applied Energy Research, University of Kentucky, Lexington, Kentucky

Fly ash from the high- and low-sulfur units were separated into size fractions and examined with a petrographic microscope to determine the abundance of major phases. Differences in the composition of the size fractions may provide clues to the distribution of trace elements. A special focus of this study was the amount and maceral composition of carbon particles. High carbon content makes the fly ash unsuitable for most beneficial uses.

Raw fly ash samples from the November, 1994, collection were wet screened at 100 mesh, 200 mesh, 325 mesh, and 500 mesh. The dried fractions were then weighed, split for petrographic analysis and prepared as polished pellets, and analyzed for ash yield and carbon content. The percent recovery, ash yield, carbon content (ultimate analysis), and petrography of the size fractions is given in Table O1. The three ashes have a similar size distribution in the +325 mesh fractions (Fig. O1). The size partitioning between the unit 3 coarse-side and fine-side ashes is somewhat surprising in that they have similar distributions of material. Based on experience with other power plants, we would have expected the coarse-side ash to have coarser-size distribution than the fine-side ash.

The distribution of carbon forms in the fly ashes is shown on Figures O2-O4. The overall trends mimic that seen in other fly ashes. Carbon tends to be most abundant in the coarse fractions. The dominance of the -325 mesh fractions in the overall size analysis implies, though, that carbon in the fine sizes is important in the utilization potential of the fly ash.

A similar analysis will be made of the December, 1994, fly ash. The December ash is actually more typical petrographically of the other monthly samples (through January, 1995) than is the November ash. Through analysis of both we should be able to gain an understanding of the range of fly ash composition produced at the plant.

Table O1. Petrographic data of size fractions of fly ash collected in November, 1994. (aniso, anisotropic; inertin., inertinite).

Unit	Size Range (mesh)	wt.%	Ash	C	glass	mullite	spinel	quartz	isotropic coke	aniso. coke	inertin.
1	+100	2.71	63.22	36.78	56.4	0.2	1.4	2.0	12.0	21.3	7.1
1	100x200	7.32	87.45	12.55	74.8	1.0	6.2	0.2	10.8	5.8	1.2
1	200x325	11.39	94.43	5.57	82.4	1.2	7.8	0.2	5.4	1.8	1.2
1	325x500	23.41	96.21	3.79	88.0	0.8	8.2	0.2	1.0	0.8	1.0
1	-500	55.17	98.82	1.18	94.2	1.1	3.7	0.0	0.8	0.2	0.0
3 coarse	+100	4.63	41.96	58.04	62.8	0.4	0.4	0.6	14.8	16.4	3.6
3 coarse	100x200	6.88	81.52	18.48	82.9	0.0	0.6	0.3	7.5	6.4	2.3
3 coarse	200x325	12.13	89.82	10.18	88.3	0.0	0.3	0.1	4.2	3.7	3.2
3 coarse	325x500	11.47	95.34	4.66	94.5	0.0	0.3	0.2	2.5	1.5	1.0
3 coarse	-500	64.89	98.97	1.03	96.0	0.2	0.2	0.4	1.6	0.6	0.8
3 fine	+100	3.61	43.93	56.07	38.8	0.0	0.0	3.6	20.0	32.4	5.2
3 fine	100x200	7.27	77.10	22.90	73.9	0.0	0.1	1.0	11.5	10.9	2.6
3 fine	200x325	11.29	82.38	17.38	89.1	0.4	0.2	0.7	4.6	2.9	2.1
3 fine	325x500	18.66	95.48	4.52	93.0	0.4	0.6	0.2	2.6	1.6	1.8
3 fine	-500	59.18	98.79	1.21	97.2	0.0	0.6	0.4	0.8	0.6	0.6

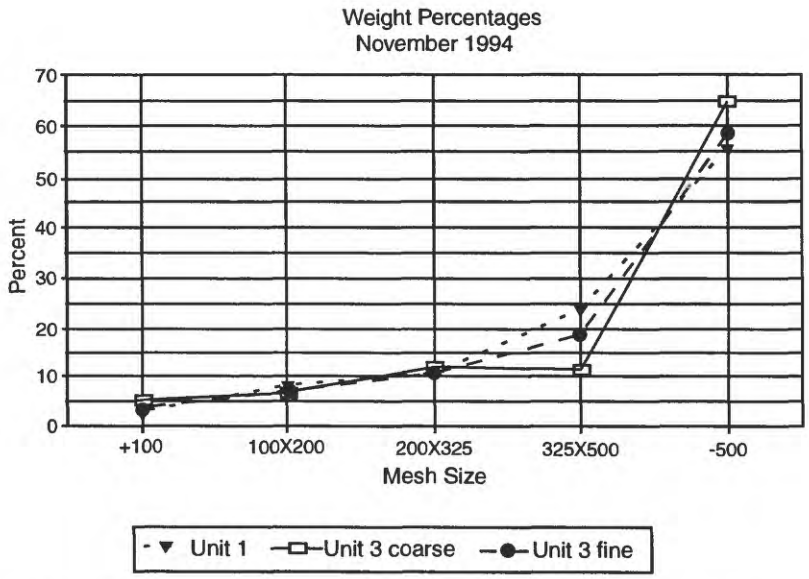

Figure O1. Distribution of size fractions (weight percent) in fly ash.

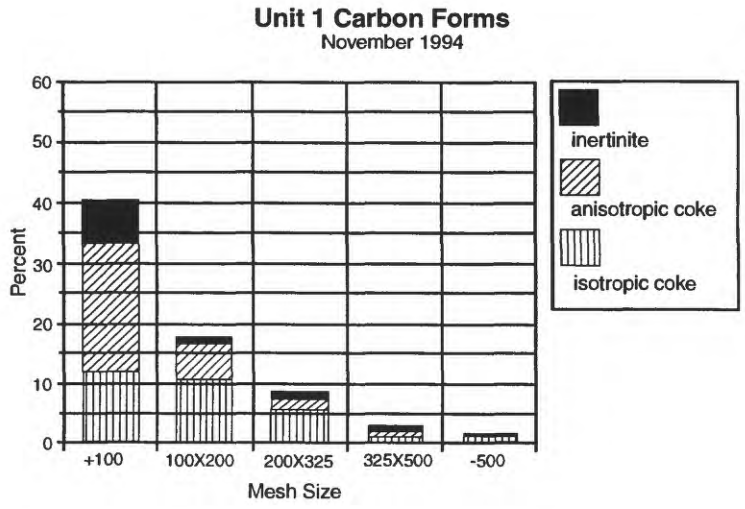

Figure O2. Abundance of carbon and maceral type in fly ash from the high-sulfur unit (unit 1).

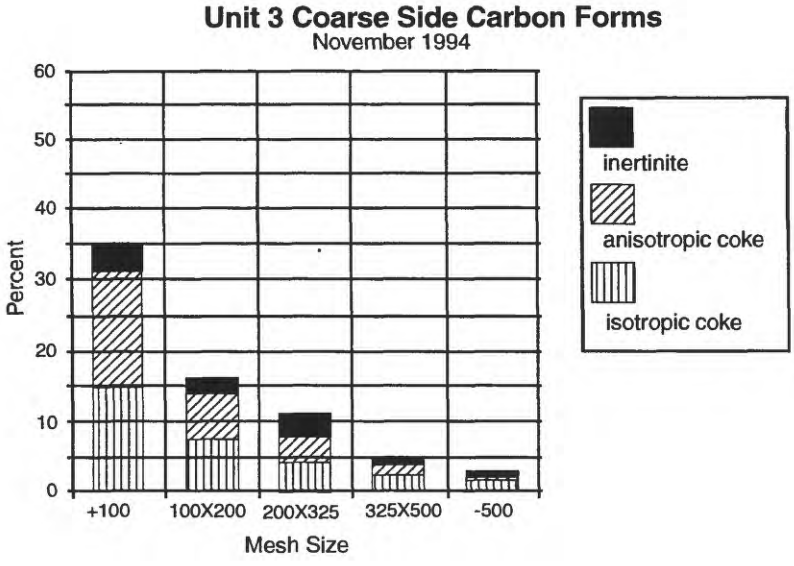

Figure O3. Abundance of carbon and maceral type in coarse-side fly ash from the low-sulfur unit (unit 3).

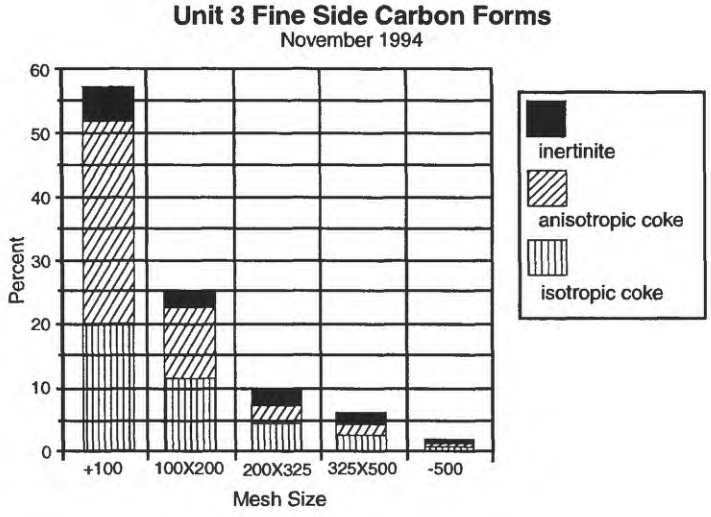

Figure O4. Carbon abundance and maceral type in fine-side fly ash from the low-sulfur unit (unit 3).

P. INITIAL REPORT ON THE SULFUR ISOTOPE GEOCHEMISTRY OF SOLID WASTE PRODUCTS FROM A COAL-BURNING POWER PLANT

by Elliott C. Spiker and Anne L. Bates, U.S. Geological Survey, Reston, Virginia

We determined the sulfur isotope composition of feed coal (FC), bottom ash (BA) and fly ash (FA) from the coal-burning power plant. Our goal was to assess the usefulness of sulfur isotopes as a tracer of the source and fate of different forms of sulfur in the solid waste products.

Methods

Sulfur isotopic analysis techniques require that the specific forms of sulfur be isolated and converted to pure SO_2. Sulfate, disulfide, and organic sulfur were isolated by using the HCl/Cr^{2+}/Eschka-fusion analytical scheme (Bates and others, 1993), similar to the method described in Tuttle and others (1986). Sulfate was removed by leaching the powdered samples with cold 6 N HCl under a nitrogen atmosphere. Minor amounts (up to .04%) of monosulfides (acid volatile sulfur, AVS) were liberated by the acid from some samples and collected. Disulfide (DS) was extracted from the HCl-leached sample by using the chromium (II) method; the H_2S gas produced was collected as Ag_2S. The organic sulfur (OS) was subsequently collected as sulfate after combusting the chromium-treated sample residue with an Eschka mixture. The products of this separation scheme were converted to SO_2, purified by cryogenic techniques, and analyzed by stable isotope mass spectrometry.

Results

It appears that most of the sulfur in the feed coal is combusted to the gas phase without significant isotope fractionation. However, the minor amounts of sulfur remaining in the bottom ash and in the fly ash show variable and sometimes large isotope fractionation compared to the feed coal. As shown in Figure P1, there can be a large positive shift in the $\delta^{34}S$ ‰ values in all forms of sulfur in the BA and FA. However, this positive isotope shift is not consistent between the 1G samples and 2G samples. This isotope shift is probably the result of the complex chemical kinetics accompanying the combustion and condensation reactions, which are a function of many variables.

Conclusion

The significant and variable isotope fractionation found in the BA and FA in 1G and 2G samples examined may be a useful indicator of combustion conditions and efficiency. Much more work is needed to confirm this; one might first attempt to correlate the isotope results with other indicators of combustion conditions. On the other hand, the positive isotope values found in some of the BA and FA samples may be useful as tracers of sulfate leachate in disposal areas.

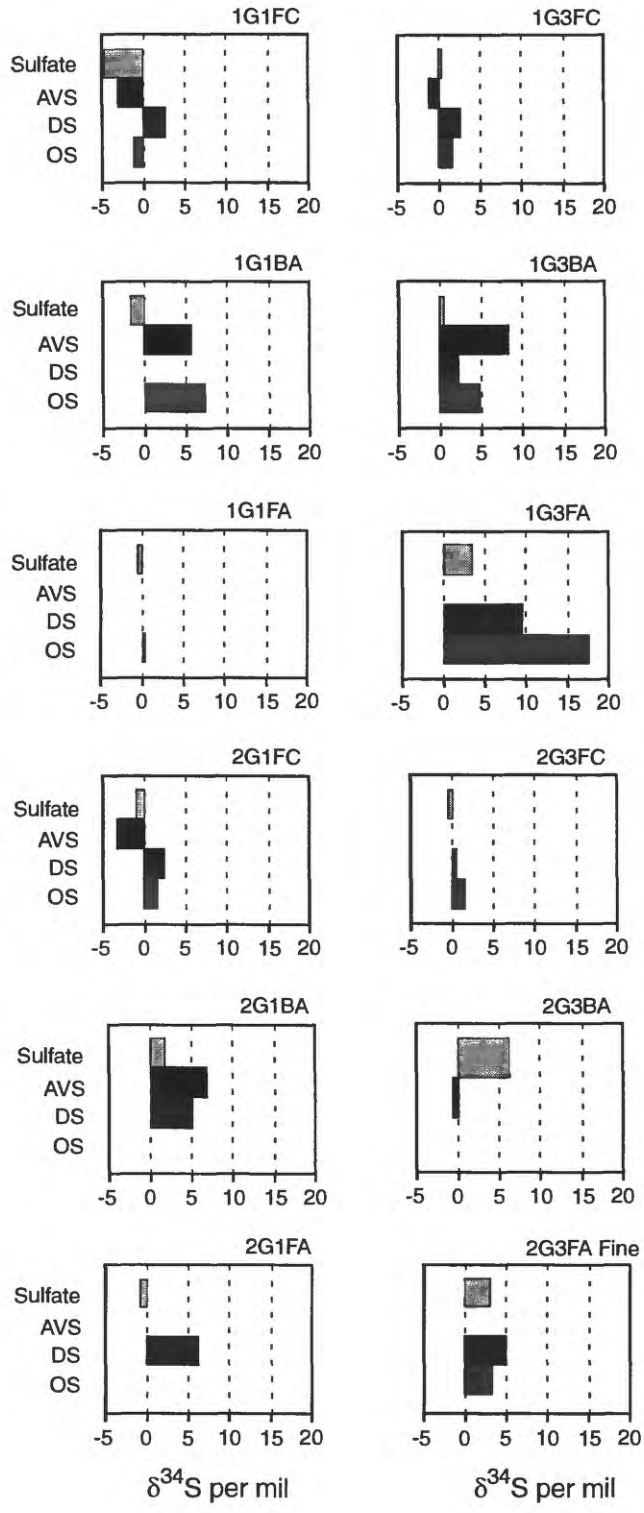

Figure P1. $\delta^{34}S$ of the various forms of sulfur determined in selected samples of fly (FA) and bottom ash (BA) from unit 1 (G1) and unit 3 (G3). (AVS, acid-volatile sulfur; DS, disulfide sulfur; OS, organic sulfur).

Q. ORGANIC GEOCHEMICAL STUDIES

by William H. Orem and Harry E. Lerch, U.S. Geological Survey, Reston, Virginia

A study of the organic geochemistry of feed coals (FC), fly ash (FA), and bottom ash (BA) from the Kentucky power plant (1G1, 1G3), and Lingan, Nova Scotia, Canada (NPS 8, 9, 10, 11, and 13) were included as part of the power plant project. The investigation focussed on (1) the amount of organic material remaining in the FA and BA after combustion, (2) the chemical composition of this organic material, and (3) the presence in the FA and BA of potentially hazardous organic compounds (e.g. polynuclear aromatic hydrocarbons (PNA), heterocyclic compounds), which could leach into surface and groundwater supplies following disposal of the ash. Chemical analysis of the FA and BA for organic constituents proved difficult due to the generally low concentrations, inert composition, and magnetic characteristics of the ash samples. Thus, the initial effort descibed herein has been largely spent in developing new organic geochemical approaches for studying these FA and BA samples. Sink/float techniques and removal of magnetic particles have been used to concentrate organic matter and prepare the FA and BA samples for gross organic characterization. We have also used a number of different solvent combinations to maximize yields of extractable hydrocarbons from the FA, BA, and FC.

Preliminary results show that organic carbon contents range from < 1 weight percent to 5 weight percent in the FA and BA samples, compared to values of 45-55 weight percent in the FC. Nitrogen contents decline from about 1 weight percent in the FC to 0.2-0.4 weight percent in the FA and BA. Hydrogen declines from 5-6 weight percent in the feed coal to 0.07-0.20 weight percent in the fly and bottom ash. Corresponding nitrogen/carbon values are about 0.02 in FA, BA, and FC, while hydrogen/carbon values ranged from 0.64 to 0.84 in the FA and BA compared to values near 1.20 in the FC. This suggests that hydrogen-rich compounds are preferentially lost during the combustion process, while nitrogen-containing compounds are retained in the FA and BA in about the same proportions as in the FC.

Structural characterization of the organic matter in the FA and BA using ^{13}C NMR was initially difficult due to the low carbon content and large magnetic component of the samples. Using techniques described above, however, we have succeeded in obtaining some preliminary NMR spectra of two BA samples and corresponding FC. Although the spectra of the BA samples are very noisy, the general features of the spectra are apparent. The spectra of the BA consists of two peaks, one in the 0-50 ppm region representing aliphatic (sp^3) carbons, and the second in the 110-150 ppm region representing aromatic carbons. The spectra of the BA samples are surprisingly similar to those of the FC samples, suggesting that the organic matter in the BA survived the combustion process with relatively little structural alteration or the carbon component was part of the pulverizer discards that bypass the furnace (Eble, this volume).

Preliminary results from gas chromatography and gas chromatography/mass spectrometry analysis of extracts from FA, BA, and FC samples for identifiable PNA are shown in Table Q1. All positively identified PNA peaks from each chromatogram were quantified and summed for listing as total PNA in Table Q1. Total PNA concentrations in the BA and FA samples are low, but still at levels that may be of environmental concern, especially if the combustion process has made them more mobile and susceptible to dissolution in water.

Table Q1. Concentrations of polynuclear aromatic hydrocarbons (PNA) in feed coal, fly ash and bottom ash samples.

SAMPLE	TOTAL PNA (μg/g sample)
1G1 FC	120
1G3 FC	117
1G1 FA	3.3
1G3 FA	2.1
1G1 BA	3.7

R. BULK X-RAY DIFFRACTION ANALYSIS

by Frank Dulong, U.S. Geological Survey, Reston, Virginia

The assemblage of minerals found in coal is substantially altered during combustion. This contribution presents the semiquantitative abundance of major minerals detected by x-ray diffraction in the feed coal, fly ash, and bottom ash. Two sample collections from the high-sulfur unit (unit 1, G1) (Table R1) and three sample collections from the low-sulfur unit (unit 3, G3) (Table R2) were analyzed.

High-Sulfur Unit

The feed coal (FC) contains roughly sub-equal amounts of quartz and kaolinite, followed in abundance by pyrite and illite with minor to trace amounts of calcite and gypsum and a trace amount of hematite. The fly ash (FA) is dominated by maghemite, followed in abundance by quartz in roughly the same relative concentration as in the feed coal, with some hematite and a minor to trace amount of mullite. The bottom ash (BA) is dominated by maghemite, followed by hematite and mullite. Quartz in bottom ash is present only in a trace amount, which is substantially less than the amount in the feed coal and fly ash (Table R1). During combustion, pyrite is altered to maghemite (Fe_3O_4) and hematite (Fe_2O_3) while the clay minerals, especially kaolinite, are converted to mullite ($Al_6Si_2O_{13}$).

Quartz was expected to be in approximately equal concentrations in the feed coal, fly ash and bottom ash. Analysis of the samples however determined that most of the quartz accumulates in the fly ash; only a trace amount ends up in the bottom ash. The quartz in the coal might be very fine-grained, which would favor accumulation in the fly ash.

Low-Sulfur Unit

The dominant mineral in the feed coal (FC) is kaolinite followed in abundance by quartz and illite. Calcite and pyrite are present in trace amounts. The fly ash (FA) and bottom ash (BA) are dominated by mullite, followed by quartz, with more hematite on the fine side (FS; Table R2).

Quartz has a similar content in the feed coal and the bottom ash; the content in the fly ash is greater than the feed coal. A substantial amount of kaolinite in the coal believed to result in mullite in both the fly and bottom ash. The small amounts of maghemite and hematite in the fly and bottom ash are accounted for by minor to trace amounts of pyrite and the small amount of iron-containing illite in the feed coal.

Table R1. Semi-quantitative relative abundance of major minerals in samples of feed coal (FC), fly ash (FA) and bottom ash (BA) from the high-sulfur unit (unit 1). (Kaol., kaolinite; Mag., maghemite; TR, trace amount (< 5 percent); MN, minor amount (≥5 and <10 percent); nd, not detected).

Sample Number	Quartz wt.%	Illite wt.%	Kaol. wt.%	Pyrite wt.%	Calcite wt.%	Gypsum wt.%	Mag. wt.%	Hematite wt.%	Mullite wt.%
1G1 FC	25	10	35	20	10	TR	nd	TR	nd
2G1 FC	30	15	30	15	TR	MN	nd	nd	nd
1G1 FA	30	nd	nd	nd	nd	nd	50	10	10
2G1 FA	20	nd	nd	nd	nd	nd	50	20	TR
1G1 BA	TR	nd	nd	nd	nd	nd	55	30	10
2G1 BA	TR	nd	nd	nd	nd	nd	50	30	10

Table R2. Semi-quantitative relative abundance of major minerals in samples of feed coal (FC), fly ash (FA) and bottom ash (BA) from the low-sulfur unit (unit 3). (Kaol., kaolinite; Mag., maghemite; TR, trace amount (< 5 percent); MN, minor amount (≥5 and <10 percent); nd, not detected; FS, fine side; CS, coarse side).

Sample Number	Quartz wt.%	Illite wt.%	Kaol. wt.%	Pyrite wt.%	Calcite wt.%	Gypsum wt.%	Mag. wt.%	Hematite wt.%	Mullite wt.%
1G3 FC	25	15	50	MN	TR	nd	nd	nd	nd
2G3 FC	25	15	55	TR	TR	nd	nd	nd	nd
3G3 FC-A	20	10	60	nd	TR	nd	nd	nd	nd
3G3 FC-B	20	10	60	TR	TR	nd	nd	nd	nd
1G3 FA	40	nd	nd	nd	nd	nd	nd	nd	60
2G3 FA/FS	35	nd	nd	nd	nd	nd	nd	15	40
2G3 FA/CS	35	nd	nd	nd	nd	nd	nd	nd	60
3G3 FA/FS	30	nd	nd	nd	nd	nd	nd	20	40
3G3 FA/CS	65	nd	nd	nd	nd	nd	nd	5	30
1G3 BA	35	nd	nd	nd	nd	nd	MN	MN	50
2G3 BA	25	nd	nd	nd	nd	nd	nd	15	40
3G3 BA	20	nd	nd	nd	nd	nd	nd	nd	85

S. FLY ASH PETROGRAPHY

by Jim Pontolillo, U.S. Geological Survey, Reston, Virginia

This section summarizes petrographic observations on fly ash from both unit 1 and unit 3 from July 1994 and December 1994. The purpose of this examination was to provide an optical description of the bulk fly ash. Detailed analysis of size fractions of the fly ash is presented by Hower and Trimble (this volume).

Descriptions were made using polished, epoxy-mounted pellets examined under reflected-light, oil-immersion microscopy at a magnification of 400x. The use of Sudan Black-doped epoxy greatly enhanced the identification of fly ash particles by eliminating the majority of the subsurface reflections common with the use of non-dyed epoxy.

Fly ash is divided into four inorganic and three organic constituents. The inorganic constituents include:

- glass - the fused alumino-silicates,
- quartz - includes crystalline quartz, which has a melting temperature higher than boiler temperatures, and other unfused silicates, in some cases these have a fused outer rim,
- mullite - ideal composition of $3(Al_2O_3)•2(SiO_2)$ but in fly ash represents a class of minerals from $3(Al_2O_3)•2(SiO_2)$ to $2(Al_2O_3)•3(SiO_2)$,
- metal oxides - ideally a class of minerals composed mainly of iron and oxygen, magnetite and hematite are the prominent members of this group.

The organic constituents include:

- isotropic and anisotropic coke - coke or char in fly ash derived from macerals, primarily vitrinite with some semi-inertinite, which passed through a thermoplastic phase and is repolymerized in the boiler,
- inertinite - the inertinite macerals from the coal which pass through the boiler relatively unaltered.

The fly ash petrography for the ashes collected from July through December, 1994, is shown in Table S1. Unit 1 fly ash consistently has a higher spinel content than the unit 3 ashes, reflecting the higher iron oxide content of the high-sulfur feed coal ash (Eble, this volume). The unit 3 fly ashes generally have a higher glass content then the unit 1 ash, with the fine-side fly ash particles being much smaller than those from the coarse-side ash.

Table S1. Abundance of major phases in fly ash as determined by petrographic microscope. Samples included those collected from July until December of 1994. All values expressed as volume percent (TR, trace amount; CS, coarse side; FS, fine side).

Sample	glass	mullite	spinel	quartz	isotropic coke	anisotropic coke	inertinite
1G1 FA	88.2	2.2	7.8	0.2	0.4	0.6	0.6
1G3 FA	95.2	0.2	0.4	0.6	1.2	2.4	0.0
2G1 FA	90.4	1.8	5.2	0.4	1.2	0.8	0.2
2G3 FA/CS	97.2	0.0	0.4	0.4	0.4	1.0	0.8
2G3 FA/FS	92.8	0.4	0.2	0.4	1.4	3.6	1.0
3G3 FA/CS	99.6	0.0	0.2	0.0	0.2	0.0	0.0
3G3 FA/FS	94.4	0.0	0.4	0.6	1.6	2.2	0.8
4G1 FA	89.0	1.4	5.4	0.4	1.2	2.6	0.0
4G3 FA/CS	86.8	1.0	0.8	0.6	5.6	5.2	0.0
4G3 FA/FS	91.0	0.2	0.6	0.6	1.8	4.6	1.2
5G1 FA	87.4	2.4	8.4	0.0	1.4	0.2	0.2
5G1 FA/CS	96.0	0.2	0.2	Tr	0.6	2.8	0.2
5G1 FA/FS	97.6	0.0	0.8	0.4	0.2	1.0	0.0

REFERENCES

Baedecker, P.A.; Grossman, J.N., 1994, The SPECTRA program library: A PC based system for gamma-ray spectra analysis and INAA data reduction: U.S. Geological Survey Open File Rep. 94-168, 47p.

Bates, A. L., E. C. Spiker, W. H. Orem, and W. C. Burnett, 1993, Speciation and isotopic composition of sulfur in sediments from Jellyfish Lake, Palau: Chemical Geology, v. 106, p. 63-76.

Bethke, C.M., 1994, Geochemist's Workbench, University of Illinois.

Chinchon, J.S., Querol, X., Fernández-Turiel, J.L., Lopez-Soler, A., 1991, Environmental impact of mineral transformatins undergone during coal combustion: Environmental Geology and Water Science, v. 18, p. 11-15

Clarke, L.B., and Sloss, L.L., 1992, Trace elements, International Energy Association Coal Research, London, IEACR/49 111p.

Davidson, R.L., Natusch, D.F.S., Wallace, J.R., and Evans, C.A., Jr., 1974, Trace elements in fly ash: Environmental Science and Technology, v. 8, no. 11, p. 1107-1113.

Day, R., Fuller, M.D., and Schmidt, V.A., 1977, Hysteresis properties of titanomagnetites: Grain size and compositional dependence: Physics of the Earth and Planetary Interiors, v. 13, p. 1206-1216.

Dekkers, M.J., and Pietersen, H.S., 1992, Magnetic properties of low-Ca fly ash: a rapid tool for Fe-assessment and a survey for potentially hazardous elements: Materials Research Society Symposium Proceedings, v. 245, p. 37-47.

Dudas, M.J., 1981, Long-term leachability of selected elements from fly ash: Environmental Science and Technology v. 15, p. 840-843.

Eary, L.E., Rai, D., Mattigod, S.V., and Ainsworth, C.C., 1990, Geochemical factors controlling the mobilization of inorganic constituents from fossil fuel combustion residues: II. Review of minor elements: Journal of Environmental Quality, v. 19. p. 202-214.

Electric Power Research Institute, 1994, EPRI TR-104614-V2 Project 3081, p.G1-G4.

Fernández-Turiel, J.L., de Carvahalho, W., Cabanas, M., Querol, X., and Lopez-Soler, A., 1994, Mobility of heavy metals in coal fly ash: Environmental Geology, v. 23 p. 264-270.

Finkelman, R.B., 1994, Modes of occurrence of potentially hazardous elements in coal: Levels of confidence: Fuel Processing Technology, v. 39, p. 21-34

Furuya, K., Yoshihiro, M., Chiba, T., and Kikuchi, T., 1987, Elemental characterization of particle size-density spearated coal fly ash by spectrophotometry, inductively coupled plasma emission spectrometry, and scanning electron microscopy -- energy dispersive X-ray analysis: ,Environmental Science of Technology, v.21, p. 898-903.

Germani, M.S., and Zoller, W.H., 1988, Vapor phase concentrations of arsenic, selenium, bromine, iodine and mercury in the stack of a coal-fired power plant: Environmental Science and Technology, v. 22, no. 9, p. 1079-1085.

Grisafe, D.A.; Angino, E.E., Smith, S.M., 1988, Leaching characteristics of a high-calcium fly ash as a function of pH: a potential source of selenium: Applied Geochemistry, v.3, p. 601-608

Hansen, LD., Silberman, D., Fisher, G.L., and Eatough, D.J., 1984, Chemical speciation of elements in stack-collected respirable-size coal fly ash: Environmental Science and Technology, v. 18, no., 3, p. 181-186.

Hassett, D.J., 1993, Scientifically valid leaching of coal converstion solid residues to predict environmantal impact: unpublished report, 29 pages.

Heulett, L.D., and Weinberger, A.J., 1980, Some etching studies of the microstructure and composition of large aluminosilicate particles in fly-ash from coal-buring power plants: Environmental Science and Technology, v.14, p. 965-969.

Hulett, L.D., Weinberger, A.J., Northcutt, K.J., and Ferguson, M., 1980, Chemical species in fly ash from coal-burning power units: Science, v. 210, p. 1356-1358.

Keefer, R.F., and Sajwan, K.S., 1993, Trace elements in coal and coal combustion residues: Boca Ration, Florida, Lewis Publishers, 308 p.

Lauf, R.J, Harris, L.A., and Rawlson, S.S., 1982, Pyrite framboids as the source of magnetite spheres in fly ash: Environmental Science and Technology, v. 16, p. 218-220.

Locke, G., and Bertine, K.K., 1986, Magnetite in sediments as an indicator of coal combustion: Applied Geochemistry, v. 1, p. 345-356.

Mattigod, S.V., Rai, D., Eary, L.E., and Ainsworth, C.C., 1990, Geochemical factors controlling the mobilization of inorganic constituents from fossil fuel combustion residues: I. Review of major elements: Journal of Environmental Quality, v. 19. p. 188-201.

McGee, J.J., Finkelman, R.B., and Pontolillo, J., 1995, Microanalysis of hazardous air pollutants in fly ash from a coal-buring power plant: GSA Abstracts with Program, v. 47, A245.

Minkin, J.A., Finkelman, R.B., Thompson, C.L., Chao, E.C.T., Ruppert, L.F., Blandk, H., and Cecil, C.B., 1984, Microcharacterization of arsenic-and selenium-bearing pyrite in Upper Freeport coal, Indiana County, Pennsylvania: Scanning Electron Microscopy, IV, p. 1515-1524

Nord, Gordon L., Jr., 1982, Analytical electron microscopy in mineralogy: Exsolved phase in pyroxenes. Ultramicroscopy, 8, 109-120.

Palmer, C.A., 1990, Determination of twenty-nine elements in eight Aragonne Premium coal samples by instrumental neutron activation analysis: Energy and Fuels, v.4, p. 436-439

Palmer, C.A.; Finkelman, R.B.; Krasnow, M.R., unpublished data.

Palmer, C.A., Finkelman, R.B., Krasnow, M.R., Eble, C.F., 1995, Laboratory leaching behavior of environmentally sensitive trace elements from fly ash and bottom ash samples: American Chemical Society, Fuel Chemistry Division,, v. 40, no. 4, p. 803-804.

Palmer, C.A., Krasnow, M.R., Finkelman, R.B. and D'Angelo, W.M. J., 1993, An evaluation of leaching to determine modes of occurrence of selected toxic elements in coal: Journal of Coal Quality, v. 12, p.135-141.

Puffer, J.H., Russell, E.W.B., and Rampino, M.R., 1980, Distribution and origin of magnetite spherules in air, waters, and sediments of the greater New York City area and the North Atlantic Ocean: Journal of Sedimentary Processes, v. 50, p. 247-256.

Turner, R.R., 1981, Oxidation state of arsenic in coal-ash leachate: Environmental Science and Technology, v. 15, p. 1062-1066.

Smit, J., and Wijn, H.P.J., 1959, Ferrites: New York, John Wiley & Sons, 369 p.

Stumm, W., and Morgan, J.J., 1981, Aquatic Chemistry, Wiley and Sons, New York, NY, 381 p.

Thorpe, A.N., Senftle, F.E., Alexander, C.C., and Dulong, F.T., 1984, Oxidation of pyrite in coal to magnetite: Fuel, v. 63, p. 662-668.

Tuttle M. L., M. B. Goldhaber, and Williamson, D.L., 1986, An analytical scheme for determining forms of sulfur in oil shales and associated rocks: Talanta, v. 33, p. 953-961.